Capture and Characterization of Circulating Tumor Cells (CTCs) in Early Lung Cancer Using a Novel High-throughput Affinity-based Microfluidic Device

by

Vasudha Murlidhar

A dissertation submitted in partial fulfillment
of the requirements for the degree of
Doctor of Philosophy
(Chemical Engineering)
in the University of Michigan
2016

Doctoral Committee:

Associate Professor Sunitha Nagrath, Chair
Professor Ronald G. Larson
Professor Jennifer J. Linderman
Associate Professor Nithya Ramnath
Assistant Professor Ariella Shikanov

DEDICATION

I dedicate this thesis to my advisor, Dr. Sunitha Nagrath, whose insight and trust in my capabilities changed my career path forever - I will always be grateful to her for being a turning point in my life; to my brother Anish Muralidhar, who gave me the impetus and courage to pursue a PhD; to my mother and father, whose endless sacrifices enabled me to get a good education; and to my husband Madhav Ramesh, whose patience and cheerfulness keeps me going.

ACKNOWLEDGEMENTS

I would like to acknowledge a multitude of people, who made this research possible. First and foremost, my advisor, Dr. Sunitha Nagrath, whose passion for research and to make a difference in the lives of cancer patients, has been a constant source of motivation and excitement in every step of my research. I would also like to thank my lab mates, for their support and feedback over the years. I am thankful to my committee members Dr. Ronald Larson, Dr. Jennifer Linderman, Dr. Nithya Ramnath and Dr. Ariella Shikanov for their valuable feedback and guidance throughout my research.

I am especially grateful to Dr. Rishindra Reddy for being a wonderful collaborator and mentor, and Dr. Nithya Ramnath for her immensely useful insights and feedback on my work. I would also like to express my heartfelt gratitude to Shari Barnett, the clinical coordinator, who made many of my experiments possible, and Melinda Shearrer, for her support. I am grateful to the entire lung cancer project team - Dr. David Beer, Dr. Mark Orringer, Dr. Jules Lin, Dr. Andrew Chang, Dr. Philip Carrott, Dr. William Lynch, Dr. Hiroe Shiratsuchi, Dr. Martin Ishikawa, Svetlana Grabauskiene, and Dr. Lili Zhao, for being a wonderful team and for providing samples, feedback, and more. I would like to acknowledge Dr. Nallasivam Palanisamy, Shannon Carskadon and Dr. Chandan Kumar-Sinha for their help with the genetic analyses. I am thankful to our collaborators Dr. Max Wicha, Dr. Ebrahim Azizi and Shamileh Fouladdel for their help and feedback. I also enjoyed working with our collaborators in the departments of dermatology and otolaryngology – Dr. Scott Mclean, Dr. Alison Durham, Nisha Meireles, Dr.

Monique Verhaegen and Dr. Andrzej Dlugosz. Additionally, I am grateful for the Rackham International Student Fellowship and the Rackham Conference Travel grants which helped me greatly in my research. I would also like to acknowledge the Lurie Nanofabrication Facility (LNF), the Microscopy and Image Analysis Lab (MIL) at University of Michigan, and the Takayama lab. And most importantly, I am very grateful to all the patients who participated in our study, and kindly provided blood for our research.

TABLE OF CONTENTS

LIST OF TABLES

LIST OF FIGURES

Chapter 1

Introduction

1.1. Circulating Tumor Cells (CTCs)

Circulating tumor cells (CTCs) are cancerous cells that are shed by a tumor, which are then circulated in the blood circulation to different parts of the body. These cells may then proceed to get lodged into distant sites (a process known as 'seeding') and form secondary tumors (**Figure 1.1A**). This process of the spread of cancer (or metastasis) is believed to be caused by circulating tumor cells.

Circulating tumor cells (CTCs) were first discovered in 1869 during an autopsy of a patient who had died of metastatic cancer [1]. It was observed that the patient had cancer cells that resembled the originating tumor, in a site distant from the tumor itself. This suggested that in order for these cancer cells to be present in the distant site, they would have been carried by the blood circulation. CTCs have since been proposed to be involved in metastasis, a process that accounts for the majority of deaths due to cancer. While the role of CTCs in cancer has been known for more than a century, their study picked up pace in the last two decades where multiple research groups elucidated their clinical importance. CTCs have been detected from the peripheral blood of patients and hold the promise of being a real time biomarker for cancer detection and management [2]. They have been identified as useful predictors of metastasis and multiple

studies have demonstrated their potential in determining prognosis in metastatic breast, colorectal and prostate cancers [3]. Cristofanilli et. al. showed that CTCs can predict survival in metastatic breast cancer patients [4]. In ovarian cancer, Fan et al. found that stage III/IV (advanced stage) cancer patients exhibited a higher mean CTC count than stage I/II patients, suggesting that elevated numbers of CTCs were present in more advanced stages of disease [5]. Elevated CTCs numbers during treatment have also been shown to be associated with disease progression [6, 7]. CTCs are thus useful candidates for clinical monitoring of cancer patients. For example, in patients with metastatic breast cancer, the number of CTCs before and during treatment is an independent predictor of progression free and overall survival [4, 6]. Nagrath *et al.* surveyed patients from different cancers in advanced stages over their treatment course and showed that changes in CTC numbers could predict changes in the tumor burden [8]. Furthermore, CTCs have also been able to detect mutations related to treatment resistance,

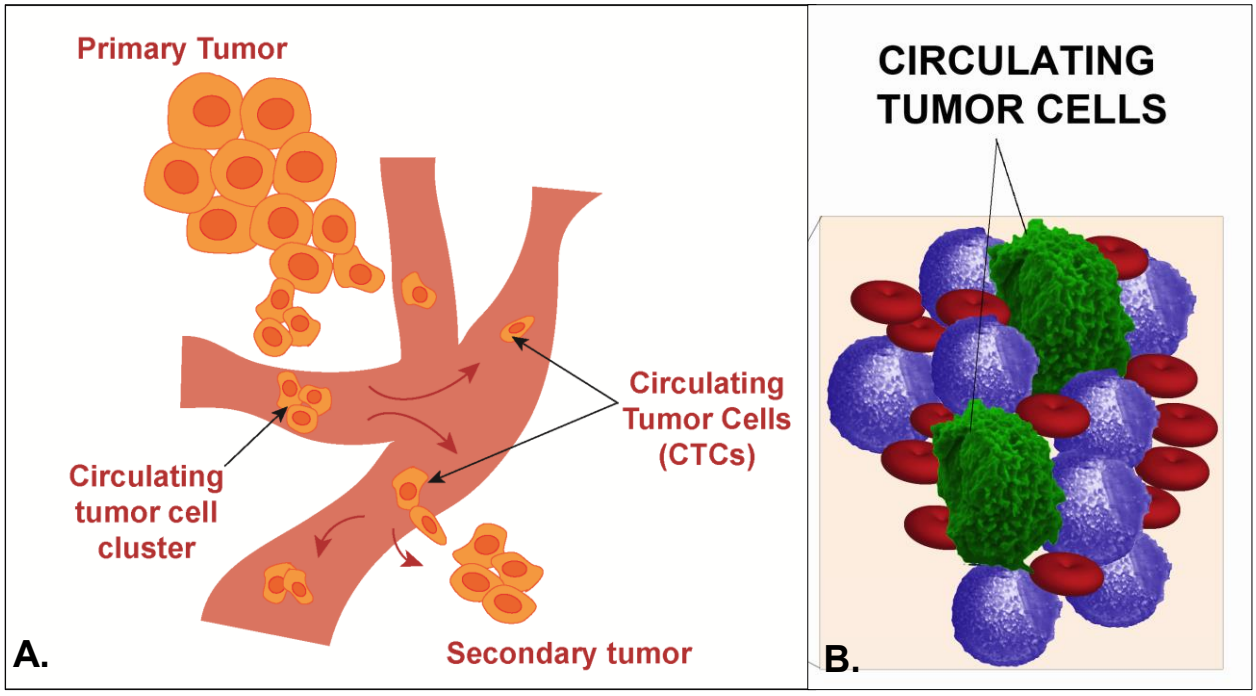

Figure 1.1 Circulating tumor cells (CTCs)
(A). Diagram represents circulating tumor cells being shed from a primary tumor and entering and circulating in the blood, consequently seeding a secondary tumor at a distant site, (B). Circulating tumor cells are rare and are found in frequencies of 1-20 among millions of white blood cells (purple) and billions of red blood cells.

thereby demonstrating their clinical utility in therapeutic monitoring [9].

CellSearch, a platform that utilizes antibody coated ferrofluids for CTC capture [10], is currently the only FDA-approved platform for CTC detection available for clinical use [3]. It has successfully demonstrated clinical utility by monitoring CTCs in blood from patients with breast, colon and prostate cancer wherein it was shown that CTCs correlate with poor prognosis [5, 11]. CTCs have also been used as investigative biomarkers in clinical trials; two recent clinical trials in lung cancer [12, 13] analyzed CTC numbers to predict survival among patients undergoing treatment. Molecular analysis of the CTCs was performed by investigating mutations for primary tumor matching [12] or FISH analysis of the CTCs indicating the potential use of CTCs in determining mutation status of patients undergoing therapy [13]. CTCs were also investigated in a pancreatic cancer study to evaluate two different technologies for CTC isolation and the possible use of CTCs as a novel biomarker for tumors that are difficult to biopsy [14].

However, their rarity (1-2 CTCs in 1 mL of blood containing ~10^9 blood cells, **Figure 1.1B**) prevents important downstream analysis that could provide useful insights into tumor biology and metastasis [8, 15, 16]. More efficient processing of higher volumes of blood in order to obtain a significant number of these cells thus becomes critical and has the potential to establish the role of CTCs as potential biomarkers for early detection of cancer. The vast majority of the background cells (blood cells) contribute to not only challenges in enriching for the target cells (CTCs), but purity issues during downstream molecular analyses [17]. Attempts at increasing CTC concentrations by expanding them after isolation are hardened by viability issues [18]. Hence, the key aspects of any CTC isolation technology should be a high recovery rate without compromising on purity and viability [18]. A plethora of microfluidic technologies have risen to these challenges with promising results. With their help, scientists are now analyzing complex

fluids such as blood *in vitro*, as a means to investigating non-invasive alternatives for cancer detection, patient prognosis and therapeutic monitoring [2].

Approaches toward this endeavor started with the first detection of CTCs from melanoma using reverse-transcription polymerase chain reaction (RT-PCR) [19]. The investigators used PCR to detect the tyrosinase gene, a gene specific to melanoma cells, from blood which was indicative of the presence of melanoma cells [19]. They demonstrated CTC detection in four out of seven melanoma patients. This study opened the arena for future research exploring different methods to sensitively and effectively isolate CTCs.

1.2. Role of microfluidics in CTC studies

Microfluidic devices have had a major impact on the field of CTC research [20]. Such efforts have been facilitated by the automation of labor-intensive experimental processes involved in isolating and characterizing CTCs. As a consequence, the microfluidic field has been gaining pace especially in the handling of rare cells [18, 21]. Different materials ranging from traditional silicon and glass to elastomers have been used for making these devices. The use of poly-dimethylsiloxane (PDMS), an elastomer, has made rapid prototyping an easy and preferred method, leading to widespread use of microfluidic technologies for investigating CTCs [15, 16]. Their smaller dimensions allow precise manipulation of fluid flow in the devices, translating to better control over the cells. The smaller volumes also demand lesser reagents [15]. Following the initial success of using CTC technologies in predicting patient survival [4], many microfluidic CTC isolation technologies [8, 11, 15, 16, 22-27] have been developed to date employing immuno-affinity or physical separation techniques, as they offer a more compact technology with efficient use of resources.

Microfluidics for CTC isolation gained popularity with the reporting of the CTC-chip [8]. Over the years, a large number of similar and innovative microfluidic platforms have come up, each exploiting specific properties of CTCs to separate them from blood cells. The different properties may be biological such as target antigens, or physical such as size, density, deformity [16, 28].

1.3. Separation Principles and Technologies for CTC Isolation

Microfluidic technologies are mainly categorized by their exploitation of CTCs' distinctive (i) biochemical properties or (ii) biophysical properties (**Figure 1.2**). The former is based on the expression of cell surface markers, while the latter includes size, deformability, density, and electric charge [29]. For either of these strategies, it is imperative that developing an optimal CTC isolation method meet the following criteria: (i) high recovery, (ii) high purity of CTCs by removal of contaminating blood cells, and (iii) high system throughput to ensure handling of large sample volumes as expected for clinical settings [18]. Capture or retrieval of CTCs is followed by identification by immunocytochemical staining demonstrating positive signals for Cytokeratin(s) and the nuclear stain DAPI (4',6-diamidino-2-phenylindole), with the absence of the leukocyte marker CD45 [8].

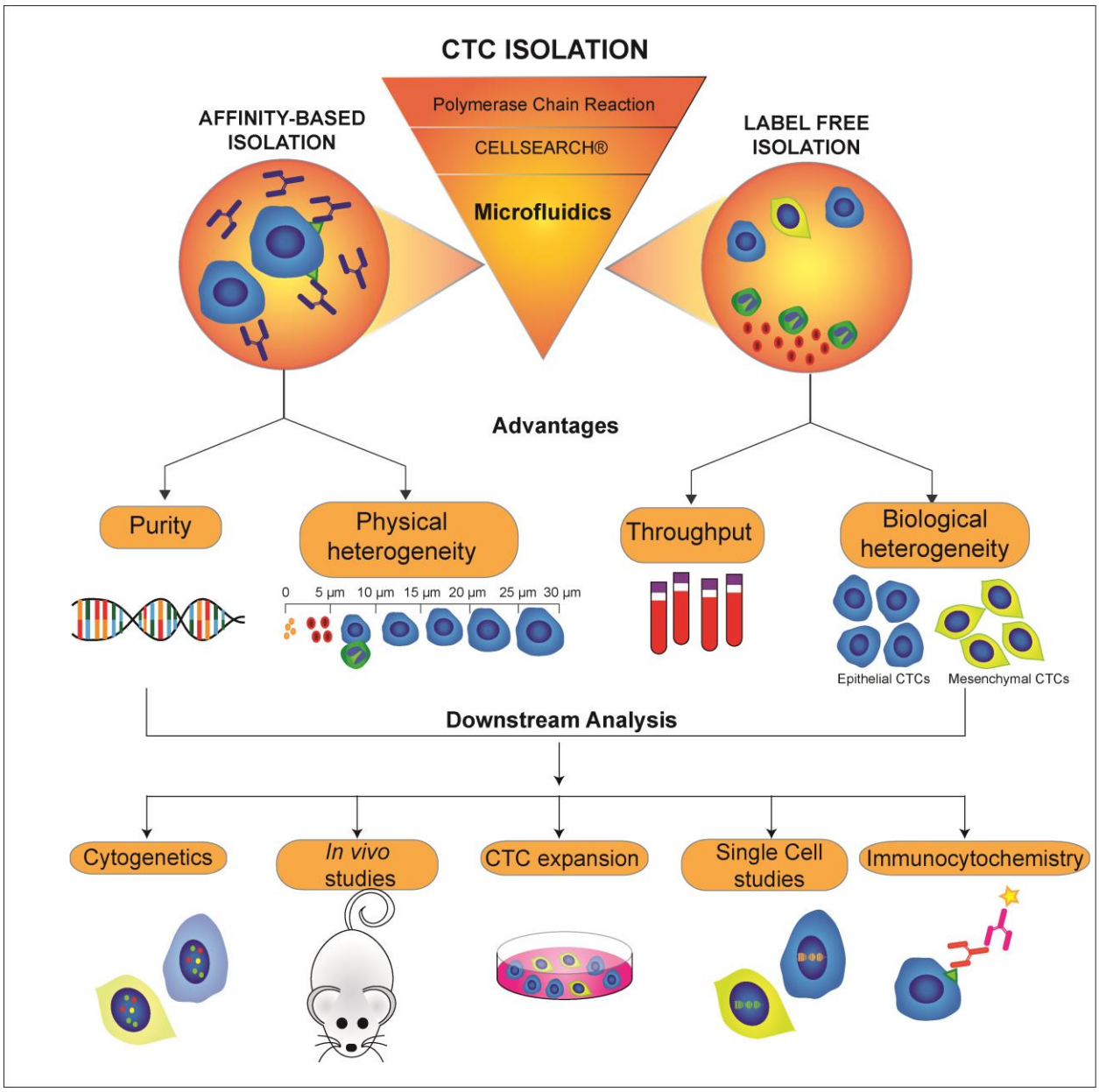

Figure 1.2 CTC isolation methodologies
Figure shows the two most-commonly employed methods of CTC isolation – affinity and size-based. Affinity-based methods utilize antibody-antigen interactions to target CTCs for capture. Size-based methods utilize size differences between CTCs and blood cells for separation. The advantages of each method are listed, followed by potential downstream assays involved in CTC studies.

1.3.1. Affinity-based Isolation of CTCs

Affinity-based isolation, the main principle of technologies such as CellSearch and the CTC-chip [8], make use of the affinity of an antigen to its corresponding antibody. Antigens or surface markers present on the membrane of CTCs are targeted by specific antibodies that can be immobilized onto a solid surface [30]. The antigens (and hence the cell) can grab on to the target antibodies under ideal conditions of affinity-binding. The bound cells can then be separated and/or identified for further assays, depending on their method of capture. The commonly used antigen for CTC capture is the Epithelial Cell Adhesion Molecule (EpCAM), and is considered to be expressed by epithelial cancers [2]. While recent findings have brought into question the utility of EpCAM in identifying the aggressors [31], it still remains the most widely adopted choice of capture antibodies. Combinations of antibodies are also being employed to widen the capture net [31].

The first immuno-capture microfluidic technology for CTCs, the CTC-chip [8] consists of a series of 100 μm tall microposts coated with antibodies against EpCAM, which can interrogate whole blood for capturing CTCs expressing the antigen. The novelty of this technology lay in its ability to capture CTCs from whole blood with high sensitivity and viability [8]. Following this, a number of technologies with varying degrees of sensitivity and purity were developed. The HTMSU device [32], CEE channel [24], Herringbone HB-chip [15], the graphene oxide chip [33], all performing EpCAM-based CTC capture, improved upon the above parameters. The NanoVelcro CTC chip, another recently developed immuno-capture device, makes use of nano-sized structures coated with EpCAM for CTC capture [34, 35]. The GEDI chip developed in 2010 [26] has a similar approach and enabled CTC isolation with an antibody against prostate specific membrane antigen (PSMA). They showed an improved purity over the CTC-chip and

also opened the arena for achieving CTC capture with antibodies other than EpCAM. Different antibodies or antibody cocktails have since been explored to capture different populations that may have been otherwise missed. Galletti *et al.* demonstrated the use of anti-Her2 for studying CTCs from breast and gastric cancer [36]. Yu *et al.* used a mixture of EpCAM, EGFR and Her2 to capture CTCs from breast cancer [37]. Pecot *et al.* used an interesting approach wherein the cells are tagged with a cocktail of antibodies, followed by capture by functionalized microchannels [24, 31].

Immuno-magnetic capture is also a popular method of affinity isolation wherein magnetic beads coated with antibodies are made to bind to cells in order to separate CTCs from WBCs [17]. MACS (magnetic activated cell sorter) is one such technology, that operates by separating cells bound to magnetic beads through a target antibody followed by purification under a magnetic field [38]. Magnetic nanoparticles are also used to label cancer cells through anti-EpCAM to separate them from blood cells with high efficiency at a high flow rate of 10 ml hr^{-1} [39]. Another novel immunological approach was developed by Shi *et al.* in which microbubbles enveloped with anti-EpCAM were used for CTC isolation [35].

Affinity-based capture also holds negative selection under its umbrella, in which the target cells are made to pass through while leukocytes (WBCs) are targeted by antibodies against CD45 [11, 40], and/or CD15 [11]. The advantage of negative selection lies in its capability of isolating CTCs that may or may not express epithelial markers [11]. This approach has been used in the CTC-iChip [11], and by Wu *et al.* [41]. Casavant *et al.* used magnetic beads coated with anti-CD45 as a means of depleting white blood cells as a precursor to CTC enrichment [40]. An *in-vivo* CTC detection technology, the GILUPI CellCollector, employing anti-EpCAM to capture

CTCs in venous blood flow is also an example of a system that demonstrates CTC isolation even under high physiological shear stresses (20 ml min^{-1}) present in the circulation [42].

1.3.1.1. Advantages of Affinity-based CTC Isolation

Affinity-based methods of isolation offer very high specificity of the recovered CTCs since the target CTCs are validated by the capture antigen in addition to identification by immunostaining procedures. The method also enables recovery of an assorted pool of CTCs, regardless of morphological considerations such as size. Whilst many size-based technologies may capture CTCs with high yields, the wide variability of CTC sizes previously reported [16, 35, 43] makes the smaller CTCs highly probable to be missed in size based techniques which are usually biased towards the larger cells. Indeed, CTCs within a patient have been shown to have a wide range of sizes (>4 to 30 um) and many of them may overlap in size with that of the blood cells [16]. Affinity-based methods can indiscriminately capture such size-variable populations, and are also capable of doing the same without the need for preprocessing steps such as dilution or red blood cell lysis, invariably required by physical separation techniques [35]. The specificity also allows for better downstream analysis which may have clinical utility. One such application was demonstrated by Maheswaran et al. who performed downstream sequencing studies on CTCs captured on an affinity platform (the CTC-chip) from lung cancer patients [9].

Affinity capture also allows high purity of the recovered CTCs [26]. Since these cells are rare, any downstream applications are dictated by the accompaniment of contaminating blood cells. The specificity of CTC capture by affinity techniques is also reflected in the retained background cells. The targeted capture not only allows for low non-specific retention but also washes away most red blood cells, eliminating the need for red blood cell lysis as a precursor to blood

analysis. The highly specific and pure CTC yield facilitated by immuno-capture combined with the viability is also conducive to CTC culture and expansion [44].

In order to efficiently study the diverse properties of CTCs, their isolation needs to be tailor-made to answer the relevant biological questions. Immuno-affinity offers a beautiful platform for this purpose as antibody-based capture techniques can be customized to target different subpopulations of CTCs. A combination of antibodies consisting of the traditional anti-EpCAM with another marker, or successive captures with the respective individual antibodies can yield the desired populations [31, 45]. For instance, Riethdorf *et al.* utilized HER2 as a target agent to identify CTCs among patients undergoing neoadjuvant treatment for a HER2 inhibitor [46]. Pecot *et al.* used an interesting cocktail of antibodies to target both epithelial cells and potential CTCs undergoing epithelial-mesenchymal transition (EMT) [31]. Affinity-based capture techniques are thus widely capable of specific targeting of cell subpopulations, an area requiring deeper attention as more and more studies illuminate tumor cell heterogeneity [47].

Affinity based methods also offer high utility with respect to capturing rare events such as CTC clusters [15, 48]. These clusters may sometimes be larger than the detection range of physical separation techniques and/or may clog the channels [49]. CTC clusters are believed to have more metastasizing capability than single cells in the circulation, as shown by Aceto *et al.* [48]. Larger clusters containing a heterogeneous mix of cells may also be captured if some of the cells in the cluster express the target antigen, thereby achieving capture of potentially "unfamiliar" populations using "known" targets. Furthermore, the generally lower shear experienced by cells in immuno-affinity capture [50] also enables collection of CTCs that are possibly circulating in conjunction with platelets. Platelets are believed to be implicated in metastasis and platelet-

enveloped CTCs may be important in disease progression as they are able to evade immune surveillance [48, 51-53].

1.3.1.2. Disadvantages of Affinity-based CTC Isolation

Traditionally preferred for CTC isolation [2], affinity methods have validated their utility in a number of CTC analyses studies. However, they suffer from a few limitations. Throughput is a major concern with antibody-based CTC recovery chips such as the CTC-chip and HB-chip [11]. This is due to the limited shear conditions under which affinity binding occurs [50]. Microfluidic flow-based affinity capture requires optimal velocity and shear conditions for antibody-antigen binding [8, 30]. A very high shear may disrupt any bonds if formed, while a very low shear is conducive to non-specific cell binding [50]. An optimal binding condition would provide adequate capture of target cells, with minimal amount of blood cells retained; in other words, a high efficiency with minimal contamination. These optimal conditions limit the velocity of flow during capture. The CTC-chip and its successors operating on similar principles therefore had an operating flow rate of 1-3 ml hr^{-1} [50]. In the CTC-chip itself, increasing the flow rate from 1 to 3 ml hr^{-1} diminished the capture efficiency [8]. This limits the blood volume that can be analyzed due to the time constraints it places on the experiments. Of late, a number of technologies have overcome the throughput limitation by introducing novel designs to circumvent the issue of optimal binding conditions [50].

Epithelial-to-mesenchymal (EMT) transition, a process in which cells lose their epithelial characteristics and become more mesenchymal, is believed to be an important process hampering the study of CTCs on the basis of EpCAM alone [43]. As these cells undergo the change, their EpCAM expression decreases, and they may be missed by EpCAM targeted capture [43, 54]. These EMT-undergoing cells are believed to be important players in metastasis [54] and may be

able to provide useful information about the dissemination of tumor cells [43]. Combinations of antibodies are therefore being employed to capture not only epithelial cells, but also the mesenchymal ones [31].

Many microfluidic affinity based technologies employ surface modifications for antibody conjugation and immobilization [8]. This poses problems as many of the bonds are irreversible and cannot be easily degraded and/or may affect the viability of these rare cells themselves in the process [55]. Subsequent assays such as single cell analysis and CTC derived xenografts may not be feasible in such cases due to cell release difficulties [55] . Many genetic analyses performed on CTCs thus depend on nucleic acid extraction from the pool of cells captured on these devices, which may create background noise as the captured populations contain impurities such as blood cells [17].

1.3.2. Physical properties based separation of CTCs

The use of physical properties allows a label-free isolation, aimed to overcome biased cell selection using biological-based separation methods. This method tends to exploit the size differences among CTCs and other blood components. More specifically, CTCs are generally considered to have a diameter of 13 to 25 μm in diameter [21], larger than the rest of the blood cells such as leukocytes with diameter ranges from 8 to 11μm [56], and red blood cells (RBCs) with diameters in the range of 5–9 μm [57]. Compared to immuno-affinity based approaches, the biomarker independent CTC isolation technologies are still evolving. While many of these have been optimized with cancer cell lines, few have been validated with clinical specimens. The use of cancer cell lines as a CTC model makes an ideal model for the optimization of a new technology. However, cell lines do not represent the heterogeneous morphology found in clinical

specimens [58]. Some subpopulations of CTCs will indeed be more deformable and smaller than cancer cell lines. Therefore, using cell lines to optimize new technologies may not serve as a true test of efficiency as their clinical utility will only be determined by testing clinical samples [59]. Filtration, hydrodynamic separation, dielectrophoresis and density-gradient separation are major methodologies using physical properties to isolate CTCs.

Size-based Filtration

Membrane filtration is the simplest form of physical separation method, that operates based on cell size and deformability and makes use of constrictions to trap larger CTCs while allowing smaller blood cells to flow through [59]. Membranes typically have pore sizes around 7-8 μm, with a few studies reporting pore sizes of 11 μm [60]. Vona *et al.* proposed ISET (Isolation by Size of Epithelial Tumor Cells), a filtration based technology that uses a polycarbonate membrane-filter [61]. This technology uses 8 μm cylindrical pores to capture CTCs. However, its large variability in CTC capture efficiency and low purity caused by membrane clogging left opportunities for further improvement. Integrating microfabricated filtration membranes into microfluidic devices has since emerged as an optimized approach for CTC separation. Materials such as polycarbonate [62-64], parylene-C [65-67], nickel [68] and silicon [69] have been demonstrated to be appropriate materials to enhance CTC capture. Lin et al. reported a label free parylene membrane microfilter that sampled CTCs from 57 cancer patients, and reported higher sensitivities than the CellSearch system [66]. Lim et al. developed an integrated microfluidic system making use of a microsieve consisting of a dense array of pores that could capture CTCs at high throughput, and was also compatible for fluorescence in-situ hybridization (FISH) analysis of these cells [69]. Since viability of captured CTCs was a concern with filtration based

devices, the ‘separable bilayer microfilter’ developed by Zhou et al. addressed this by a design that was conducive for capture of viable CTCs [70].

Hydrodynamic Separation using Inertial Microfluidics

Hydrodynamic based approaches have shown the highest throughput capability [71]. Recently, inertial migration of particles has been introduced and applied in various studies to achieve high throughput separation based on particle size [72]. Briefly, the particles migrate and are focused in microchannels due to the equilibrium of two inertial lift forces which act on the particles in opposite directions- shear gradient lift force and wall lift force [72]. Some other technologies exploit a secondary flow called Dean flow that takes place in curvilinear channels [73]. Another approach, termed deterministic lateral displacement (DLD), in which microposts are strategically placed to divide the flow into several laminar streams, are also used for separation of CTCs from blood cells [74]. Regardless of the type of hydrodynamic based technologies, the goal is to impart different flow velocities based on cell size differences to separate the target cells with high efficiency. Lee *et al.* developed a lab-on-a disc platform that utilizes centrifugal force to rapidly transfer unprocessed whole blood samples from one chamber to another [75]. The selective isolation of CTCs was achieved through the use of a commercially available track-etched polycarbonate membrane filter on a lab-on-a-disc system. Hou *et al.* developed a spiral microchannel for separation of CTCs using centrifugal forces, a principle known as Dean Flow Fractionation [76]. Sollier *et al.* developed the Vortex Chip, which uses micro-scale vortices and inertial focusing to isolate CTCs [77]. Hyun *et al.* developed a parallel multi-orifice flow fractionation (p-MOFF) device in which contraction/expansion microchannels were placed in a parallel configuration for CTC separation [78]. Warkiani *et al.* developed the trapezoid chip, which uses a trapezoidal design and exploits Dean forces and lift forces to isolate CTCs [79].

More recently, Warkiani *et al.* reported an ultra-high-throughput spiral device [80] consisting of three stacked spiral microfluidic chips with two inlets and two outlets, in which the combination of the inertial and Dean forces focuses the cells at certain equilibrium positions of the channel cross-section.

Dielectrophoresis (DEP)

Dielectrophoresis (DEP) is a CTC isolation method that relies on a cell's dielectric properties where CTCs and other cells are separated from each other depending on their different responses to an electric field [81]. DEP allows the identification of cells with different phenotypes, but is limited by very low throughputs (<1 ml/hr) [82]. Shim *et al.* used a continuous flow microfluidic processing chamber into which CTCs are isolated from clinical samples using a combination of DEP, sedimentation and hydrodynamic lift forces [83].

1.3.2.1. Advantages of Physical Properties based CTC Isolation

Physical CTC separation methods have the potential to address the shortcomings involved in biological marker based separation methods. Overcoming biased cell selection using molecular markers permits heterogeneity studies on CTCs, where different subpopulations can be analyzed. As previously mentioned, CTCs that have undergone EMT are associated with a loss of expression for epithelial markers, such as EpCAM and CK. As a result, the most aggressive cancer cells could potentially be the least likely to be captured and identified using EpCAM based technologies [21, 31].

Isolated CTCs can be analyzed using molecular characterizations. For instance, Shim *et al.* used continuous flow dielectrophoretic field flow fractionation (DEP-FFF) method and also

performed molecular studies on isolated CTCs [83] wherein they showed concordance between the amount of KRAS mutation positive cells and the proportion of cytokeratin positive cells. Warkiani *et al.* performed DNA fluorescence *in situ* hybridization (FISH) to evaluate the HER2 status of isolated CTCs from breast cancer patients using their trapezoid chip [84, 85].

Unlike most immuno-affinity based isolation systems which only allow on-chip growth of CTCs [44] due to difficulties in post-separation retrieval [55], inertial-based technologies simplify CTC culture by using off-chip standard cell culture techniques since cells can be recovered in suspension. This advantage gives rise to multiple CTC expansion approaches, such as the use of extracellular matrix (matrigel or collagen) for CTCs growth or a 3D culture system [44]. Sollier *et al.* showed that A549 cells processed with the Vortex Chip and collected in a well-plate proliferate over 3 days [86]. Similarly Hou *et al.* used their device to demonstrate this advantage by successfully culturing sorted MCF-7 cells for 5 days [35]. Moreover, they also show the retrieval of intact MCF-7 cell clusters. Despite the high throughput of the label free devices, these technologies are still able to preserve cell clusters, which are of greater interest to study the metastatic ability of CTCs [48, 87].

1.3.2.2. Disadvantages of Physical Properties based CTC Isolation

Physical or label free CTC isolation methods have gained popularity only recently in CTC studies. While technologies are still evolving, it is notable that physical separation methods suffer from certain limitations. The primary drawback stems from the hypothesis of differential sizes of CTCs and blood cells. Although on average CTCs are shown to be larger than leukocytes, there is a significant overlap in the size of CTCs and leukocytes that may hinder label-free separation efforts. It is now known that CTCs as small as 4 μm may be detected [16].

Marinnucci *et al.* also reported findings on CTCs that were the same size or smaller than leukocytes [88]. This variability in size can cause the loss of CTCs or, to overcome such problem, low sample purity. Although greatly studied, filter-based approaches encounter clogging difficulties when processing large sample volumes [89]. Moreover, high flow rates and the need for prior fixing may also prevent downstream studies such as expansion and gene expression analysis, which require cells to be viable [70]. Cell viability also remains a concern with the high pressures exerted in filtration based CTC recovery [70]. CTC clusters, which have clinical implications due to their higher metastatic ability, may also be missed by the size restricted separation technologies as clusters may clog channels or get trapped elsewhere [49]. Dielectrophoresis (DEP) methods generate gases such as hydrogen and oxygen in addition to high temperatures by Joule heating which may diminish cell viability [90].

1.4. The Future of CTC Technologies

Both affinity and size-based methods of CTC isolation need dramatic improvements to their systems to enable highly efficient CTC recovery [17]. Affinity isolations have the potential to provide key information that may be missed by size-based techniques as outlined in their advantages above. Refinements such as increasing throughputs, targeting multiple populations with the use of multiple antibodies may be the important steps needed to further improve these technologies. Use of biomaterials and reversible conjugation of antibodies that may enable CTC release will offer more robust CTC analysis modules, as these CTCs can then be utilized for downstream assays [55]. Using immuno-capture methods, different populations of CTCs can be segregated for further analysis that may be able to identify tumorigenic CTCs, such as xenograft studies [91]. As for label free technologies, their future is driven by exploiting the physical

differences between CTCs and leukocytes, with the goal of achieving selective separation of CTCs. For example, cell deformability can be combined with CTC size properties to develop new label free technologies [59]. Regardless of the technological approach, emerging technologies should not compromise throughput or sensitivity, while still targeting heterogeneous CTCs.

Past the improvement upon current microfluidic technologies, we predict an increase in effort on the molecular understanding of CTCs, encompassing multiple downstream analyses that advances personalized treatment. The comprehensive investigation of CTCs is hampered by their low numbers, making this one of the biggest challenges in this field [18]. For better understanding of CTCs, there needs to be an increase in technologies that not only aim for the isolation of such cells, but also to perform *in situ* expansion on such devices. For example, Zhang *et al.* expanded CTCs from early lung cancer patients using a co-culture 3D device that uses cancer associated fibroblast and a combination of collagen and matrigel to resemble the tumor microenvironment [44]. Recently, several groups have successfully performed *ex vivo* expansion of CTCs from breast cancer [92] and from colon cancer [93]. Overcoming the limitation of low numbers of CTCs by expanding them will allow for phenotypic and genomic characterization of CTCs, which in turn will lead to personalized treatment strategies. The establishment of cell lines from cancer patients could guide the course of drug therapy at an individual level to ensure optimal treatment outcome [94, 95].

Heterogeneity among CTCs makes their isolation and characterization a challenging task. The molecular characterization of CTCs has revealed indications of the genotype and phenotype of these tumor cells and demonstrated a striking heterogeneity of CTCs [96]. Thus, the present setback is the identification of the functional properties of the different CTC subsets. This could

be achieved through the use of functional assays that reveal the biology of CTCs, with particular emphasis on the discovery of the most aggressive subset of CTCs. At present, such assays are limited by the very low concentration and yield of CTCs. Single cell studies could serve as an essential tool to assess the heterogeneity among CTCs. The study of single CTCs by their molecular characterization provides high clinical relevance by potentially aiding in early cancer detection and revealing new therapeutic targets for personalized medicine [97].

While CTC enumeration has shown tremendous potential in terms of clinical utility [98], researchers are now exploring their validity as more than just an enumerable measure of disease intensity or spread. The prognostic and diagnostic utilities of CTCs are now an area of extensive focus through analysis of gene expression profiles [99], single cell analysis [100], RNA and DNA studies [9, 101], and cytogenetics to detect gene amplifications or rearrangements [102, 103]. Examining epigenetic modifications and their after effects on the metastatic cascade may be a useful tool for determining therapeutic efficacy. Chimonidou *et al.* analyzed CTCs and cell-free DNA in breast cancer for methylation of a tumor suppressor gene SOX17 promoter [104]. In another study of breast cancer, methylation of a metastasis suppressor gene was studied in primary tumor and CTCs, and the authors investigated its effect on survival [105]. Whilst the rarity of CTCs offers challenges in enrichment and downstream assay feasibilities, cell free DNA suffer from similar limitations with respect to available amounts [106]. Malara *et al.* identified CTC subpopulations that are enriched for methylated DNA using folate receptors. Methylation of cancer cells is believed to be implicated in metastasis, and the authors found that patients with high methylation of CTCs had a risk of relapse [106]. Albeit CTC enumeration has seized attention as a possible endpoint in clinical trials due to their prognostic utility [46], a comprehensive analysis of the genome and epigenome will likely compliment traditional

diagnostic methods and open the arena for more frequent patient monitoring, leading to timely decision making. This also has the potential to circumvent invasive tissue biopsies [8]. CTCs also offer a means of personalized therapeutics through their tumorigenic capabilities [91]. CTC expansion on in vitro microfluidic models, one of which has recently been demonstrated by our group [44], propose a method for testing of drugs or drug combinations [91, 92], which can be used to make quicker decisions for therapeutic management. Resistance to treatment can be monitored similarly by analyzing CTCs [9]. The idea that all of the above could possibly be accomplished through venipuncture, a relatively low discomfort means to achieving a higher end, in a field as vast and challenging as cancer management, is both an exciting and formidable notion. The future of CTCs thus looks promising toward patient-specific tumor monitoring.

1.5. Microfabrication and Lithography

Since the success of the semiconductor industry, microfabrication has been employed widely in the manufacturing of microfluidic devices. Silicon and glass have widespread applications as suitable materials for microfabrication, and more recently, polymers have proven to be more economical for the microfluidics industry [107]. Polymers such as poly-dimethyl siloxane (PDMS) and poly-methyl methacrylate (PMMA) have been employed in a variety of microfluidic cell sorting applications due to their

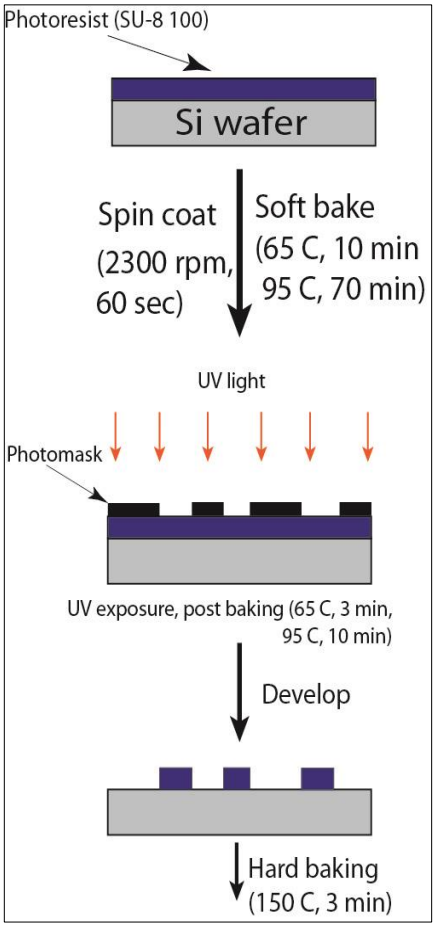

Figure 1.3 Photolithography
Figure shows a negative photoresist (SU-8) spin coated onto a silicon wafer followed by baking and exposure through a photomask, and developing to achieve the desired pattern.

low cost and rapid prototyping [107, 108]. PDMS is a popular choice of material due to various properties such as optical transparency, biocompatibility and ease-of-use [107, 108].

Silicon master molds can be used to create templates for PDMS molding by the process of photolithography (**Figure 1.3**) [109]. The master molds are fabricated in a clean room environment. A photoresist is spin-coated onto a silicon wafer, following by baking and UV exposure through a pattern (photomask). Depending on the type of photoresist, exposed or unexposed areas polymerize forming the desired pattern [110]. Photoresists can be positive resists, where the UV exposed region gets polymerized to form structures, or negative resists, where the unexposed regions create the structured patterns [111]. The patterns can then be used to create PDMS channels by soft lithography [109].

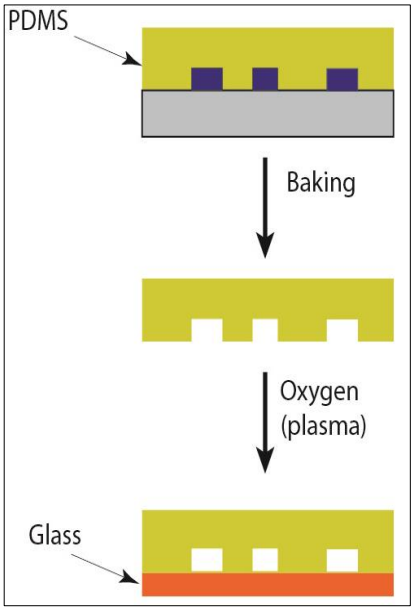

Figure 1.4 PDMS bonding
The silicon master mold is used to create PDMS molds, which are bonded to the substrate (glass) by plasma bonding.

PDMS can be prepared by mixing two liquid components- a base and a curing agent followed by curing to generate a solid polymer. PDMS can be bonded to substrates either by reversible methods using van der Waals interactions, or irreversibly by tuning its surface properties. The surface of PDMS can be altered by various techniques that change its hydrophobicity which can be adapted to introduce various

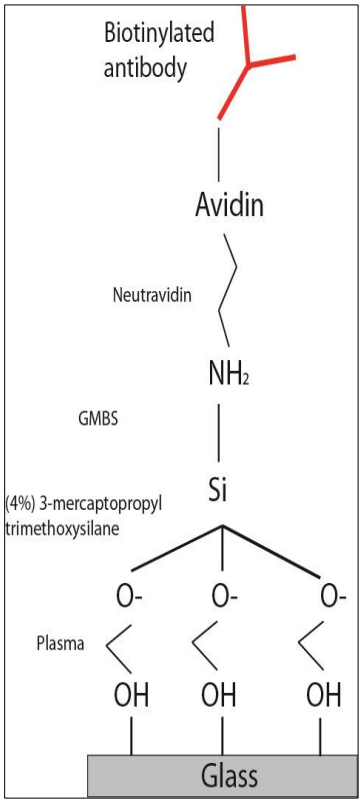

Figure 1.5 PDMS surface modification
Antibodies can be immobilized on PDMS by silanization

functional groups on its surface. One such technique is plasma activation (**Figure 1.4**), where the surface of PDMS and the substrate (glass or PDMS) are exposed to oxygen plasma that produces silanol groups, which can then seal irreversibly to the substrate. The activated surfaces can then be modified by silanization for attachment of the biomolecule avidin **(Figure 1.5)**. This can then be used for immobilization of biotinylated-antibodies through avidin-biotin covalent binding [112].

1.6. Conclusion

Circulating tumor cells (CTCs) have thus been widely recognized as a non-invasive cancer monitoring tool, with current studies exploring their biology in depth [2]. Clinical trials are also underway to investigate their utility as biomarkers for therapeutic efficacy [46]. Microfluidics provides an efficient and economic platform, with control over cells on microscale dimensions, which makes for delicate processing of rare cells such as CTCs [15]. Microfluidic devices also show higher sensitivity of CTC analyses [2] in comparison to macroscale technologies. We have thus chosen to develop a microfluidic device for CTC capture using affinity-based isolation, due to the higher specificities offered by targeting cell surface antigens [50]. In order to interrogate larger volumes of blood and increase CTC yields, the goal is to develop an affinity-based microfluidic device that can operate at high-throughputs. Once achieved, the device will be tested for applicability to detect CTCs in early lung cancer.

Chapter 2

Development of a high-throughput radial flow microfluidic device for affinity-based CTC capture

2.1. Abstract

Circulating tumor cells (CTCs) are believed to play an important role in metastasis, a process responsible for the majority of cancer-related deaths. But their rarity in the bloodstream makes microfluidic isolation complex and time-consuming. Additionally the low processing speeds can be a hindrance to obtaining higher yields of CTCs, limiting their potential use as biomarkers for early diagnosis. Here a high throughput microfluidic technology, the OncoBean Chip is reported, which employs radial flow that introduces a varying shear profile across the device enabling efficient cell capture by affinity at high flow rates. The recovery from whole blood was validated with cancer cell lines H1650 and MCF7, achieving a mean efficiency >80% at a throughput of 10 mL hr^{-1} in contrast to a flow rate of 1 mL hr^{-1} standardly reported with other microfluidic devices. Cells were recovered with a viability rate of 93% at these high speeds, increasing the ability to use captured CTCs for downstream analysis. Broad clinical application was demonstrated using comparable flow rates from blood specimens obtained from breast, pancreatic and lung cancer patients. Comparable CTC numbers were recovered in all the samples at the two flow rates demonstrating the ability of the technology to perform at high throughputs.

2.2. Motivation

Affinity-based microfluidics operate at low flow rates (1-3 mL hr^{-1}) due to shear constraints at high flow rates that may rupture antibody-antigen bonds. The CTC-chip [8, 113] that captures epithelial cancer cells circulating in blood at an operating flow rate of 1 mL hr^{-1} by using anti-Epithelial Cell Adhesion Molecule (anti-EpCAM) coated on microposts, was the first successful immuno-affinity based microfluidic platform. Subsequently, a second generation platform was developed, known as the Herringbone -Chip (HB-Chip) with a design flow rate of 1.5-2.5 mL hr^{-1}[15]. Gleghorn et. al. developed a geometrically enhanced differential immunocapture (GEDI) device that manipulated the flow dynamics around microposts to capture CTCs with high purity at a throughput of 1 mL hr^{-1}[26]. The high throughput microsampling unit (HTMSU) designed by Adams et. al. was an integrated device that could both isolate and enumerate CTCs from 1 mL of blood in about 37 min [32]. Many aptamer based technologies were also designed to improve the specificity of capture. One such device was developed by Sheng et al. with a higher flow rate of 600 nL s^{-1} (or 2.16 mL hr^{-1}) [22]. In 2011, Dickson et al. introduced a device that studied cell lines with different antigen densities for capture at 18 µL min^{-1} (1.08 mL hr^{-1}) [24]. Higher throughputs of isolation have been achieved in subsequent years. An immunomagnetic separation device with a throughput of 10 mL hr^{-1} was developed by Hoshino et. al. in 2011[39]. While the throughput is significant for an affinity-based CTC isolation, the sample pre-processing steps such as dilution and centrifugation may lead to cell loss [39, 114]. Mittal et. al. developed a permeable affinity-capture device operating at 6 mL hr^{-1} [30] which was subsequently multiplexed to increase throughput [115].

More recently, two new integrated platforms were brought forth for CTC isolation. Liu et al. introduced an integrated device that separates blood cells and CTCs by deterministic lateral

displacement, followed by an affinity-based enrichment [25]. The CTC-iChip by Ozkumur et. al. combines inertial focusing with affinity-based capture employing both positive and negative selection [11]. The device works by magnetically labeling cancer cells in whole blood, followed by a series of separation steps involving deterministic lateral displacement, inertial focusing and magnetic separation [11]. While both these technologies showed a high throughput, 9.6 mL hr^{-1} and 140 µl/min (or 8.4 mL hr^{-1}) respectively [11, 25], the need for multiplexing and pre-processing of blood samples is cumbersome. Labeling of cells in whole blood may also compromise the purity of isolation [11]. Processing higher volumes of blood becomes critical from a clinical standpoint as technologies are becoming geared toward single cell mutational analysis of CTCs to monitor patient status [12, 13, 116]. Thus, despite advances in the field, a need exists to further improve microfluidics platforms to efficiently monitor and analyze CTCs with minimal pre-processing of blood to preserve these rare cells.

In the exploration for such a device that ensures specificity through antibody-based methods without compromising the volume of blood processed, we developed a radial flow model in contrast to current microfluidic affinity-based capture devices that employ linear flow. We hypothesized that the constant velocity across every cross-section experienced in linear flow based devices is a major limitation for effective capture of cells at higher flow rates. Radial flow provides an alternative to overcome this drawback as the velocity decreases with increasing cross-sectional area, thereby providing varying shear rates across the radius. Cells would thus experience different shear rates at every radius and would get captured at an optimal shear rate that would be determined by their surface antigen expression. A high surface area for capture was also achieved by designing a bean-shaped micropost with its concave side toward the incoming flow.

We hereby report a radial flow microfluidic device, the OncoBean Chip, inspired by the CTC-chip [8] that efficiently isolates CTCs in one step at high flow rates using an affinity reaction between the Epithelial Cell Adhesion Molecule (EpCAM) antigen expressed by epithelial tumor cells and anti-EpCAM coated on bean-shaped microposts on the microfluidic chip. The OncoBean Chip **(Figure 2.1)** is designed to operate at a flow rate of 10 mL hr^{-1}, capturing rare CTCs through a radial flow design that provides varying shear across the device for optimal capture conditions even at high flow rates.

2.3. Materials and Methods

2.3.1. Finite Element Simulations

Finite element simulations were performed in COMSOL Multiphysics 4.2 (Comsol Inc.) with an inlet flow rate of 10 mL hr^{-1} on a 6 mm radial section and 30° arc of the proposed device. Navier-Stokes equations for incompressible fluid flow were used for the study. A symmetry boundary condition was applied on the two similar boundaries flanking the posts. Wall (no slip) boundary condition was applied on the post outlines. The particle tracing plot was simulated with rigid particles 15 μm in size, with a condition of sticking to any encountered wall being applied.

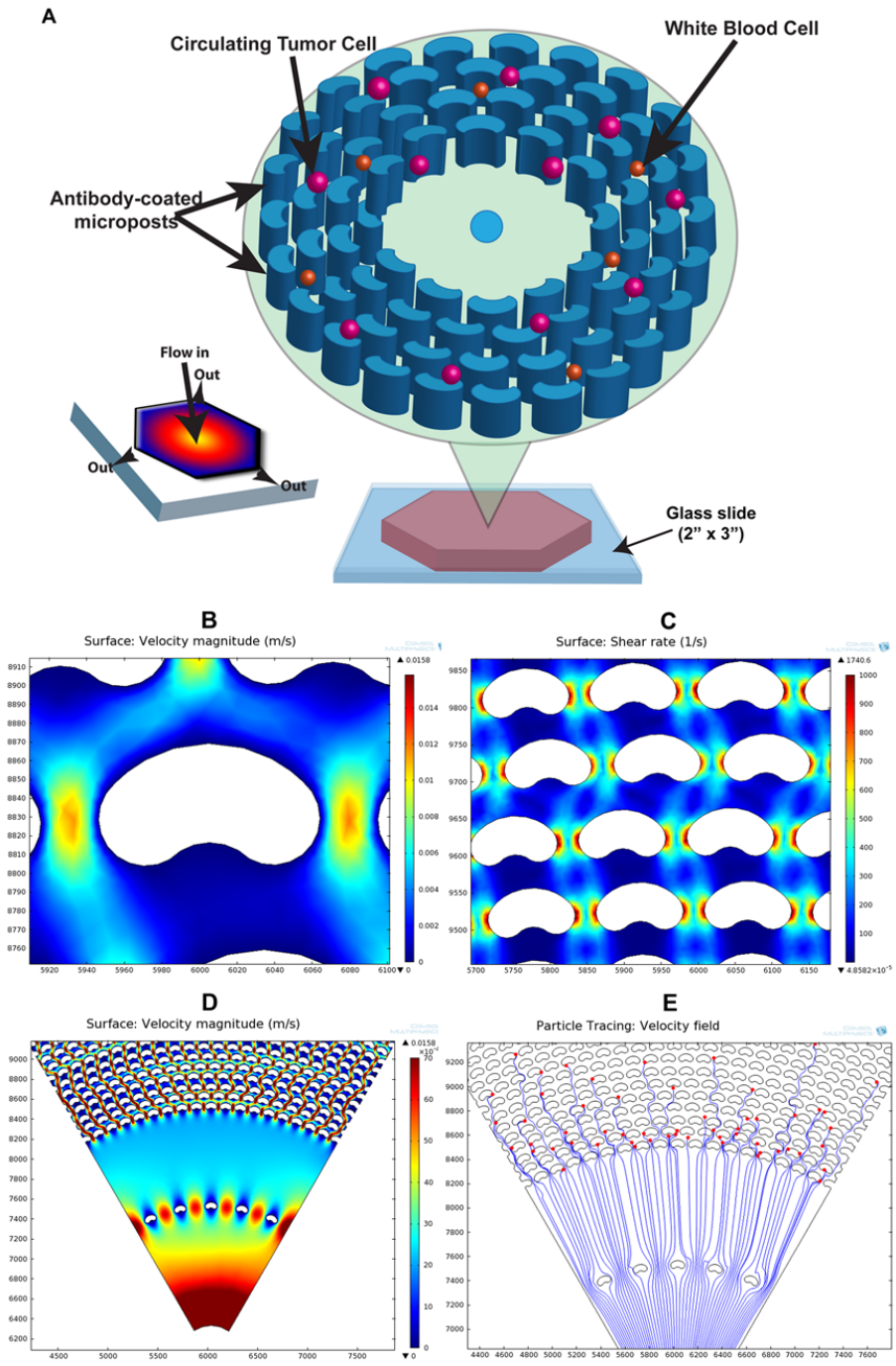

Figure 2.1 Schematic of OncoBean Chip and finite element simulations
(A) Schematic representation of the OncoBean Chip shows cancer cells (pink) being captured on antibody coated bean-shaped microposts. Inset shows a flow profile representation with velocity decreasing from red to blue. Finite element simulations on a section of the OncoBean Chip show (B) velocity magnitude of flow around a single post (magnified image) and flow converging behind the post, (C) surface plot of shear rate around the posts indicating slowing down of flow near the post face (concave side) (D) velocity magnitude profile across posts near the inlet (bottom arc) (E) particle tracing plot around microposts near the inlet demonstrating typical streamlines (blue) and capture of 15 µm rigid particles (red) upon encountering a wall (post). Flow occurs from bottom toward top in these images.

2.3.2. Device fabrication

The design was prepared using AutoCAD software with the following dimensions: bean width 50 µm, arc angles 90°, adjacent (lateral) post spacing 25-32 µm. The design was converted to a photomask (FineLine Imaging) and used to prepare a mold by traditional photolithography. Briefly, a negative photoresist SU-8 100 (MicroChem Corp) was spin coated onto a silicon wafer at 2350 rpm. This was followed by soft baking at 65 °C for 10 min and 95 °C for 70 min, and then UV exposure of the pattern onto the wafer for 15 sec. Post exposure baking was done at 65 °C for 3 min and 95 °C for 10 min and the pattern was developed in SU-8 developer. The wafer was then hard baked at 150 °C for 3 min. A post height of 100 µm was achieved. Poly-dimethoxysilane or PDMS (Ellsworth Adhesives) was prepared in a monomer to curing agent ratio of 10:1 and baked overnight after degassing. The PDMS was peeled from the master mold, cut and prepared for surface modification.

Each PDMS chip was bonded onto a glass slide using plasma bonding. 3-mercaptopropyltrimethoxy silane (Gelest) was infused and incubated for 1 hour. This was followed by washing with ethanol and addition of N-gamma-Maleimidobutyryloxy-Succinimide (GMBS) (Thermo Fisher Scientific), a cross linking agent for 30 mins. The devices were washed again and Neutravidin (Invitrogen-Life Technologies Inc.) was added and the devices were stored at 4 °C. Before experiments, the devices were incubated with biotin-conjugated anti-EpCAM (RnD Systems).

2.3.3. Cell culture

Human lung cancer cell line H1650 and human breast cancer cell line MCF7 were cultured in RPMI-1640 and DMEM (Invitrogen - LifeTechnologies, Inc.) respectively. The media were

supplemented with 10% fetal bovine serum (Invitrogen - LifeTechnologies, Inc.). Both additionally contained 1% antibiotic-antimycotic solution. Cells were grown at 37 °C and 5% CO_2 and medium was renewed every 2-3 days. Cells were passaged with 0.05% Trypsin - 0.53 mM EDTA (Invitrogen - LifeTechnologies, Inc.).

2.3.4. Cell capture and analysis

The cells were harvested with 0.05% Trypsin - 0.53 mM EDTA and labeled with CellTracker Green fluorescent dye (Invitrogen - LifeTechnologies, Inc.). They were counted with a hemocytometer and spiked into healthy blood or serum free medium. Informed consent was obtained from all healthy blood donors. The devices were incubated with anti-EpCAM prior to experiments. 3% bovine serum albumin (Sigma Aldrich) was used as a blocking agent to reduce non-specific binding. Two of the three outlets in the device were looped in order to increase the resistance and thereby the residence time of the fluid in the device. The fluid spiked with known number of cells was then processed through the device at the respective flow rates. This was followed by washing with phosphate buffer saline (PBS) and fixing and permeabilizing with BD Cytofix/Cytoperm (BD Biosciences). DAPI (4',6-diamidino-2-phenylindole) (Invitrogen - LifeTechnologies, Inc.) was then applied to stain the nucleus followed by a last washing step. The devices were stored at 4 °C until visualization with Nikon Eclipse Ti fluorescence microscope.

Statistical analysis was performed with the software OriginPro 9.0. A standard two-sample t-test was used for comparison between the groups.

2.3.5. Blood Collection and Analysis from Cancer Patients

Informed consent was obtained from all donors. Whole blood from cancer patients was processed through the OncoBean Chip at the designated flow rates in equal volumes, followed by washing with phosphate buffer saline. The cells were fixed with 4% paraformaldehyde and refrigerated at 4 °C until immunofluorescent staining. Before staining, the cells were permeabilized with 0.2% Triton-X 100, followed by blocking with 2% goat serum in 3% bovine serum albumin. Primary antibodies anti-Cytokeratin 7/8 (BD Biosciences) and anti-CD45 (BD Biosciences) were applied in 1% bovine serum albumin for all samples with the exception of pancreatic cancer specimens where anti-Cytokeratin 19 (SantaCruz Biotechnology Inc.) and anti-CD45 (SantaCruz Biotechnology Inc.) were used. After a quick wash, secondary antibodies AlexaFluor 488 and AlexaFluor 546 or 568 (Invitrogen-Life Technologies Inc.) were applied in 1 % bovine serum albumin. DAPI was applied as the final step before microscopic imaging.

2.3.6. Cell Viability Assay

H1650 cells were harvested and spiked into serum free RPMI 1640 and processed through the OncoBean Chip at 10 mL hr^{-1}. The live/dead reagent consisting of calcein AM and ethidium homodimer-1 (Invitrogen - LifeTechnologies, Inc.) was prepared as specified by manufacturer and applied to the cells in the device. Following 15 min of incubation, several fields of view were microscopically imaged under 10 x magnification.

2.4. Results

2.4.1. Engineering Design and Flow Characteristics in OncoBean Chip

The design of an optimal capture platform with structures relies largely on channelizing the flow in order to have maximum cell contact with functionalized post surfaces. Reducing the flow

separation is one way to increase the contact of the cell with the post surfaces, thereby increasing the chance of capture. A circular micropost as in the CTC-Chip [8] shows a large flow separation behind the post and the area behind the flow remains largely unused for capture. To overcome this, we hypothesized that a bean-shape would provide a better flow utilization for capture. The flow dynamics of a series of different designs of bean-shapes that varied by arc angles and length, followed by a qualitative estimate of boundary layer thickness from fluid simulations was performed using COMSOL Multiphysics 4.2 software.

The OncoBean Chip was designed with bean-shaped posts conceived from an arc angle of 90°, with the structures measuring 50 µm wide and 118 µm along the longest axis. The posts were placed 25-32 µm apart in polar arrays, with subsequent arrays being rotated to introduce interjection of flow. **Figure 2.1B, C, D** demonstrate velocity magnitude and shear rate profiles on simulated sections. As was expected, for a flow rate of 10 mL hr^{-1} the simulations predicted maximum velocity (0.0158 m/s) for the simulated inlet dimensions and a decreasing trend on moving radially outward as the cross sectional area increased. Similar to the velocity profile, the shear rate decreased on moving toward the outlets. This continuous decrease in shear even at a high flow rate of 10 mL hr^{-1} makes it feasible to capture cells with a heterogeneous expression of antigens. A particle trajectory was also simulated to predict hydrodynamic efficiency and to observe streamline paths. The plot (**Figure 2.1E**) shows 15 µm rigid particles and their corresponding streamlines as the particles navigate around the post structures (walls). The simulation predicted 94.3% of particles (33 of 35 particles sent) interact with bean posts within the first 600 µm array of dense posts, with the remaining 2 particles being interjected at other post regions. The simulation thus indicated a high hydrodynamic efficiency and a good streamline trajectory with sufficient cell-post interaction for a sensitive capture.

2.4.2. Optimization of OncoBean Chip for Cancer Cell Capture

The OncoBean Chip was optimized for capture with the epithelial lung cancer cell line H1650 with anti-EpCAM as the capture antibody. Capture efficiency was calculated as the percentage of captured cells on the device to the total number of cells sent, normalized against the OncoBean Chip 1 mL hr^{-1} to account for cell spiking errors. Briefly, fluorescently labeled H1650 cells were spiked into healthy blood at a concentration of 1000 cells mL^{-1}. To validate the effectiveness of the OncoBean Chip against a standard affinity-based microfluidic device, the OncoBean Chip was compared with a PDMS based version of the CTC Chip (henceforth referred to as the CTC Chip). The following conditions were analyzed: OncoBean Chip 1 mL hr^{-1}, OncoBean Chip 10 mL hr^{-1}, CTC Chip 1 mL hr^{-1} and CTC Chip 10 mL hr^{-1}. Upon comparison of performance with the CTC Chip, the OncoBean Chip showed high capture efficiencies with mean yields of 100% and 82.7% at both 1 mL hr^{-1} (n=4) and 10 mL hr^{-1} (n=4) respectively (**Figure 2.2A**), in close agreement with the mean capture yield of 90.7% obtained in the CTC Chip at 1 mL hr^{-1}.

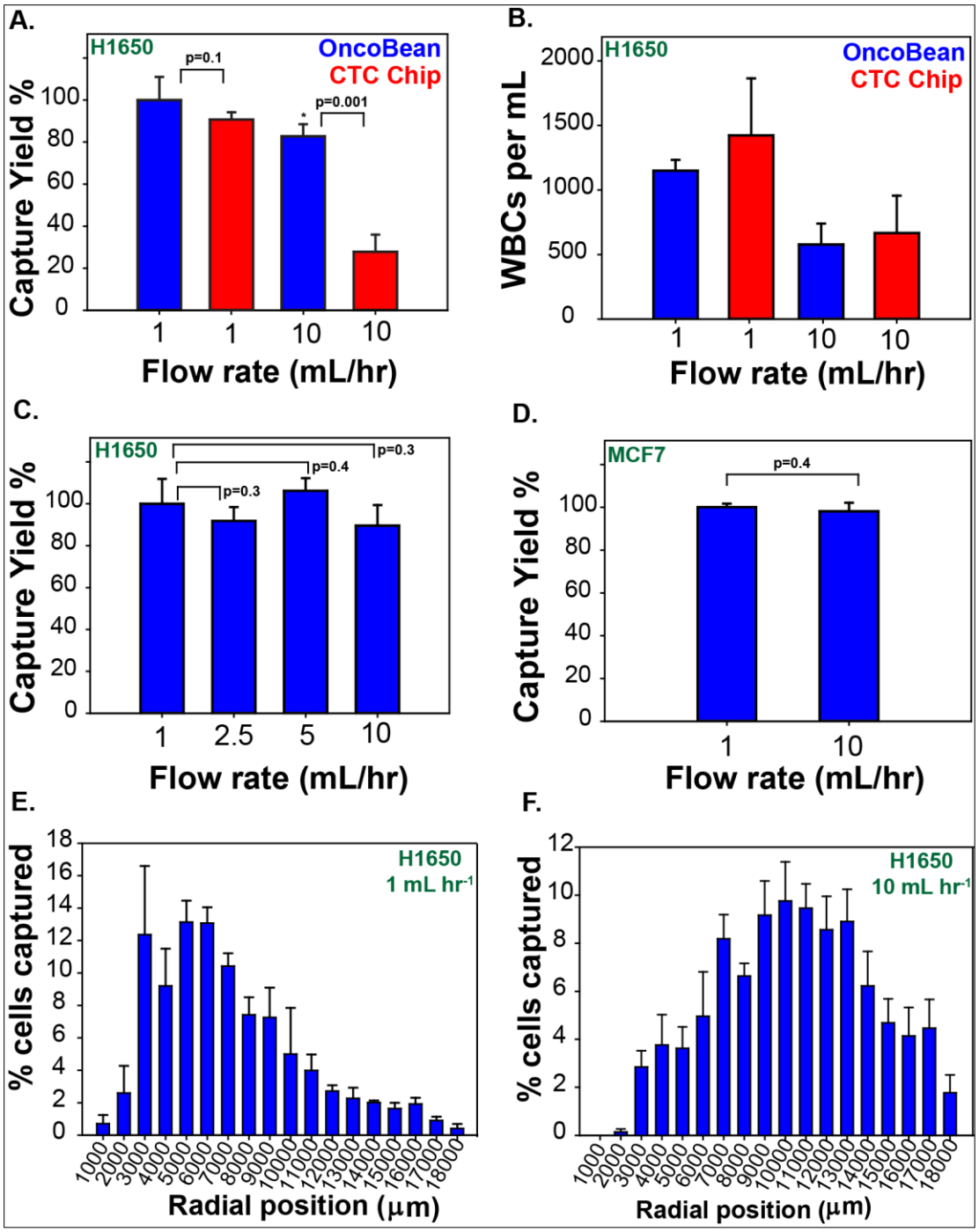

Figure 2.2 Optimization of capture efficiency of the OncoBean Chip

(A) Comparison of H1650 cell capture from whole blood between OncoBean Chip vs CTC Chip at 1 and 10 mL hr^{-1} normalized to OncoBean Chip at 1 mL hr^{-1} (B) Non-specific white blood cell capture for the experiment in (A) represented as the number of white blood cells per mL of whole blood. (C) Effect of flow rates on capture of H1650 cells spiked into whole blood by the OncoBean Chip shows capture yields at 1, 2.5, 5 and 10 mL hr^{-1} (D) Capture of MCF7 cells from whole blood by the OncoBean Chip at 1 and 10 mL hr^{-1} (E) and (F) show capture profile or position of H1650 cells captured from serum free medium across different radial distances along the OncoBean Chip at 1 mL hr^{-1} and 10 mL hr^{-1} respectively.

On the other hand, the high capture rate achieved by the CTC Chip at 1 mL hr^{-1} dropped to a mean rate of 27.8% with the same chip at a flow rate of 10 mL hr^{-1} (n=3). This greater than 3-fold drop can be explained by the linear flow profile in the CTC Chip, which may not be conducive for capture at high flow rates due to the high velocities present constantly throughout the device. The OncoBean Chip combats this in its radial flow design as there is a continuous drop in the velocity on moving outward.

The effect of flow rates on the capture efficiency in the OncoBean Chip was tested under four conditions: 1 mL hr^{-1}, 2.5 mL hr^{-1}, 5 mL hr^{-1} and 10 mL hr^{-1} on anti-EpCAM coated devices to test the robustness of the capture platform at different velocities. As seen in **Figure 2.2C** the capture efficiency had no significant drop on increasing the flow rate from 1 to 10 mL hr^{-1}, with the mean capture yield being greater than 80% at all the above flow rates. The lowest mean capture efficiency was 89.5% at 10 mL hr^{-1} indicating a high yield even at this maximum flow rate. A similar trend in efficiency is observed in the absence of other cells, as is seen in the capture of H1650 cells spiked into serum free medium. The OncoBean Chip recovery was also tested with the breast cancer cell line MCF7, and the device achieved a mean capture yield of 98% at 10 mL hr^{-1} normalized against the same device at 1 mL hr^{-1} at a spike concentration of 1000 cells mL^{-1} (**Figure 2.2D**). This data suggests that it is possible to obtain similar recovery of CTCs with a process that is 5-10 times faster than many standard affinity isolation methods.

2.4.3. Capture Purity

Non-specific background blood cells are a major hindrance during molecular analysis of CTCs and it is essential not only to achieve effective CTC isolation, but also minimal contamination of these background cells. The purity of capture in the OncoBean Chip was determined by

measuring the number of white blood cells (WBCs) per mL of whole blood captured on the device. Due to variations in WBC counts between different donors, a purity percentage was not calculated; a relative comparison caused by increase in flow rates was performed. As shown in **Figure 2.2B**, the high flow rates tend to have an advantageous effect on reducing the non-specific capture of contaminating WBCs, with a 2-fold drop in the WBC count at 10 mL hr^{-1} compared with 1 mL hr^{-1} (OncoBean Chip: 1 mL hr^{-1} range 1060-1240 cells per mL, 10 mL hr^{-1} range 390-740 cells per mL, CTC Chip: 1 mL hr^{-1} range 930-2010 cells per mL, 10 mL hr^{-1} range 330-850 cells per mL). This may be attributed to the high velocities at high flow rates which reduce the residence time for binding of these cells. The non-specific cell numbers show large variation in capture between the OncoBean and CTC Chips but they indicate similar trends between the flow rates suggesting that the radial gradation in shear does not increase non-specific white blood cell capture.

2.4.4. Cell Capture Profile

The varying shear stress model proposed in the OncoBean chip suggests there are differential regions of capture on the OncoBean, dependent on antigen density. For a given flow rate, capture of a high EpCAM expressing cell would require less residence time for binding than a low EpCAM expressing cell [30, 31, 117]. This translates to distance traversed within the device, or the number of antibody-coated posts encountered by the cell. At low flow rates, the cells would be captured within a small distance into the device due to the radial drop in shear in addition to the already-low shear rates. At high flow rates, a larger capture distance is required as the velocity needs to slow down sufficiently for the cells to bind. To test this hypothesis, H1650 cells were spiked into serum free medium and captured at 1 mL hr^{-1} and 10 mL hr^{-1}. The cells captured were manually counted at 1000 μm radial intervals. The capture profile plot (**Figure**

2.2 E, F) shows the distribution of captured cells along various radial positions in the OncoBean Chip. It was observed that with H1650, a cell line with high EpCAM expression (greater than 500,000 antigens per cell) [8], most cells are captured within the first half radius of the device at 1 mL hr^{-1} (**Figure 2.2E**), while the capture is more widespread at 10 mL hr^{-1} (**Figure 2.2F**), utilizing a larger area of the device at the higher flow rate. This was in accordance with our predictions. A similar capture profile was observed for MCF7 cells as well.

2.4.5. Cell Viability at High Flow Rates

For optimal use of microfluidic platforms to capture CTCs, cell viability is an important readout as it determines the feasibility of performing critical downstream assays on CTCs, such as genetic profiling [18]. Since high flow rates can induce high shear rates which can be detrimental to cell health [8], the cell viability was assessed in the OncoBean platform using the Invitrogen Live/Dead Assay. Briefly, H1650 cells were spiked into serum free medium and processed through anti-EpCAM coated OncoBean Chip at a flow rate of 10 mL hr^{-1}. Live/Dead reagent was flushed through the device and incubated for 15 minutes, followed by microscopic imaging of several 10x magnification fields on view. The first four fields of view were considered as accurate estimates of cell viability. Live and dead cells were manually counted in a blinded manner and cell viability was defined as the percent ratio of number of cells alive to the total number of cells

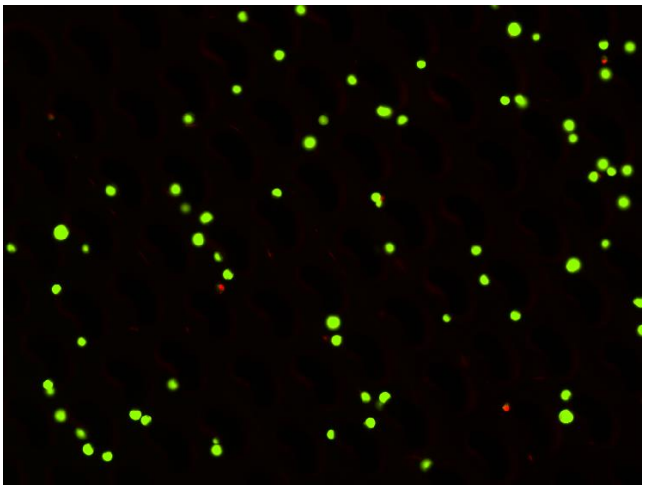

Figure 2.3 Cell viability at high flow rates
Invitrogen Live/Dead viability assay shows live H1650 cells (green) and dead H1650 cells (red) in one section of the device after capture at 10 mL hr^{-1} on the OncoBean Chip.

in the field of view. Using this assay, 92.91 ± 1.63% (mean ± s.d.) of the cells were found to be viable after flow at high throughput, comparable to the mean viability of 98.5% reported for the CTC Chip [8]. These data indicate that despite facing an initial momentary high stress at higher flow rates, cell viability is not diminished compared to lower flow rates, perhaps due to the continuous drop in shear stress that is produced by the radial flow (**Figure 2.3**).

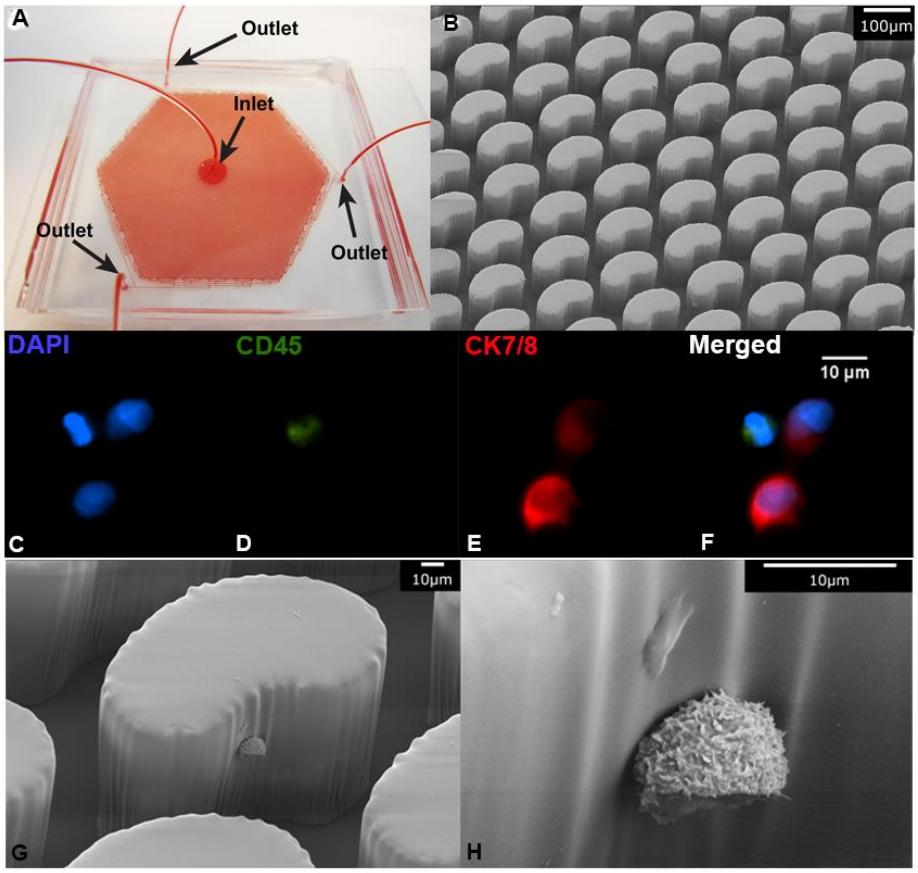

Figure 2.4 Cell capture on the OncoBean Chip
(A). The OncoBean Chip with blood flow shows inlet and outlet positions (B) Scanning electron micrograph of the device shows bean-shaped micropost structures. H1650 cells in blood captured by the OncoBean Chip: panel shows immunofluorescence images of cells stained for nucleus with DAPI (C), CD45 – a white blood cell marker (D), cytokeratin 7-8 that stains the H1650 cancer cells (E), and a merged field (F) showing all fluorescent stains. (G) is a scanning electron micrograph of a H1650 cell captured on a bean-shaped micropost, with (H) showing a magnified view of the cell.

2.4.6. CTC Capture in Cancer Patients

The strength of the technology was assessed by testing clinical specimens from different cancers.. Whole blood from healthy donors (n = 4) was processed as controls at 10 mL hr-1 to test for the specificity of capture against anti-EpCAM. **Figure 2.4A** shows the whole blood flowing through the device, and a representative scanning electron micrograph of the posts is shown in **Figure 2.4B**. After fixation of the cells on the device, the cells were permeabilized and stained for anti-Cytokeratin (CK) (tumor specific epithelial marker), anti-CD45 (leukocyte marker) and DAPI (nuclear stain) and respective secondary antibodies for immunofluorescent imaging. **Figure 2.4C-F** presents representative images of immunofluorescence staining of H1650 lung cancer cells along with WBCs captured on the chip, whereas **Figure 2.4G-H** shows SEM image of a H1650 cell captured on the side of an OncoBean post. The criteria for CTC enumeration was a CK+, CD45- and DAPI+ expression profile [8]. The healthy controls gave a recovery of 1.4 ± 0.89 CTCs per mL (range 0.91-2.67 CTCs per mL, median 1.13 CTCs per mL) as per the above enumeration criteria (Figure 2.5). Following this, a threshold of 2 CTCs per mL was set for CTC detection in clinical specimens [33]. Whole blood from pancreatic (n = 2), breast (n = 2) and lung (n = 2) cancer patients were processed through the OncoBean Chip at 1 and 10 mL hr-1 in equal volumes to observe CTC recovery using an anti-EpCAM antibody. According to this criteria, CTCs were detected by the device in 100% of the samples, with a recovery of 4.2 ± 0.65 CTCs per mL at 1 mL hr-1 (range 3.33-5 CTCs per mL, median 4 CTCs per mL) and 4.33 ± 0.85 CTCs per mL at 10 mL hr-1 (range 3-5 CTCs per mL, median 4.67 CTCs per mL). The high flow rate of 10 mL hr-1 gave equivalent recovery in 5 of 6 samples. Because of the small cohort

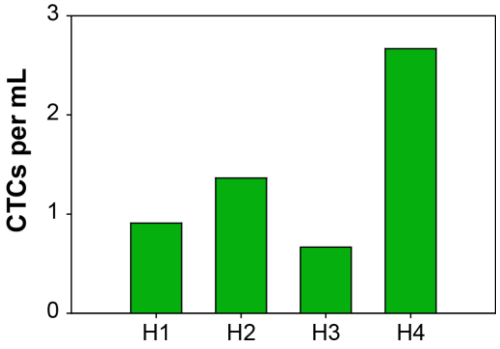

Figure 2.5 Healthy controls
Healthy controls processed through the OncoBean Chip at 10 mL hr^{-1} against anti-EpCAM showing number of CK+, CD45-, DAPI+ cells.

of specimens tested, statistical significance was not observed. The CTC yields across the different cancers at the two flow rates are shown in **Figure 2.6**. It can be seen that the high flow rate has a similar CTC recovery capacity to that at a low flow rate in the various cancer specimens processed.

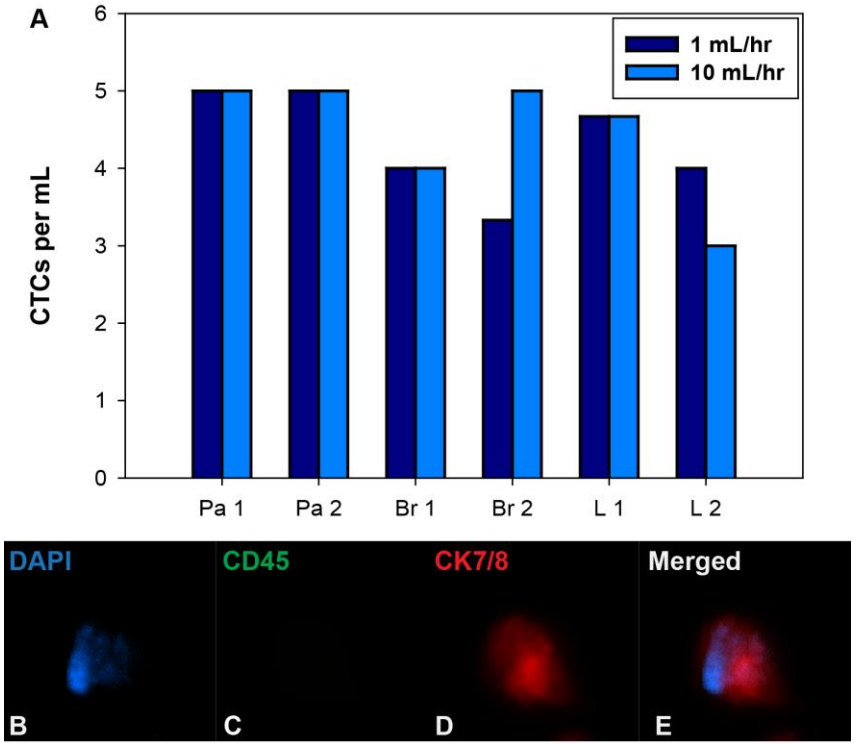

Figure 2.6 Testing of OncoBean Chip with patient specimens
(A). Clinical performance of the OncoBean Chip showing CTC recovery from patients with pancreatic (Pa), breast (Br) and lung cancer (L) at 1 and 10 mL hr^{-1}. Panel at the bottom shows immunofluorescent staining of a lung CTC recovered at 10 mL hr^{-1} showing (B) nucleus, (C) absence of CD45, (D) cytokeratin 7/8 and (E) a merged field with all channel staining.

2.5. Discussion

High throughput analysis has remained a major hurdle in the retrieval of circulating tumor cells from cancer patients and is a critical issue in the development of new microfluidic technologies to measure CTCs [18]. While many physical separation methods and integrated systems have been developed, to our knowledge, no affinity-based one-step cell recovery technologies have

yet been developed for high throughput analysis. The OncoBean Chip is a first of its kind immuno-enrichment technique offering the specificity of antibody-based capture in a high throughput manner (10 mL hr^{-1}). It works by isolating CTCs from whole blood in a single step, without the need for pre-processing or dilutions. It achieves its high throughput functionality through a simple technique of a radial flow channel. Fluid simulations and theoretical calculations show that the fluid velocity in the radial flow OncoBean Chip varies as $1/(2\pi rh)$, where r and h stand for the radius and height of the channels, respectively. While increasing the height of the channel is an alternative to achieving high throughput, microfabrication of a high aspect ratio channel as well as microscopic imaging are challenging. A flow profile which dynamically varies with distance thus offers an economical and compact technology that enables the processing of high volumes of fluid samples, which is highly advantageous in the context of rare circulating tumor cells. The design of the OncoBean Chip is thus optimal for this purpose, as it achieves an average capture efficiency (>80%) comparable to that of the CTC Chip, which still remains a benchmark for microfluidic CTC extraction by immuno-affinity methods [16, 28].

Immuno-affinity based microfluidic platforms like the CTC Chip and others perform poorly at high flow rates due to the linear flow profile wherein many cells either escape the substrate interactions or are travelling at a constantly high velocity throughout the device in order for binding to occur [8, 15]. The OncoBean Chip shows stable binding at high flow rates due to the drop in velocity at every radial position toward the outlets. Reducing shear at different cross sections in the chip also allows a high flow rate without compromising cell viability, increasing the feasibility of downstream processing of these cells to obtain molecular characteristics and genetic information [18, 99].

While high volumes of blood used for CTC analysis potentially offer higher yields of these rare cells, the detection methods also face the issue of an increased background contamination owing to the quantity of sample. We observed that WBC contamination was not a major concern in the OncoBean Chip as the high velocities prevented high non-specific binding. There is a greater than 2-fold drop in the contaminating WBCs when run at 10 mL hr^{-1} in contrast to 1 mL hr^{-1}, and also a continuous drop in non-specific binding with increasing flow rates. This is expected as the higher velocities reduce the interaction time of these non-specific cells with the tumor-specific-antibody coated posts, thereby reducing contamination. The higher levels of purity coupled with higher CTC yields in a one-step strategy should enhance accuracy in molecular analyses of the recovered CTC population [9].

Affinity-based microfluidics are dependent on antibody-antigen kinetics, and antigen density is an important parameter controlling the rate of capture [30, 31, 117]. The capture profile plot shows that a cell with high EpCAM expression such as H1650 would be captured early in the device as the antigen density would enhance bond formation, whereas a cell with lower EpCAM expression would be concentrated around the latter half of the device, nearer to the outlets, as the cells would need to be at a sufficiently lower velocity for binding to occur due to the smaller number of binding sites [30, 117]. The OncoBean is thus conducive to capturing cells with a wide range of EpCAM antigen expression. It is also possible that multiple antibody combinations could be used in the OncoBean Chip in the future to further fine tune CTC capture.

As with all diagnostic technologies, bench-to-bedside remains the deciding factor for the device's competence. The OncoBean Chip shows initial promise with clinical samples, capturing CTCs from the blood of patients with epithelial cancers by the use of anti-EpCAM as the capture antibody. Out of the 6 patient samples tested, 5 show equivalent capture at 10 mL hr^{-1} compared

to capture at 1 mL hr^{-1}. This demonstrates the potential of this technology as a high-throughput platform to evaluate CTCs in different cancers. The technology also enables the processing of 7.5 mL of blood in under an hour, which is not only unprecedented in many other microfluidic technologies, but also attractive from a clinician's perspective. The OncoBean Chip is thus a potential tool for blood based diagnostics that can quickly become part of routine clinical tests. The healthy controls also indicate the specificity of capture by this technique. Although the small cohort of patients and the volume of blood processed for unbiased comparison with that at low flow rate restrict a rigorous sensitivity analysis of the device, the capture efficiency of the device shows potential for using higher volumes of blood for recovery of higher CTC numbers. While a few high throughput affinity isolation technologies have recently been developed, they invariably require working with diluted blood, or multiplexing and integration of devices [11, 25, 30, 39, 115]. Also, immunomagnetic technologies suffer from limitations such as reduction in the binding affinities of antibodies on magnetic particles, requiring higher amounts of antibodies to screen larger cell populations [114, 118]. Tumor heterogeneity brings forth another set of challenges for physical separations as CTCs are observed to be widely different, with size heterogeneity being the most evident [18, 62, 76]. Hou et al. witnessed a range of 10-22.5 μm in the CTC sizes isolated using their physical separation device [76]. While many such devices perform at commendable throughputs, such size variations may result in significant CTC loss.

2.6. Conclusion

We have demonstrated that high-throughput processing with immuno-affinity CTC capture is possible even without multiplexing such as in physical separations which in many cases involve complex handling to reduce the blood volume [11, 25]. We have validated the efficacy of the technology with cancer cell lines and also with clinical specimens. In addition, it has also been

shown that the ultra-high throughput used is not detrimental to the cell viability, yields good purity and can be capitalized for downstream studies. The major highlight of the OncoBean Chip lies in its design of radial flow, which can be easily incorporated into other microfluidic chips, such as the graphene oxide chip developed by our group [33] and other devices that may be utilized for CTC culture [44]. Also, the captured cells may be released by the incorporation of cell recovery techniques as performed for the HTMSU device [23, 32] or those described by Shah et al. [55]. The OncoBean Chip would thus be useful in the cases of early stage cancers where there may not be sufficient number of cells in the circulation in order to be detected in 1-3 mL of blood and thus shows great promise as an early diagnostic tool.

Chapter 3

Capture and characterization of CTCs from pulmonary and peripheral vein blood of early stage lung cancer patients

3.1. Abstract

Despite the "curative" intent of surgical resection of early stage non-small cell lung cancer, the majority of patients will recur and die from metastatic cancer. Early detection of metastasis or tumor progression can be aided by liquid biopsies such as circulating tumor cells (CTCs) which also have the potential to predict early relapse. As the numbers of CTCs present in peripheral blood in early stage lung cancer are limited, we investigated CTCs in pulmonary vein blood accessed during surgical resection of tumor as a presumably enriched source of CTCs, in addition to peripheral blood. Pulmonary vein (PV) and peripheral vein (Pe) blood specimens from patients with suspected lung cancer were drawn during the perioperative period, with multiple draws of Pe blood at different time points. The specimens were assessed for CTC burden using affinity capture on a high-throughput microfluidic device, the OncoBean Chip. From 108 blood samples analyzed from 36 patients, the intra-operative pulmonary vein had significantly higher number of CTCs compared to both pre-operative peripheral ($p<0.0001$) and intra-operative peripheral ($p<0.001$) blood. Rare CTC clusters with large number of CTCs were observed in 50% of patients, with the PV more often revealing larger clusters. Majority of patients with larger clusters had moderate or poorly differentiated tumors. Longitudinal

monitoring of patients with CTC clusters revealed persistent CTCs in the majority (66%) of patients with higher number of clustered CTCs. Long term surveillance of patients in this study indicated that 85% patients who recurred had CTC clusters. Gene expression analysis of PV and Pe samples by RT-qPCR revealed EMT genes were expressed in CTCs from both the sources, with the PV having higher differential expression of mesenchymal genes (ZEB1, BMi1), whereas the Pe had higher levels of immuno-suppressing genes such as NANOG, IL6, LGALS3BP. Ki67 expression was detected in 46% of PV samples and 38% of Pe samples, with majority (83%) of patients positive for Ki67 expression having single CTCs. Furthermore, 90% of all Ki67+ patients had a moderate or poor tumor differentiation grade indicating the ability of CTCs to reflect disease aggressiveness. Gene ontology analysis also revealed upregulation of cell migration and cell survival pathways in CTC clusters. Comparing p53 status of primary tissue to CTCs, we discovered that CTCs in circulation have no to low p53 expression despite high positivity in primary tumors by IHC. This suggests that EMT-like cells in the PV have downregulated p53 expression. Taken together, CTCs leave primary tumor even in early stages of lung cancer and could be presented in cluster form. The cells in circulation exhibit EMT phenotype with high migratory and immuno suppression signature along with low tumor suppression, revealing markers of tumor aggressiveness, progression and recurrence.

3.2. Early detection of lung cancer

Improving the early detection of lung cancer, a disease that causes approximately one fifth of all cancer related deaths in the world [119, 120], is critical as early stage tumors have a greater than 70% 5-year survival, compared to less than 5% for patients with metastatic disease [121]. Most lung cancers are diagnosed when they are too advanced for surgical intervention. The National

Lung Screening Trial has shown that early detection of lung cancers results in improved long term survival. Over 50,000 patients were screened using either low dose CT scans or chest X-rays. Of patients screened by CT scans, 24% had "positive" scans, with 96% of those found to be false positives. Nonetheless, there was a 20% reduction in lung cancer specific mortality and a 7% reduction in all-cause mortality [122]. Despite these improvements, increased radiation from CT scans has been implicated in increasing long term cancer risk for some, and is not the ideal screening method [123]. Other concerns with the current paradigm of diagnosing lung cancers include the high costs and complications associated with lung biopsies, performed to diagnose indeterminate nodules. Almost 20% of patients can have complications from their lung biopsies [124]. Alternative methods to detect early stage cancers that can supplant or complement CT screening is an unmet need to increase specificity of screening tests and one that can be more widely used. The identification of circulating biomarkers such as CTCs to detect cancers by blood sampling offers an attractive, less invasive alternative to tissue biopsies.

3.3. CTCs in lung cancer

Circulating cells may be shed from solid organ tumors into the blood stream. Recent research has shown that metastasis may not just be a late event, but may be present very early in disease progression [125]. Investigators have demonstrated this in breast cancer using transgenic mice models [125]. They found that tumor cells may be released even before the tumor is presumed to be invasive, and some of these cells may form metastatic tumors. Their findings are supported by reports of tumor spread even after resection of early stage cancers [125].

In lung cancer, Izbicki et al. studied the presence of micrometastases in lymph nodes and their association with patient survival [126]. In another study, Maruyama et al. analyzed paraffin

sections of lymph nodes from stage I patients to predict recurrence from lymph node metastasis [127]. They observed presence of tumor cells in lymph nodes in 70% of patients, some of whom recurred [127]. Both studies found a reduction in survival among those patients that tested positive for micrometastatic cancer cells in the lymph nodes. Both of these studies suggest that the presence of these cells indicates that tumor resections might not completely eliminate disease, and further action such as adjuvant therapy may be needed to detect these 'previously undetected' cells [126, 127]. The presence of micrometastatic disease in the lymph nodes may also serve as a source for future CTCs found in the blood stream [128]. While there has been debate about the path of cell shedding, namely, whether cancer cells extravasate into the lymph nodes first or the bloodstream first [128], it is now generally believed that undetectable micrometastases may be present before tumor spread to other organs is evident [126, 127].

3.4. CTCs in early lung cancer

CTC detection in early stages of cancers is gaining momentum as a means of early diagnosis and intervention. A number of studies have demonstrated the presence of CTCs in patients with early breast cancers, with more recent work being done in lung cancer also [105, 129-131]. Advancing such studies to larger cohorts and detailed molecular analyses of these cells may lead to timely treatment decisions and surgical interventions [131, 132]. Surgical intervention is the most commonly used "cure" for lung cancers when detected early [133]. However, CT scans are limited by their ability to identify very small nodules, and predicting malignancy of nodules. CTCs or other blood based markers can complement standard screening tests for early detection [134]. CTCs in early stage lung cancer have the potential to be interrogated for detailed molecular and genetic characterization.

Ilie et al. used CTCs in conjunction with CT scans to identify high risk patients for having occult lung cancer [131]. Those individuals who tested positive for CTCs despite having no detectable lesions on CT scan were followed over 4 years, with all developing CT-scan-identifiable lung cancers which were resected. The study represents a promising direction for future research wherein CTCs could inform the risk of patients with or even without lung nodules having lung cancer. Ex vivo assays such as growth of enriched CTCs has also been demonstrated from early stage lung cancer patients. Zhang et al. captured lung CTCs using a microfluidic post-based device, and expanded them for downstream assays including sequencing [44]. They also showed concurrent mutations of the p53 gene among CTCs and primary tumor in a few samples. Wendel et al. studied CTCs from different stages of lung cancer including early stages [135]. While no statistical differences were found between CTC numbers from the various stages, they did observe a high number of CTCs and CTC clusters even in some early stage patients. This provides scope for further analysis on individual cells and clusters.

3.5. Challenges in CTC studies

The biggest challenge in the field of circulating tumor cells is posed by their rarity [8]. Overcoming this challenge requires the development of more sensitive technologies that can efficiently pick out these cells from hordes of contaminating cells. Certain factors such as low frequency and low throughputs limit the scope for further CTC analysis [17, 18]. Downstream sequencing studies require very high purity of these cells, and enriched CTCs tend to be either tethered onto the capture device and/or or contaminated with blood cells, thereby increasing noise [2, 17, 55].

Functional assays such as culturing of these cells require CTCs to be viable and proliferating [136]. Majority of CTCs in circulation are presumed to undergo anoikis or apoptosis, thereby explaining why all disseminated cells do not form secondary tumors. While this poses a big challenge for expanding these cells to perform drug testing and other tumorigenicity assays, it also calls for the use of multiple markers to shed light into why some cells survive physiological shear stresses while others do not [137, 138]. Indeed, even apoptotic CTCs may be able to predict prognosis, as shown in the aforementioned study by Kallergi and authors [139].

Another interesting challenge is posed by the theory that these cells may be undergoing various changes in different steps of the metastatic cascade. Epithelial to mesenchymal transition (EMT) is one such change that is believed to be an important part of metastasis, which is mostly attributed to disseminating cells [37, 140]. Cell motility and the ability to intravasate into the blood stream is explained by EMT, while the reverse process or mesenchymal to epithelial transition (MET) is believed to occur during extravasation to secondary sites [49]. In light of EMT, there is a general debate about inadequacy of epithelial markers such as Epithelial Cell Adhesion Molecule (EpCAM) to be able to capture the wide variety of heterogeneous CTCs [54]. This is currently being overcome by the use of multiple antibodies, or by the use of antigen-independent methods of enrichment.

3.6. Aims and scope of lung CTC study

Lung cancer has tremendous potential for early detection and intervention, which can dramatically improve overall survival [141]. In the proposed study, we aim to investigate circulating tumor cells from early lung cancer patients. Since early stages of cancers have low CTC yields, we aim to maximize the recovery by analyzing blood from the pulmonary vein. The

unique anatomy of the lung offers an opportunity to obtain CTCs from the venous drainage directly from the tumor containing lung lobes, i.e. the pulmonary vein [142]. CTCs from this source would presumably be present at a higher abundance, therefore aiding in subsequent molecular analyses. Initially, the pulmonary and peripheral vein CTCs will be compared by enumeration. This will be followed by genomic characterization using RT-qPCR to study the genotypic differences or similarities at a molecular level. The aim of the study is to understand the characteristics of CTCs at the time of shedding and in circulation, such that new biomarkers can be revealed which may be useful in predicting disease progression or recurrence even in early stages of the disease.

3.7. Motivation

Circulating tumor cells (CTCs) and cell-free DNA are emerging as promising tools for rapid, convenient and less-invasive screens for detecting and monitoring a patient's cancer [2]. CTCs play an important role in metastasis, which accounts for majority of cancer deaths [4, 143-145]. These cells can provide useful prognostic information and can also be utilized to make therapeutic decisions in clinical cancer management [4, 8, 27, 143, 146]. The biology of CTCs have been explored extensively mostly in advanced stages of cancer wherein their typically larger frequencies enables useful downstream analysis [147]. Such studies in early stages have been limited by the low number of these cells [148]. In order to understand early events and the role of CTCs in initiation of the metastatic cascade, it is essential to understand phenotypic and genotypic characteristics of CTCs in early stages of cancer.

Lung cancer, the leading cause of cancer-related deaths across the world [135, 141, 143, 149] provides a potential model to study the utility of CTCs with applications in disease screening.

The disease has a poor survival rate of 5% for stage IV disease with the dismal survival rate attributed to the lack of early detection [141]. The high incidence and pressing need to improve survival calls for improved early diagnostic tools. Assessing CTCs has the ability to offer repeated monitoring of patients, a useful way of observing patients for relapse after resection [150]. In this study we aimed at identifying specific characteristics of CTCs in patients undergoing surgery for early stage lung cancer. However their rarity in the bloodstream (few CTCs among millions of blood cells) required alternate strategies for sequestering them to better examine their biological potential [8, 151].

In order to overcome the limitation of the low frequency of CTCs, we decided to study these cells when enriched near their origin, i.e. from the pulmonary vein of the affected lobe which can be accessed at the time of tumor resection. There have been few studies documenting the presence of CTCs in the pulmonary veins of patients with lung cancer [152, 153]. One study showed that the presence of CTCs in the pulmonary vein indicated a poor prognosis relative to those with an absence of CTCs in the tumor draining vein [153]. Also, the pulmonary vein shows a significantly high number of CTCs relative to that obtained through conventional peripheral vein methods [142, 152]. The higher yields obtained from the PV offers a useful strategy to study CTCs and their role in tumor progression. While a few studies have investigated the pulmonary vein as a potential source of increased CTCs [152-157], most of these studies utilized the CellSearch EpCAM-based platform, negative selection and/or centrifugation for enriching PV CTCs. This study is to our knowledge, novel in the following aspects: (a). None of the previous studies examined the differences in characteristics of CTCs from these different sources, especially at genetic level, (b). In our study, CTCs were examined at multiple (≥ 2) time-points around surgical resection; this comparison of different time-points during the perioperative

period would presumably indicate actual differences in CTCs obtained from different sources, (c). CTCs were isolated from the pulmonary and peripheral veins using microfluidics, a more sensitive platform for CTC detection [2] with the incorporation of multiple antibodies to capture diverse CTC populations, (d). Patients were monitored longitudinally to study the CTC changes from resection to follow-up, and (e). Gene expression profiling by RT-qPCR for 96 genes revealed differentially expressed genes between the different CTC sources. We thus hypothesized that PV CTCs could offer a useful strategy for obtaining higher CTC yields from early stage lung cancer where peripheral CTCs might be inadequate; furthermore CTCs from the pulmonary vein may provide molecular markers of invasion and metastasis that could inform surveillance biomarkers during follow-up to detect early recurrence and metastasis.

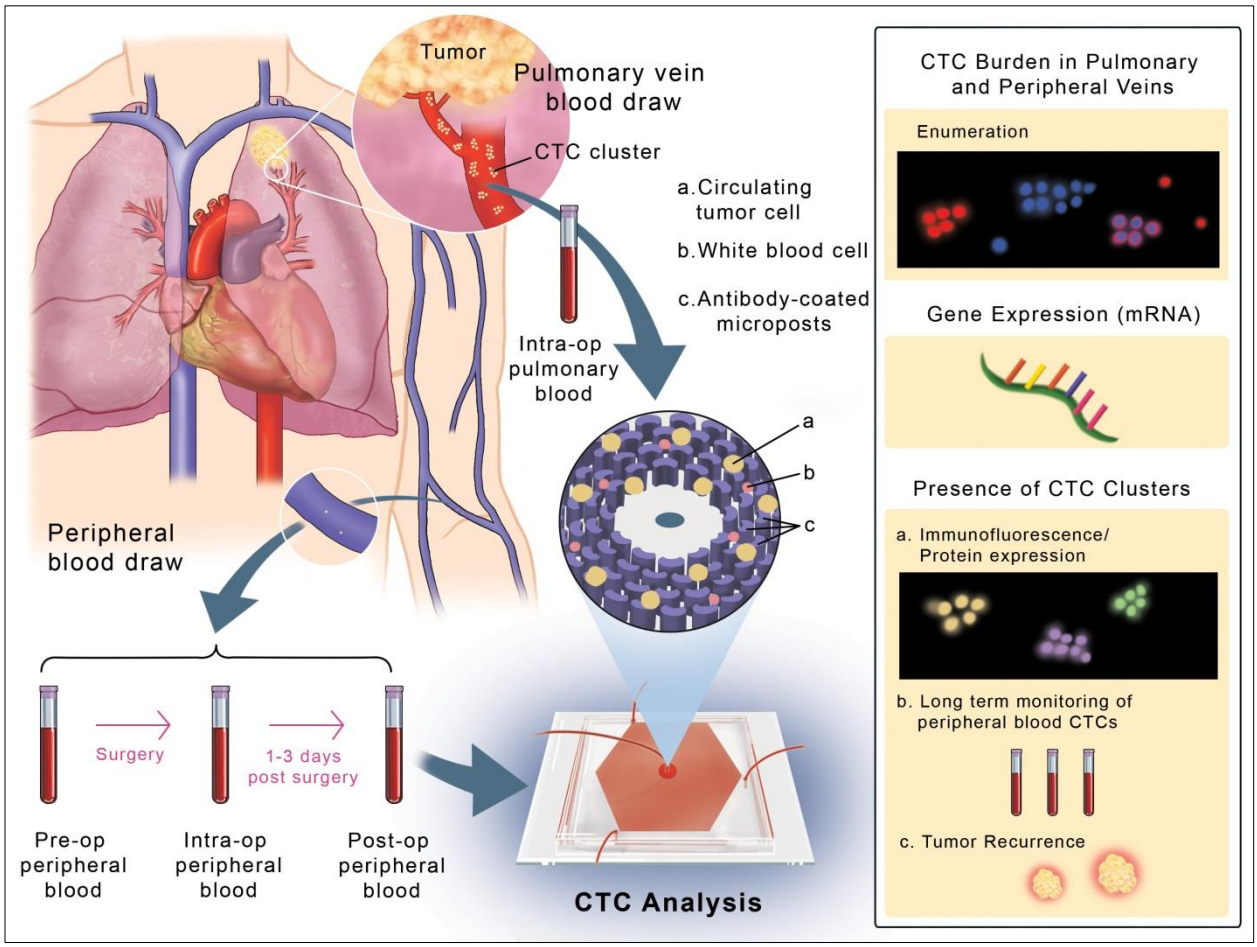

Figure 3.1 Strategy of lung CTC study
Study schematic representing the anatomy of the lung displaying the pulmonary vein (PV) and peripheral veins (Pe). Blood was drawn from the veins at different time-points around tumor resection and processed through the OncoBean Chip, followed by analysis by enumeration and genomic profiling (inset on right). Illustration by Lisa D'Angelo.

3.8. Materials and Methods

3.8.1. Strategy of lung CTC study

Pre-operative peripheral (Pre-op Pe) blood was collected 0-2 hours prior to surgery. During the initial phases of the operation, the pulmonary vein branches draining the cancer containing lobe of the lung were identified (**Figure 3.1**). Blood was drawn from the pulmonary vein (Intra-op

PV) via a 25- gauge needle early in the operation, prior to significant lung or tumor manipulation. Simultaneously, blood was drawn from a peripheral vein or arterial line (Intra-op Pe). Finally, a post-operative peripheral (Post-op Pe) blood draw was performed within 1-3 days of surgery. Follow-up blood was drawn via a peripheral vein at the time of follow-up visits. Blood specimens were collected in EDTA tubes and processed on the same day for CTC analysis.

Whole blood samples were processed using a high-throughput radial flow microfluidic device, the OncoBean Chip [50] at a flow rate of 5 ml/hr, using different combinations of antibodies against Epithelial Cell Adhesion Molecule (EpCAM), Epidermal Growth Factor Receptor (EGFR) and CD133.

3.8.2. Patient demographics

Patients with surgically resectable (clinical stage I-III) lung cancer were enrolled into the study at the time of surgery. Thirty-six patients underwent surgery (NSCLC=35, SCLC =1) (**Table 3.1**). Among NSCLC group, there were 20 patients with adenocarcinoma and 15 with squamous cell lung cancer. When broken down by pathologic stage, among the NSCLC patients, 19 patients were stage I, 7 were stage II and 8 were stage III. One patient was found to have stage IV disease, with metastatic disease found 3 weeks after surgery. The median age of patients was 70 years, and the population consisted of 15 males and 21 females.

Table 3.1 Clinical characteristics of patients in lung CTC study

Index	Age	Gender	Histology	Stage	Differentiation
P1	66	m	Squamous	IB	Poor
P2	91	f	Adenocarcinoma	IB	Moderate
P3	81	f	Adenocarcinoma	IIIA	Moderate
P4	92	m	Squamous	IA	Moderate
P5	52	f	Adenocarcinoma	IIIA	Poor
P6	57	m	Small cell	IIB	High grade
P7	70	f	Adenocarcinoma	IIA	Moderate
P8	85	f	Adenocarcinoma	IIB	Moderate
P9	86	m	Adenocarcinoma	IA	Well
P10	77	m	Squamous	IIIA	Poor
P11	62	m	Squamous	IB	Poor
P12	73	f	Adenocarcinoma	IIIA	Poor
P13	65	m	Squamous	IA	Moderate
P14	75	f	Adenocarcinoma In Situ	IB	Well
P15	60	m	Adenocarcinoma	IB	Moderate
P16	70	m	Squamous	IIA	Moderate
P17	58	f	Squamous	IB	Moderate
P18	71	m	Adenocarcinoma	IA	Moderate
P19	82	f	Adenocarcinoma	IA	Moderate
P20	57	m	Squamous	IB	Poor
P21	72	f	Adenocarcinoma	IB	Well
P22	54	m	Squamous	IIIB	Poor
P23	73	f	Adenocarcinoma	IA	Moderate
P24	66	f	Adenocarcinoma	IIIA	Poor
P25	58	f	Adenocarcinoma	IB	Moderate
P26	73	m	Squamous	IB	Moderate
P27	68	m	Squamous	IA	Poor
P28	77	m	Squamous	IIB	Clear cell features
P29	79	f	Adenocarcinoma	IIB	Poor
P30	72	f	Squamous	IV	Moderate
P31	53	f	Adenocarcinoma	IA	Moderate
P32	58	f	Squamous	IIIA	Poor
P33	67	f	Adenocarcinoma	IA	Moderate
P34	74	f	Adenocarcinoma	IA	Well
P35	67	f	Squamous	IIB	Poor
P36	60	f	Adenocarcinoma	IIIB	Poor

3.8.3. Isolation of pulmonary and peripheral vein CTCs

Blood specimens were processed through the OncoBean Chip at a flow rate of 5 ml/hr, using combinations of antibodies against Epithelial Cell Adhesion Molecule (EpCAM), Epidermal Growth Factor Receptor (EGFR), and CD133. Previously described protocol for blood sample processing [8, 50] was followed with a few modifications. Briefly, following antibody incubation the devices were blocked with 3% bovine serum albumin (BSA). An average of 4.3, 4.0 and 2.0 ml of Pre-op Pe, Intra-op Pe and Intra-op PV blood was processed for CTC analysis through each device. Blood was processed through the device at 5 ml/hr followed by washing with phosphate buffered saline (PBS). After washing, the cells captured on the device were fixed with 4% paraformaldehyde (PFA) for enumeration. Devices were stored at 4 °C until immuno-staining was performed.

Immunofluorescent staining was performed by first permeabilizing the cells with 0.2% Triton-X 100, followed by blocking with 3% BSA + 2% normal goat serum. Primary antibodies Cytokeratin 7/8 and CD45 and secondary antibodies Alexa Fluor 546 and Alexa Fluor 488 respectively were used to identify the cells.

3.8.4. CTC identification and analysis

Cells captured on the device were stained for Cytokeratin (CK) 7/8, CD45 and DAPI. The devices were automatically imaged by Nikon Ti Eclipse fluorescence microscope. CTCs were counted based on positive staining for CK and DAPI and negative staining for CD45.

3.8.5. Other immunocytochemistry

Devices containing CTC clusters and pre-stained for enumeration were additionally stained for anti-CD44 and visualized by Alexa Fluor 647. Positive staining among CTCs was identified by CK7/8+, CD44+, CD45- and DAPI+.

3.8.6. Statistical analysis for CTC enumeration

Statistical analyses were performed using OriginPro, SAS, and R [44] . Enumerated CTCs from peripheral and pulmonary veins were compared by the Wilcoxon Signed Rank test for each pair of sources. CTC clusters were also analyzed by the Wilcoxon test. Significance is determined if $p<0.05$.

3.8.7. RNA extraction and RT-qPCR

For RNA extraction the captured cells were lysed on chip immediately after PBS wash using Arcturus PicoPure RNA Extraction buffer. The lysate and the device were incubated at 42 °C for 30 min, followed by a wash with water and collection of effluent. All effluents were stored at -80 °C until RNA analysis. The second effluent collected was processed to isolate RNA for cDNA synthesis and multiplex gene expression analysis. The total RNA samples were used to synthesize cDNA that were preamplified for the target 96 genes using pool of TaqMan assays. The preamplified cDNA were subjected to qPCR to determine expression patterns of target 96 genes forming a "comprehensive CTC panel" using TaqMan assays and the Biomark HD system (Fluidigm).

3.8.8. Gene data analysis

Raw Ct values generated by Biomark HD (Fluidigm) were normalized to *GAPDH* for each sample using the -ΔCt method [158, 159]. Undetected transcripts automatically generate a Ct

value of 999, which were changed to Ct of 40 for numerical analyses [158, 159]. Statistical analysis was performed using R software [61]. Wilcoxon rank sum tests were used to calculate differential expression. Log fold change was calculated from median expression ($2^{-\Delta Ct}$) values for each group of samples. Heat maps were generated using the *heatmap.2* function under the gplots library of R. The p-values generated by the Wilcoxon rank sum tests, and the logFC from median expression values were input into a pathway analysis software, IPathwayGuide (Advaita Bio). For gene ontology enrichment analyses, a logFC cut-off of 2.0, and a p-value cut-off of 1 was used.

3.9. Results

3.9.1. CTC burden in different venous sources

Captured cells were enumerated by immunostaining for Cytokeratin (CK) 7/8 and CD45, in addition to DAPI. Cells positive for Cytokeratin 7/8 and DAPI, and negative for leukocyte specific marker CD45 were scored as CTCs (**Figure 3.2A**). Since PV blood volumes were most often limited to 3 ml, CTC numbers are reported per 3 ml. From 36 patients analyzed, CTCs were detected in the pre-op peripheral (pre-op Pe), intra-op peripheral (intra-op Pe) and intra-op pulmonary vein (intra-op PV) in 77.8%, 69.4% and 83.3% of patients respectively. The range of detected CTCs in the pre-op Pe varied from 0-15 CTCs per 3 ml, with a median of 1.5 CTCs per 3 ml. The intra-op Pe had a detection range of 0-28.5 CTCs per 3 ml with a median count of 1.3 CTCs per 3 ml. The intra-op PV specimens showed CTCs in the range of 0-10,278 per 3 ml, with a median of 7.5 CTCs per 3 ml (**Figure 3.2B, C**). Microfluidic capture confirmed that a significantly higher number of CTCs were detected from the PV when compared to the pre-op ($p < 0.0001$) and intra-op ($p < 0.001$) Pe samples, as determined by the Wilcoxon Signed Rank test

(**Figure 3.2C**). The pre-op and intra-op Pe samples did not show a significant difference in CTC numbers ($p = 0.34$).

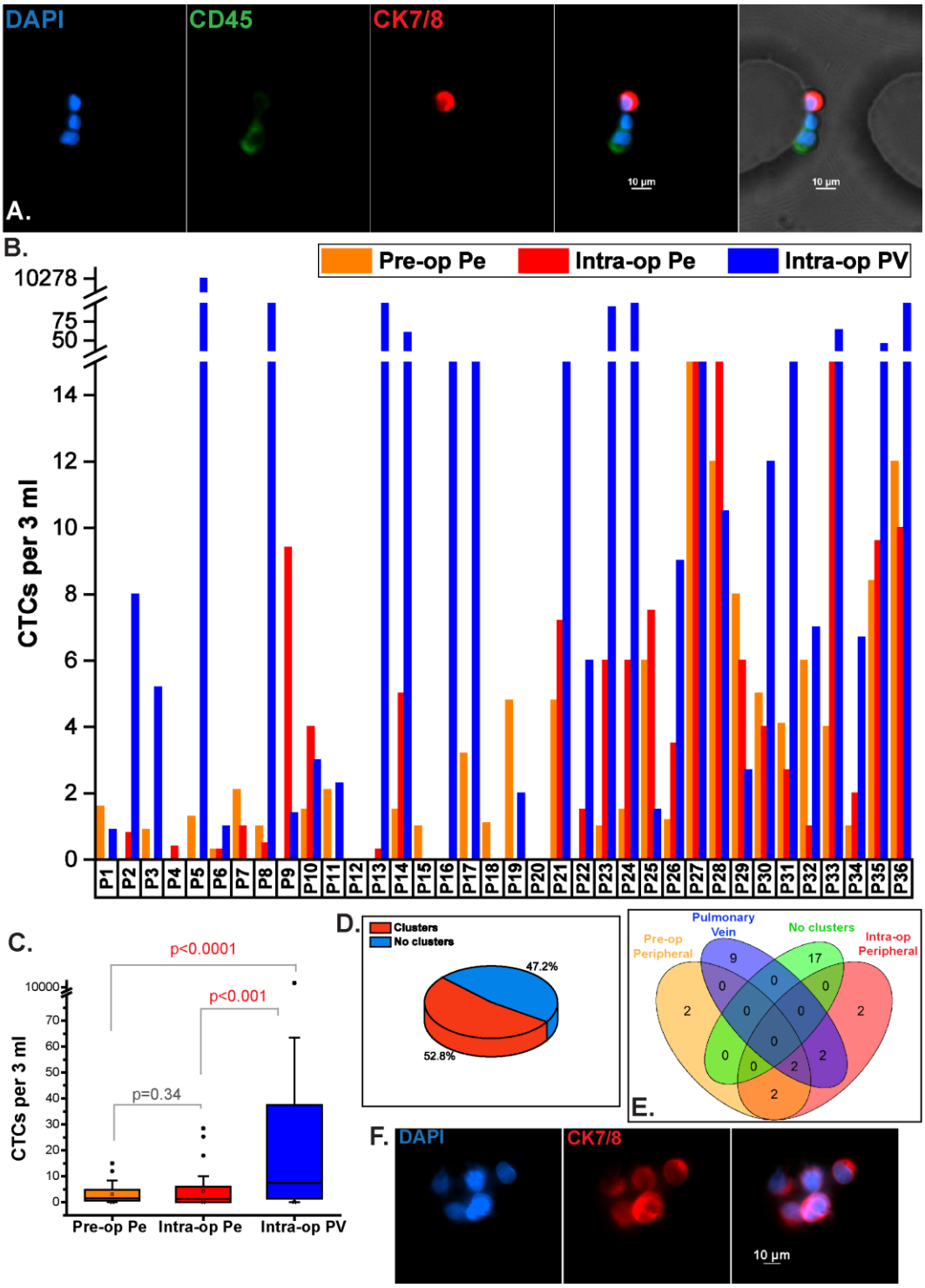

Figure 3.2 CTC enumeration from different venous sources

(A). Immunofluorescent staining of captured cells showing a CTC (CK7/8+, DAPI+, CD45-) captured next to CD45+ blood cells on the OncoBean Chip, (B). CTC burden from pre-op Pe, intra-op Pe and intra-op PV samples across 36 patients, (C). Range of CTCs from different sources showing higher CTC abundance in PV, (D). Frequency of CTC clusters observed in all patients at any time-point, (E). Individual incidence of CTC clusters in each venous specimen among all samples, (F). Immunofluorescent staining of CTC clusters captured in a lung cancer patient, (G). Confocal merged image of a CTC cluster captured on the OncoBean Chip.

3.9.2. CTC cluster analysis

CTC clusters have been detected in a few cancers, and studies indicate that they have a greater capability to metastasize [48]. CTC clusters, defined here as groups of 2 or more CTCs captured within close proximity of each other were observed in large numbers in the pulmonary vein of one patient (P5) early on in our study, which led to further investigation of these aggregates in subsequent samples in the different blood sources. CTC clusters were detected in 52.7% of patients across all samples (n=36) irrespective of the blood source (**Figure 3.2D**). Among patients with observed clusters (19/36), the average volumes of blood processed were 3.5 ml of pre-op Pe, 3.3 ml of intra-op Pe and 1.8 ml of PV. Clusters in PV were observed in 13/36 (36.1%) patients, while 6/36 (16.6%) and 8/36 (22.2%) patients had clusters in pre-op and intra-op Pe samples respectively, with 6 patients having clusters in multiple time-points (**Figure 3.2E**). Representative immunofluorescence staining images of clusters are shown in **Figure 3.2F**.

The clusters in PV varied in size from 2 CTCs to >200 CTCs, while those in either Pe group ranged from 2-9 CTCs. A total of 9 clusters (range 0-3) were observed in pre-op Pe, 22 clusters (range 0-6) were detected in intra-op Pe, and 1116 clusters (range 0-885) in PV were observed among all patients. Of these, 593 (53.1%) of PV clusters consisted of >= 5 CTCs, and 319 (28.6%) of these clusters were comprised of >=10 CTCs. Examples of different CTC cluster sizes are shown in **Figure 3.3A**. A distribution of the clusters segregated by their size is also shown in **Figure 3.3B**. With the exception of patient P9, the peripheral blood yielded small clusters (<5 CTCs), while the PV had a heterogeneous size distribution of captured CTC clusters in 7/13 samples (**Figure 3.3B**). In patient samples, in which clusters of CTCs were found (n=19), the number of CTCs in clusters compared to the total number of CTCs present as both clusters

and single cells was analyzed. The PV showed a higher median percentage of clustered CTCs to total CTCs when compared to pre-op Pe and intra-op Pe. The PV also showed capture of bigger clusters than the two peripheral sources ($p<0.05$) for clusters with ≥5CTCs and for clusters with ≥10CTCs), whereas no difference was observed among the peripheral sources. Importantly, the number of clusters with >5 or >10 CTCs increased with the disease stage (**Figure 3.3C**). Also, 6/7 (85.7%) patients with >10 CTC clusters had a moderate or poor tumor differentiation grades.

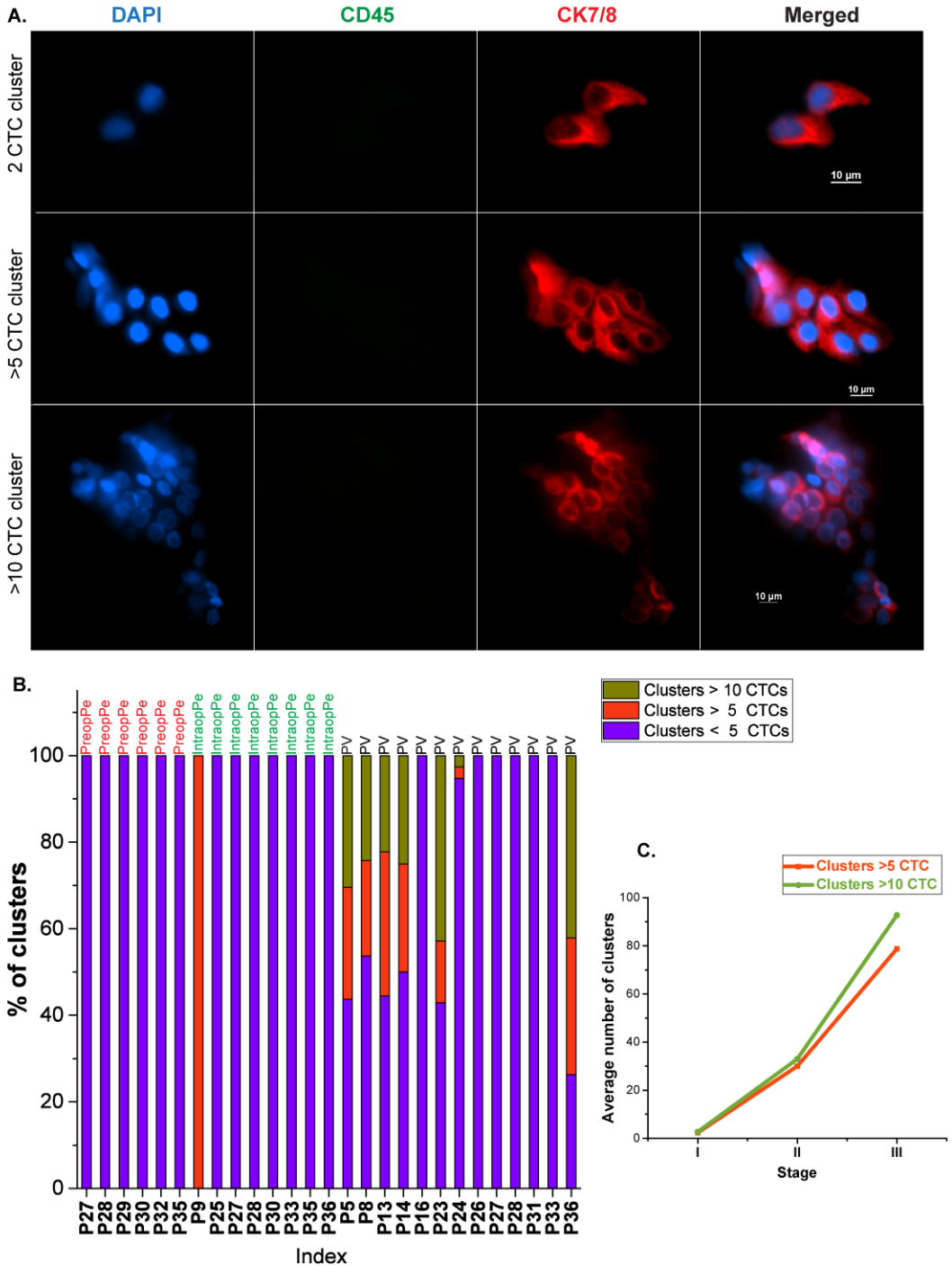

Figure 3.3 CTC clusters in lung cancer patients
(A). Immunofluorescent staining images of captured CTC clusters showing a 2 CTC cluster, >5 CTC cluster, and >10 CTC cluster, (B). Distribution of sizes of the clusters obtained from cluster positive specimens, (C). Trend of average number of 5 CTC and 10 CTC clusters with stage

3.9.3. Monitoring of patients with CTC clusters

CTC clusters have been shown to be associated with a poor prognosis [48, 155]. It is also believed that the cells within clusters can escape cell death [28]. Considering their prognostic significance and their ability to survive, we sought to monitor patients with detectable perioperative CTC clusters. The objective was to examine if the CTC numbers in the peripheral vein during follow-up were associated with the presence of clusters or by higher numbers of CTCs in the PV at the time of resection. For 12 patients, 6 had >1 follow-up time-points, and the median duration at time of follow-up blood draw was 10 months, with a range of 2-26 months. Original analysis had revealed that 4 of these patients had clusters with >10CTCs, one patient had clusters with >5CTCs, 7 patients had clusters of 2-5CTCs evident in their PV, pre-op Pe or intra-op Pe. **Figure 3.4** represents CTCs per 3 ml from the peripheral vein at pre-op, intra-op and post-op Pe time intervals in addition to the follow-up longitudinal time-point(s). CTCs per 3 ml from the PV are also shown for each patient. 7/12 (58.3%) patients had persistent CTCs (>2 CTCs per 3 ml) at their last follow-up time point, and 9/12 (75%) patients had persistent CTCs at any long term time-point. Interestingly, 6/9 (66.7%) patients with at least 50% CTCs found in clusters in any blood source had persistent CTCs at last follow-up. Moreover, surveillance data indicated that out of 7 patients in our cohort who were positive for recurrence, 6 patients had CTC clusters in one or more of their blood sources.

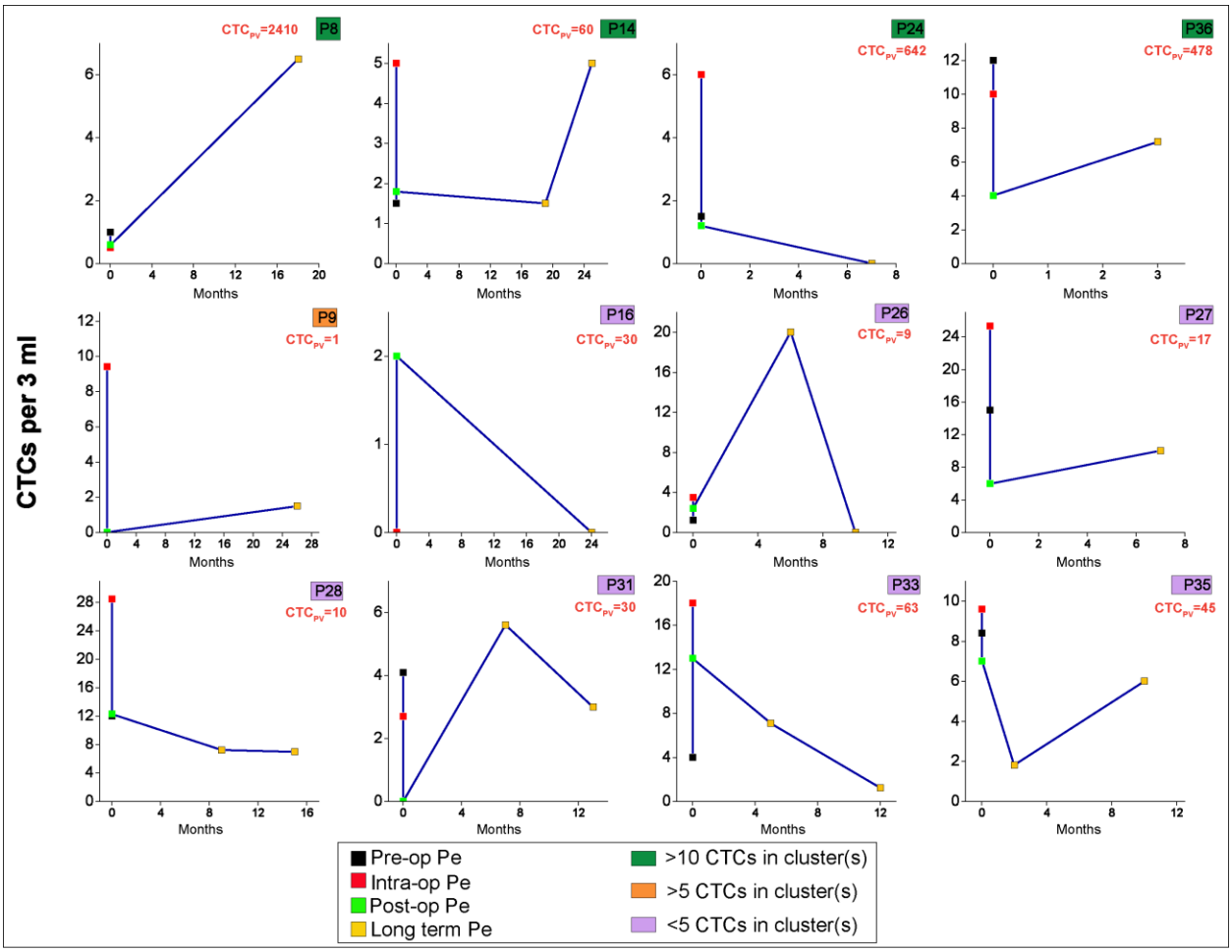

Figure 3.4 Longitudinal monitoring of patients with CTC clusters
PV CTC numbers at initial analysis are indicated in orange. Color keys shown in green, yellow and pink represent cluster sizes.

3.9.4. mRNA expression profiling of captured CTCs

The PV and Pe as sources of CTCs demonstrated macroscopic differences in enumerated CTCs and also populations of cells captured (single or clusters). In order to compare genotypic differences, we examined the CTCs at mRNA transcript level using Fluidigm HD system to perform quantitative RT-PCR for a 96 gene "comprehensive CTC panel". After normalization to internal house-keeping gene *GAPDH* using the ΔCt method [158, 159], the gene expression patterns for PV and Pe specimens were compared (**Figure 3.5, Figure 3.6**).

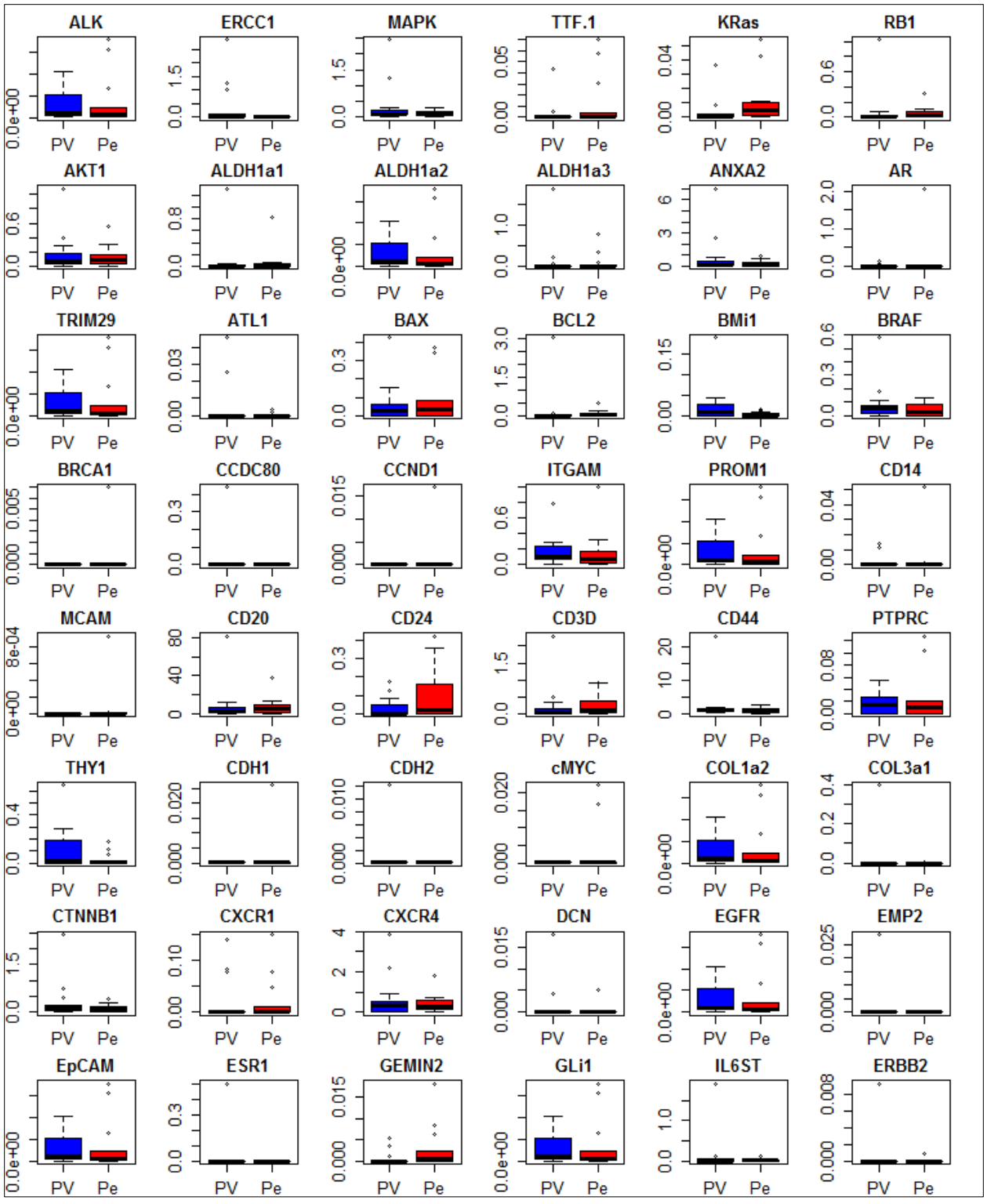

Figure 3.5 Gene expression of CTCs from PV and Pe
Gene expression $2^{-\Delta Ct}$ of selected genes showing expression range among pulmonary vein (PV) and peripheral (Pe) samples from all patient specimens analyzed.

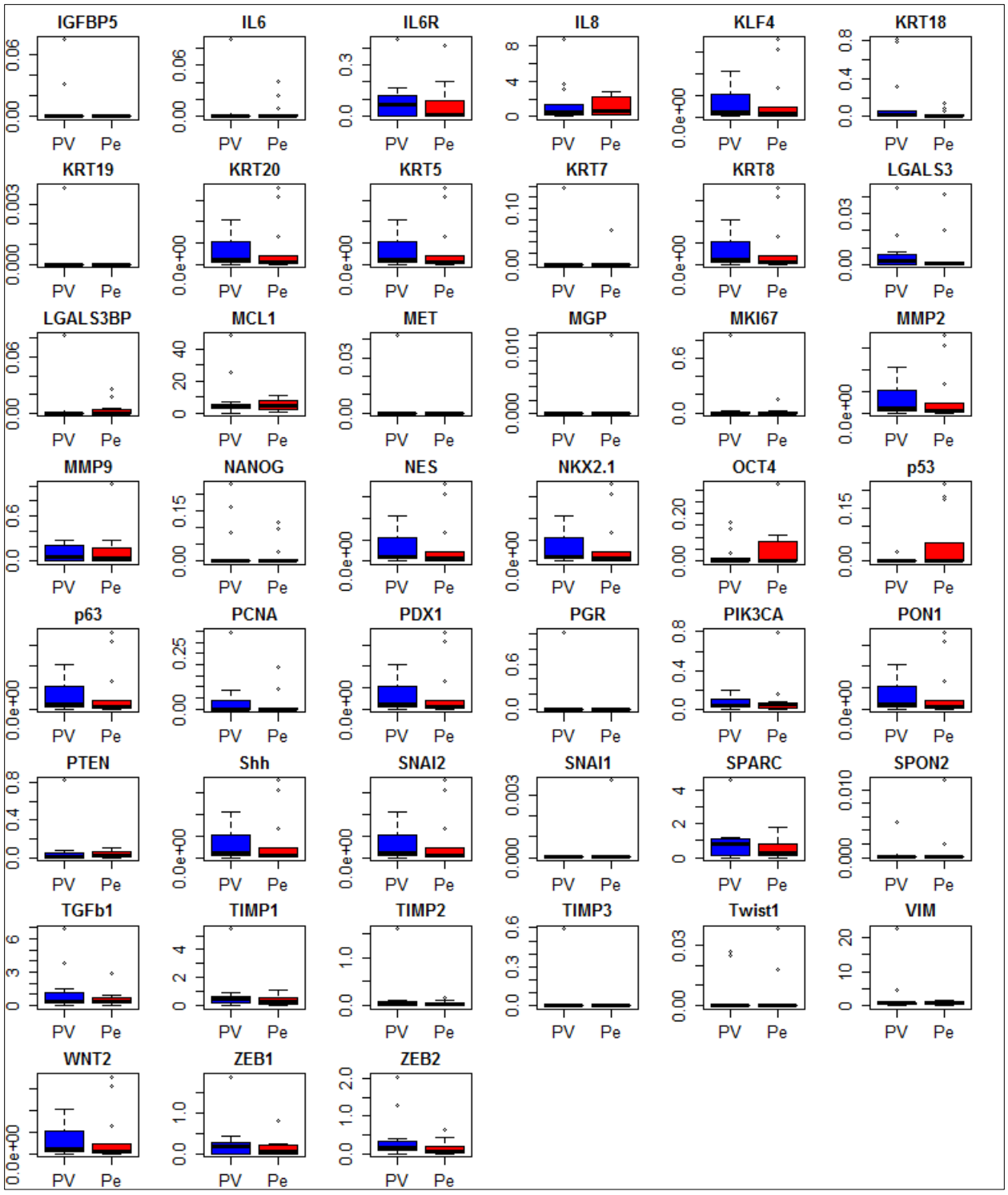

Figure 3.6 Gene expression of CTCs from PV and Pe (continued)
Gene expression $2^{-\Delta Ct}$ of selected genes showing expression range among pulmonary vein (PV) and peripheral (Pe) samples from all patient specimens analyzed.

Figure 3.7A shows a heat map of expression levels of genes among PV and Pe samples grouped according to histology. **Figure 3.7B** shows the range of expression levels relative to *GAPDH* ($2^{-\Delta Ct}$) of the top genes with relative log fold changes (FC) of median PV expression compared to median Pe expression greater than 2. While there were several genes that showed similar expression patterns between PV and Pe, there were many genes differential in expression among the two groups. The genes that are expressed in both sources include "stem" or mesenchymal genes namely *TGFβ1*, *VIM* (Vimentin) and *CD44*, oncogenes including *PIK3CA*, *MAPK1*, *BRAF* and *KRAS*, extracellular matrix (ECM) related genes such as *ANXA2*, *SPARC*, metastasis genes including *MMP9*, *TIMP1*, *TIMP2*, apoptotic genes such as *BAX*, *BCL2* and *MCL1*, and inflammatory or cytokine related genes such as *CXCR4* and *IL8*. Analyzing the differentially expressed genes between the two sources we observed that PV CTCs had higher expression of stem/mesenchymal genes (*ZEB1* and *BMi1*), whereas the Pe CTCs exhibited higher expression of immune modulating genes such as *LGALS3BP*, *NANOG*, *IL6*. Indeed, gene ontology analysis (IPathwayGuide, Advaita Bio) of PV and Pe revealed enrichment of cytokine-related and immune-related GO terms in the PV, suggestive of immune suppressing mechanisms in the Pe. *KRT18* was also noted to have higher median expression in the PV than Pe among all 13 pairs of samples. *ERCC1* also showed greater median expression in PV. The higher expressions of *KRT18*, *ZEB1* and *BMi1* in the PV indicate the presence of EMT-like cells more predominant in the pulmonary vein blood. This was also demonstrated by positive staining of anti-CD44, another EMT-related marker [160], in some of the PV clusters (**Figure 3.8**).

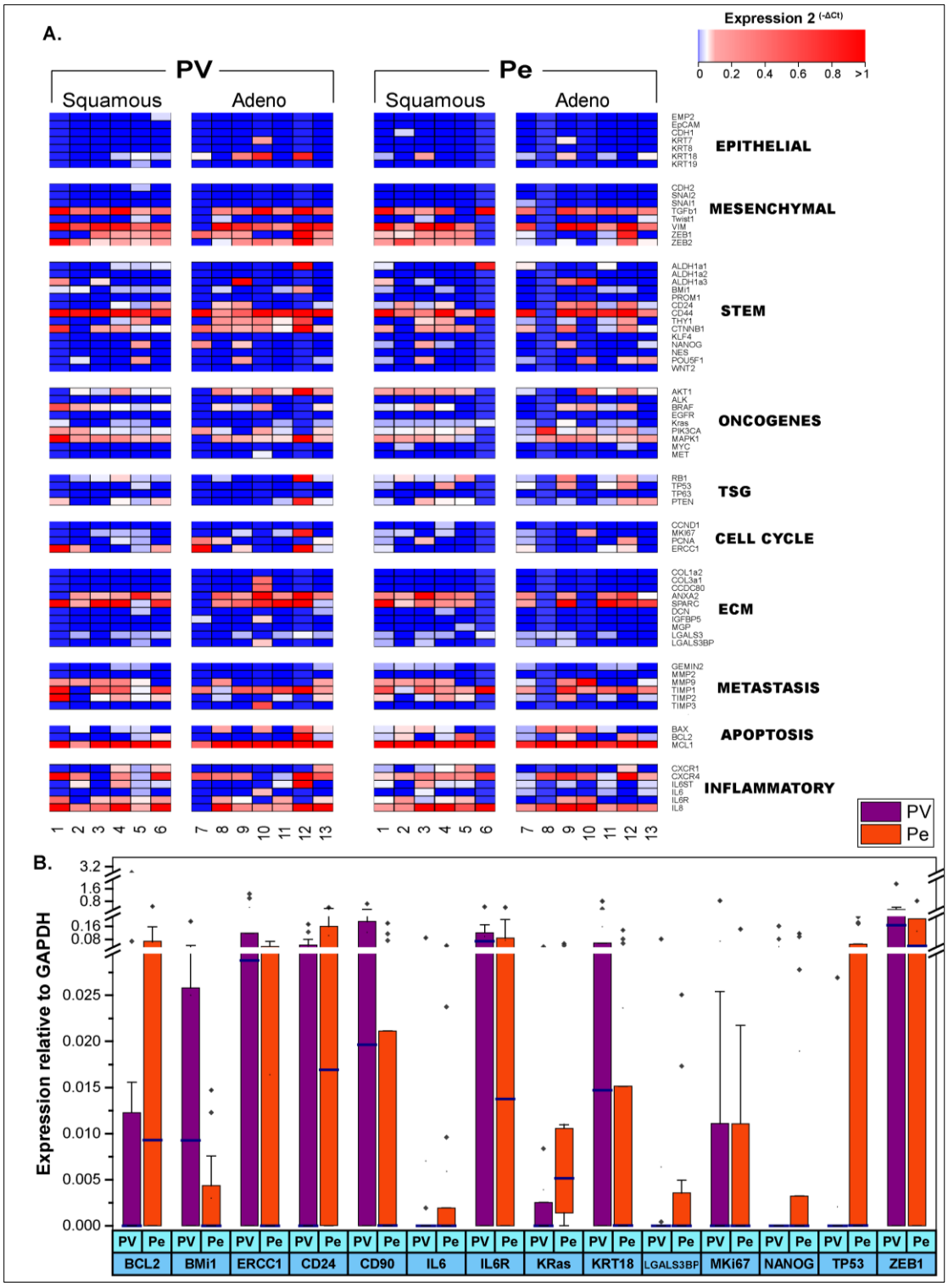

Figure 3.7 Gene expression profile comparison of PV and Pe CTCs
A). Heat map of gene expression levels ($2^{(-\Delta Ct)}$) from paired PV and Pe specimens grouped by histology. Gene categories are represented for epithelial, mesenchymal, stem, oncogenes, tumor suppressor genes (TSG), cell cycle, extra cellular matrix (ECM), metastasis, apoptosis and inflammatory genes. (B). Expression of representative genes differentially expressed among PV and Pe CTCs shown as average $\log_2$ fold change for genes with a >2 log fold change.

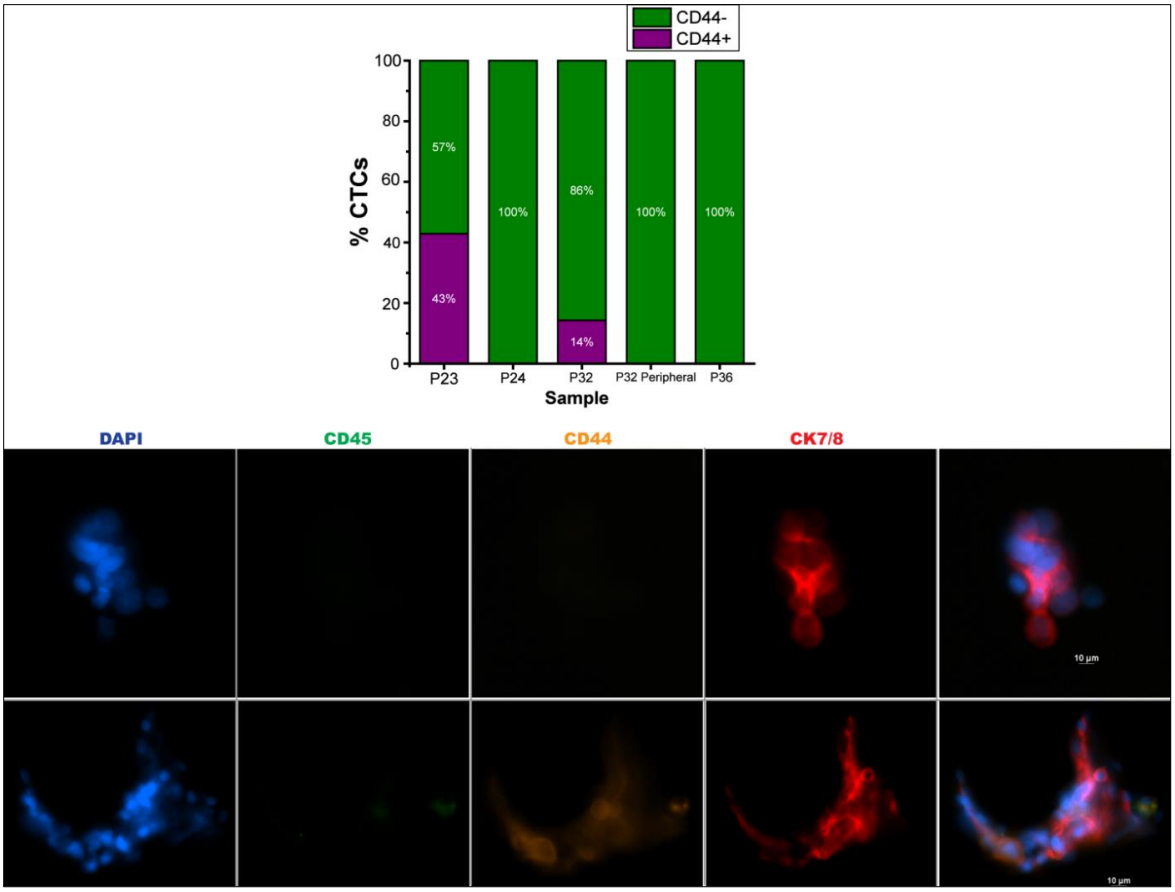

Figure 3.8 CD44 immunostaining of CTCs
CD44 immunostaining of CTCs showing percentage of CD44+ CTCs in patient samples. Panel below shows immunofluorescence images of a CD44- and a CD44+ CTC cluster.

mRNA analysis performed according to the morphological type of CTCs detected in the sample (single or clustered cells) also revealed differential gene expression between CTC clusters and single CTCs. **Figure 3.9A** shows the top genes with a >2 log fold change of the median expression in each group. The clusters showed higher expression of *KRT18* (epithelial/luminal) [31], *BCL2* (anti-apoptotic) [161] and *ERCC1* which is related to chemotherapeutic resistance [162]. **Figure 3.9B** shows a volcano plot of the genes analyzed for differential expression. For a fold change cut-off of 2, there were 14 differentially expressed genes between CTC clusters and single CTC samples. Upon pathway analysis (IPathway Guide, Advaita Bio), the CTC cluster samples showed enrichment of various gene ontology terms linked to cell migration, cell

motility, locomotion and cell adhesion, indicative of the migrative ability of CTC clusters **(Figure 3.9C)**.

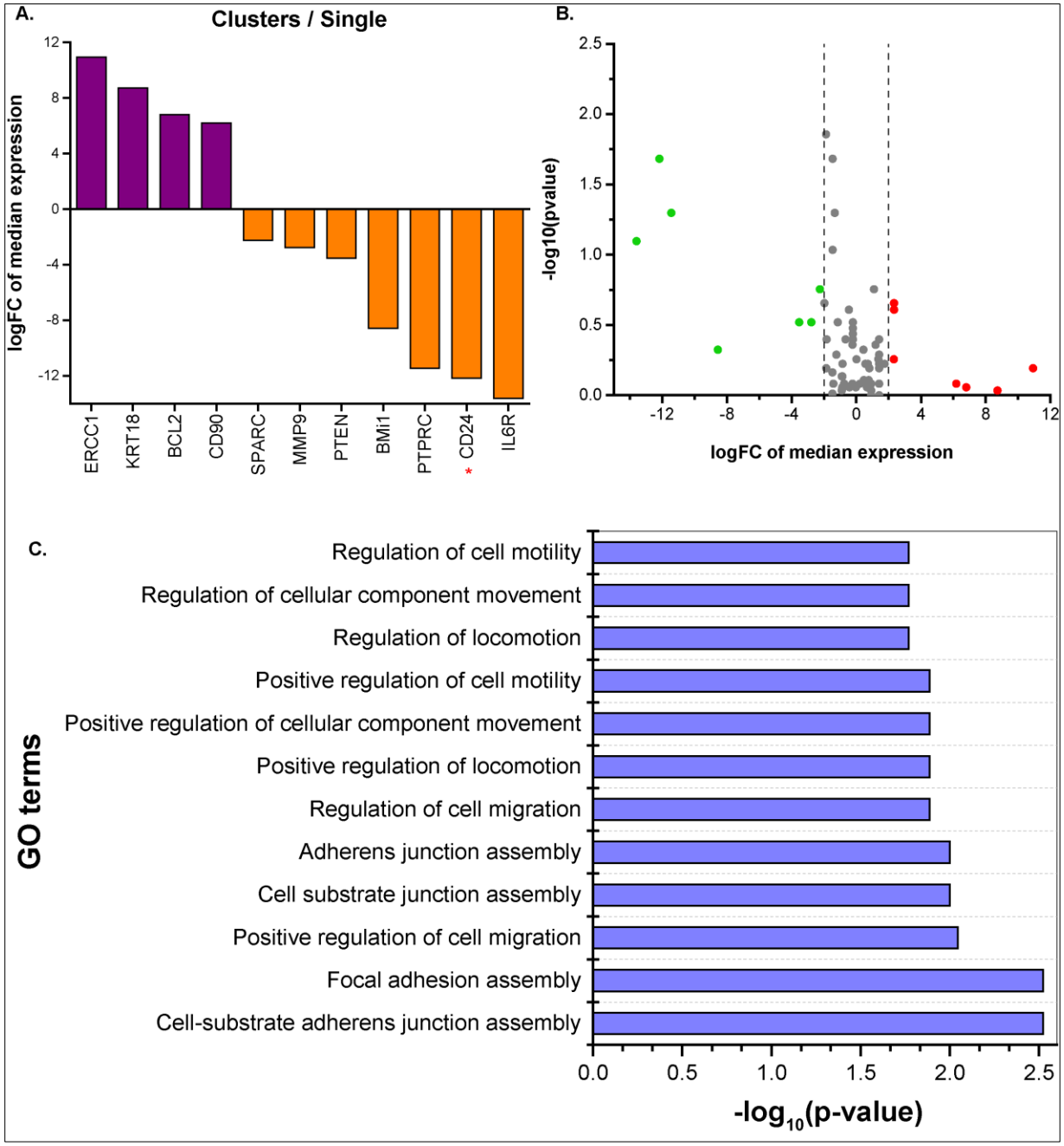

Figure 3.9 Gene expression analysis of CTC clusters and single CTCs
(A). Log_2 fold changes of median expression of clustered CTCs and single CTCs of genes with logFC>2, (B). Volcano plot showing input genes for gene ontology analysis; differentially expressed genes with provided cut-off are shown in green (down-regulated) and red (up-regulated), (C). Top gene ontology terms for cluster vs single CTC comparison.

Upon further analysis, it was revealed that *Ki67*, a proliferation marker, was expressed in 46.2% (6/13) of PV samples, and 38.4% (5/13) of Pe samples. It was also notable that *Ki67* expression was not detected in any of the healthy controls (n=4). Interestingly, 5 out of 6 (83.3%) PV samples positive for *Ki67* expression had single CTCs detected. This is consistent with literature reports indicating that absence of proliferative markers could indicate resistance to chemotherapy treatment [138]. Analysis according to tumor pathology showed that 90.9% of *Ki67* positive samples had a moderate or poor differentiation grade, which showed the potential of CTCs to reflect the aggressiveness of disease similar to pathological criteria. Representative hematoxylin and eosin staining of adenocarcinoma and squamous tumors is shown in **Figure 3.10A**, and immunohistochemistry of primary tumors for Ki67 is shown in **Figure 3.10B**.

Interestingly, the tumor suppressor gene *TP53* was expressed in 6/13 Pe samples and only one of 13 PV samples. Immunohistochemical staining of the primary tumors for p53 **(Figure 3.10C)** revealed positivity in 4 out of 6 samples in the Pe that were positive for RNA expression. Additionally, those patients with negative p53 staining by IHC indicated the same status by RNA expression in the PV with the exception of 1 patient. This seems to suggest that the origin of the pulmonary vein CTCs may be from a p53 negative region of the tumor.

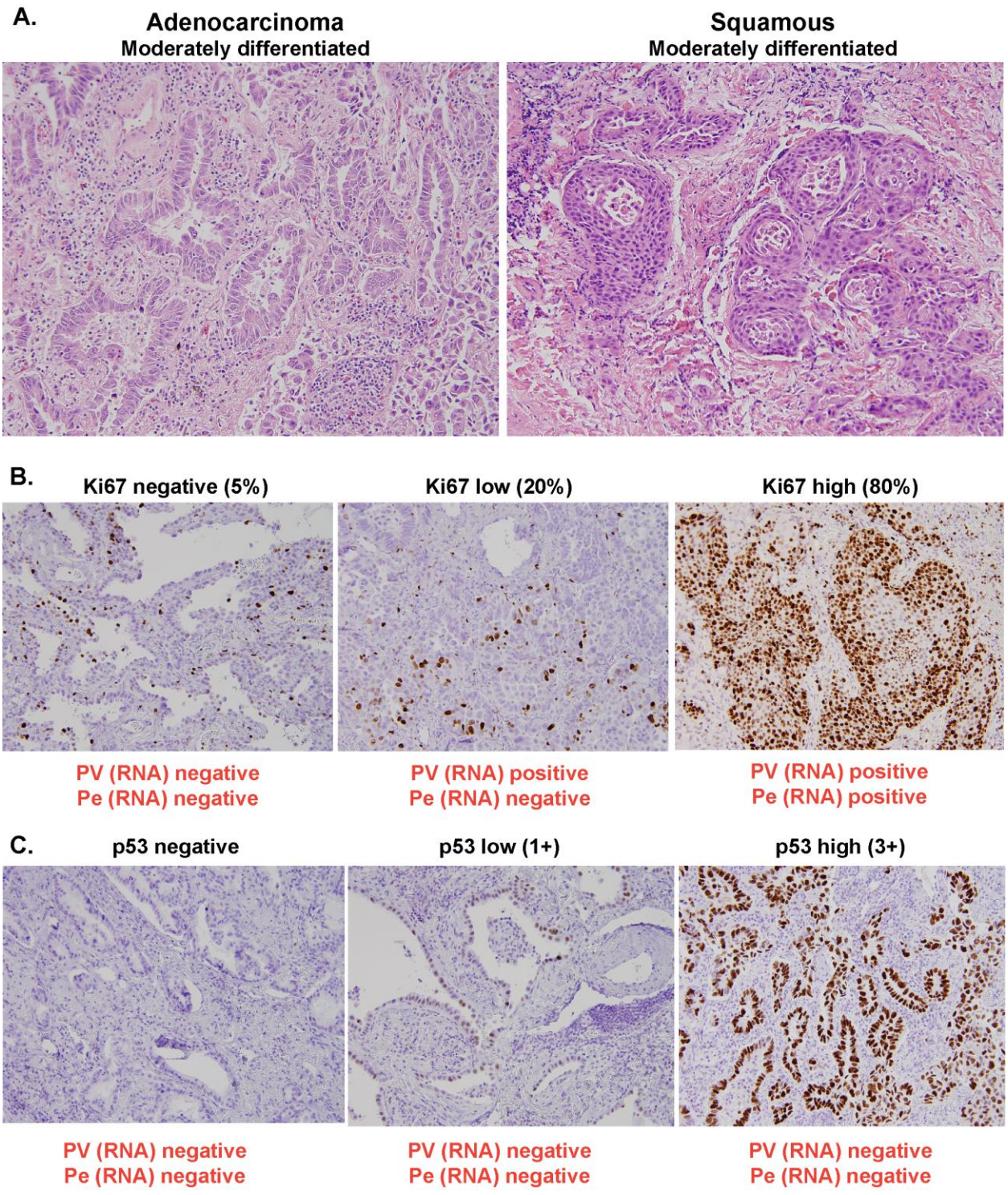

Figure 3.10 Immunohistochemistry of primary tumors
(A). Representative H&E staining images of adenocarcinoma and squamous cell carcinoma of lung cancer patients in the study, (B). Ki67 negative, Ki67 low and Ki67 high primary tumors and their corresponding CTC RNA status, (C). p53 negative, p53 low and p53 high primary tumors and their corresponding CTC RNA status.

3.10. Discussion

The field of circulating tumor cells (CTCs) research has seen many breakthroughs, most if not all, with the common underlying aspect of sampling from the peripheral blood. While the peripheral blood adds convenience to ease sampling constraints, analysis is hindered by issues of skin cell contamination during venipuncture [163], and detection of a diluted concentration of cells as the CTCs are being circulated through the entire vasculature. Despite these challenges, the peripheral blood has the advantage of more closely reflecting the metastasis initiating population of cells [164] since the identified cells would likely be on their passage to distant tumor formation. It would however be illuminating to identify CTCs at every "checkpoint" of their passage from dissemination to new tumor formation, as they can potentially indicate the dynamically changing behavior of tumor cells and the heterogeneity of tumors. We thus chose to study CTCs not only at different time-points, but also from different venous sources - the pulmonary vein presumably reflecting the origin of these escaping cells, and the peripheral vein presumably harboring cancer cells en route to distant metastasis. We have thus followed early stage lung cancer patients undergoing tumor resections through their surgery.

We demonstrate CTC capture and analysis using a high-throughput microfluidic device, the OncoBean Chip [50]. Similar studies have been previously undertaken [152-154, 156, 157, 165-167] in different cancers wherein different anatomical sources were investigated for CTCs. Morphological and molecular heterogeneity were observed in lung CTCs recovered from peripheral and pulmonary vein blood [28, 155]. While reinforcing these heterogeneities, our study also involves genomic profiling through RT-qPCR and long term monitoring of patients with CTC clusters present, as they could have potential prognostic value [48].

Despite being in early stages of tumor formation, CTCs were found in the vast majority of the patient cohort in at least one time-point of blood draw. The pulmonary vein (PV) offers the advantage of being the first tumor draining vein for CTCs before passage of the blood onto the systemic circulation, and was presumed to have an enriched source of CTCs. This was indeed observed to be the case in the present cohort wherein a higher abundance of CTCs was found in comparison to the pre-op and intra-op peripheral samples. On the other hand, the peripheral vein samples collected before and during surgery did not show differences in CTC detection rates, suggesting that the CTC numbers do not vary significantly within a few hours of sampling from the same blood source. However, our data indicate that the PV could be thought of as a "storehouse" for CTCs until such time as they are ready for distant tumor seeding through the circulation. This is supported by the findings by Seinel et al. that the presence of CTCs in the PV is associated with poorer survival [153].

An advantage of the pulmonary vein sampling in combination with microfluidic recovery using the OncoBean Chip was the detection of CTC clusters. CTC clusters were detected in close to half the patient population in at least one time point, with the pulmonary vein accounting for majority of the cluster incidence. Studies have found that CTC clusters or microemboli have more metastatic potential than single CTCs [48, 168], and that cells within the cluster may be protected from immune invasion and survive longer [28]. Liotta et al. also found that bigger clusters produced more metastasis than smaller ones [168]. This may have potential clinical relevance in predicting at resection the possibility of long term recurrence. For instance, 7 of 19 patients positive for clusters had big clusters (comprised of 10 or higher CTCs). These were only observed in the PV, while neither of the two peripheral specimens showed presence of >10 cell clusters. This suggests that most of these CTC clusters in the PV may not be able to enter the

systemic circulation, or that bigger clusters may get lodged in areas of smaller vasculature [135]. Alternatively, the PV could be accounting for the larger chunks of the tumor being shed into circulation, with most of these cells later undergoing anoikis [27, 101] or otherwise leaving the system, and only the ones with the ability to survive the stresses in circulation continuing on [28]. Additionally, 6 of 7 patients with big clusters (10 or higher CTCs) had a moderate or poor differentiation grade, possibly suggestive of disease aggression. This could have further prognostic implications.

Interestingly, many of the clusters observed in the pulmonary vein had a bright intensity of cytokeratin (CK) staining. This was in contrast to single CTCs or CTC clusters from the peripheral blood. We hypothesize that this may be due to CTCs undergoing epithelial mesenchymal transition (EMT) [54, 140] during or en route to peripheral circulation. The weaker CK staining among peripheral blood CTCs is in agreement with Wendel et al. who also suggest that brighter CK might indicate passive cells or cells that may not form new tumors [135].

Gene expression analysis by RT-qPCR revealed differences in the PV and Pe samples suggesting molecular heterogeneity in the two populations. Epithelial to mesenchymal transition (EMT) has been implicated in the tumor dissemination and metastatic process [49]. Our gene expression data reveals the presence of EMT features in cells isolated from both pulmonary vein and peripheral veins. However, the PV shows a higher expression of certain EMT genes. This is expected because these cells are closer to the primary tumor, and were presumably at the switching state from epithelial (in the primary tumor) to the motile EMT state (in circulation) [49]. This also leads us to believe that the cells already disseminated into the pulmonary vein, having migratory features, may be capable of further migrating to distant sites and causing recurrence. Indeed, authors Seinel et al. observed poorer survival of patients who were positive

for CTCs in the pulmonary vein. This has important implications in lung tumor resections, as it evidences that tumor resection must be combined with CTC-eliminating strategies in order for surgery to be “curative”.

More evidence on the possibility of CTC survival is provided by the gene expression profile of peripheral vein CTCs. Genes such as *NANOG*, *LGALS3BP* and *IL6* which are higher in expression in the Pe CTCs in our data, have been implicated in mechanisms of immune evasion [169-171] suggesting that Pe CTCs are able to survive in circulation as they are capable of avoiding immune surveillance. Indeed, *IL6* has been shown to have an activating effect on genes such as *MAPK* which can then promote anti-apoptosis signals [169]. Our data supports this by evidence of *MAPK1* expression in the Pe CTCs, in addition to the higher expression of anti-apoptosis gene *BCL2*.

CTC clusters or microemboli have been observed rarely in breast, prostate and lung cancers [15, 48, 163]. They were shown to increase metastasis in mice models of breast cancer, and also have prognostic significance in predicting survival [48, 155, 172]. Among 13 patients analyzed for mRNA expression profiles, the PV and Pe samples were segregated according to presence (clusters) or absence (single) of CTC clusters. Gene expression analysis revealed higher expression of *KRT18*, *BCL2* and *ERCC1* genes among the clustered CTCs compared to single CTCs. Recent studies in breast cancer have implied that metastatic invasion might be led by cell clusters with epithelial phenotype as evidenced by expression of various Keratins [172, 173]. It has also been demonstrated that the clusters have high expression of adhesion markers, lack of which disrupt clusters and reduce their metastatic ability [48]. The lung CTC clusters in our study exhibited high *KRT18* gene expression, which suggests similar mechanisms of epithelial and adhesion involvement in invasion. CTC clusters have also been previously shown to be

negative for apoptosis [174]. Our data supports this observation by the high expression of the anti-apoptotic *BCL2* gene in the clusters compared to single CTCs. Furthermore, mRNA expression of the excision repair cross complementation 1 (*ERCC1*) gene [175] was observed to be higher in cluster samples in contrast to the single CTC samples. This gene is involved in repair of damaged DNA, and its higher expression in lung CTCs has been correlated to worse progression free survival [175]. Taken together, the genes *KRT18*, *BCL2* and *ERCC1* indicate a survival advantage of the CTC clusters, which also coincides with literature evidence pointing to their ability to evade cell death mechanisms [174].

Gene data analysis using a pathway analysis software (IPathwayGuide, Advaita Bio) showed enrichment of various gene ontology terms involving cell migration, motility and adhesion. CTC clusters are known to have tight cell junctions regulated by various adhesion complexes. Clusters have also been shown to have a higher metastatic capability as compared to single CTCs [172]. Our data additionally indicates that CTC clusters may have higher migratory/motile ability than single CTCs, which might be useful in their metastatic route through the bloodstream.

The most interesting gene expression result in our data was indicated by *Ki67*, a gene related to the proliferation status. Patient specimens showed some level of *Ki67* expression while the healthy controls had no detectable levels of the gene. In addition, 5 out of 6 PV samples that were positive for *Ki67* had single CTCs. While there have been variable reports of *Ki67* in CTCs and CTC clusters [144, 176], it has been theorized that CTC clusters are better able to evade cytotoxic/chemotherapeutic drugs due to absence of proliferation as indicated by *Ki67* [144, 174]. This is also corroborated by the higher expression of *ERCC1* (treatment resistant marker [162]) in the PV clusters as previously mentioned. *Ki67* could thus be a potential biomarker for investigating CTCs in early lung cancer to predict disease progression.

The discordance between the p53 staining of primary tumor and the *TP53* RNA status of the pulmonary vein CTCs leads to interesting insights. This data suggests that tumor cells that are initially shed into the circulation (in the PV) may be originating in the p53 negative regions of the tumor. There have been earlier reports that p53 mutations might not be involved in the cell shedding process [177]. Authors Offner et al. found that disseminated tumor cells in the bone marrow were positive for p53 by immunostaining, despite heterogeneous expression in the primary tumor [177]. Another study showed that while p53 mutations may be acquired later on in the disease, they may not be necessary for dissemination [178]. The fact that p53 negative CTCs in the PV may still be p53 positive in the Pe, might be indicative of the dynamic changes that CTCs undergo in the circulation in order to better survive shear stresses in the flow and/or to be invasive. Another possibility is that p53 may not be transcriptionally active in the released cells [179] i.e. in the PV. DNA damage is one stress mechanism that may activate p53 [179], and the higher expression of the DNA repair gene *ERCC1* in the PV suggests that the DNA repair mechanism was active in the cells released in the PV, thereby preventing activation of p53. The contrasting expression pattern of p53 and *ERCC1* in the Pe also support this conjecture.

The finding of large clusters of CTCs in the pulmonary vein of patients undergoing tumor resections may have clinical significance which impacts long term monitoring. Our study indicates that the PV may harbor CTCs of mixed epithelial and mesenchymal features, and while some of the larger clusters may be filtered by smaller blood vessels, there still may remain a significant number to lead to metastasis and progression. This raises interesting possibilities of addressing tumor resections with therapies to eliminate the PV CTCs as they may manifest in the form of long term recurrence. Put together, the key findings suggest that the PV harbor different

populations of CTCs than the peripheral vein, which may have implications in future assessment of resections and therapy.

3.11. Conclusion

The pulmonary vein (PV) blood drawn during surgical tumor resection, provided an opportunity to assess CTCs in larger numbers than was capable by sampling peripheral vein (Pe) blood alone, in early stage lung cancer. Through this study, we observed several CTC clusters in the PV, which indicated poor prognosis with respect to disease recurrence. Our gene expression data also revealed Ki67 as a promising biomarker, which may be useful in predicting potency of CTCs, which may ultimately help in early detection of disease. Insights into tumor biology were also obtained, such as our findings on CTCs possibly being shed from regions of the tumor with low p53 expression. Additionally, the CTC clusters revealed signatures of higher cell motility and locomotion compared to single CTCs. Overall, the pulmonary vein harbors high number of CTCs even in early stages of lung cancer, which provided important indications into disease progression.

Chapter 4

Characterization of CTC clusters in early stage lung cancer

4.1. Abstract

Circulating tumor cell clusters, also known as circulating tumor microemboli are garnering attention due to their higher metastatic capability in contrast to single CTCs. Studies have shown their utility in prognosis, their ability to metastasize in mice models, and their ability to navigate through the blood circulation. Due to their reported aggressive nature, and through our earlier findings of their higher motility compared to single CTCs, we proposed to probe further into the genomic features of CTC clusters, which were frequently observed in large numbers in the pulmonary vein blood of patients with early stage lung cancer, and compare them to single CTCs. CTC clusters were obtained from the pulmonary vein blood of patients undergoing tumor resections, and clusters and single CTCs were segregated after identification by immunostaining for anti-CD45 and DAPI, followed by removal of CD45 negative cells and cell clusters. The aim of the study involves investigating the gene expression profiles of CTC clusters to understand why they are more potent or survive better than single CTCs in circulation. This preliminary work proposes future work to be undertaken to elucidate molecular characteristics of CTC clusters to understand their potential to impact disease free survival.

4.2. Motivation

Studies on metastasis and the role of circulating tumor cells (CTC) in this process have witnessed tremendous advances over the last decade, and current CTC studies are focused on understanding what makes these cells lethal. Many recent reports have found CTC clusters in patients from lung, prostate, breast, pancreatic cancer and melanoma [15, 48, 87, 163, 180, 181]. Early investigations demonstrated findings of tumor cell clusters or microemboli in the blood, and it was found that larger clusters produced more metastases [168, 182]. For a long time it was unclear whether these tumor cells aggregated in circulation, or were released by the tumor as clumps. In 2014, Aceto et al. provided evidence that tumor cell clusters in breast cancer originated from oligoclonal populations, and showed higher metastatic capability than single CTCs in mice [48]. Clusters were also found to correlate to worse prognosis in breast and prostate cancer patients. Using RNA sequencing, they identified plakoglobin, an adherens junction protein as instrumental in cell clumping and consequent metastasis formation [48]. Another independent study of breast cancer CTC clusters reported similar findings of higher metastasis and involvement of adhesion genes, and further described the implication of Keratin 14 (K14) in the invasion process [87]. Earlier theories of tumor microemboli entrapment in capillaries leading to arrest and extravasation at these sites, were also challenged by recent findings by Au et al. that clusters are indeed capable of squeezing through much smaller capillaries [183]. Through computational simulations and microfluidic models, the authors demonstrated that clusters can align themselves in a single file in order to maneuver through narrow channels [183].

Microfluidic devices are capable of capturing CTC clusters. One of the earliest evidences of microfluidic capture of CTC clusters was shown in the Herringbone (HB)-chip that captured CTC clusters of 4-12 cells against EpCAM coated surfaces from prostate and lung cancer patients [15]. Clusters of CTCs have also been detected using the CTC-iChip [11], a centrifugal force based microfluidic chip [76], and a nanomaterial based device that is capable of capture and release of CTCs [184]. Many affinity-based devices achieve capture by tethering of cells irreversibly, which can be a significant hindrance in single cell analysis [55, 185]. Biomaterials and polymer composites are now exploited in fabrication of microfluidic devices to enable reversible capture or release of viable captured cells [55, 184, 185]. One such device developed in our group, utilizes a thermal sensitive polymer, with the ability to capture cells at room temperature followed by viable cell release upon lowering the temperature [185]. In our future work, we aim to develop an improved high-throughput version of this device in order to match clinical blood volumes. As a proof of concept, we performed preliminary genomic analysis from CTC clusters using RNA extracted from fixed cells that had been captured on the OncoBean Chip.

4.3. Materials and Methods

4.3.1. Cell line optimization for CTC cluster processing

H1650 or MCF7 cells were plated on non-adherent or low adhesion well plates. After 2 days, cells were observed to clump together in suspension. If cells adhered onto the surfaces, they were released by partial trypsinization to preserve clumps [48]. Cell clusters were labeled with CellMask Orange (Invitrogen) fluorescent dye. Cells were then spiked into buffer and captured on EpCAM-coated OncoBean Chip. Following fixation with 4% para-formaldehyde, devices

were stored at 4 °C until use. Before RNA extraction, clusters were located and the PDMS chambers were punched and RNA was extracted using the RNeasy FFPE kit (Qiagen).

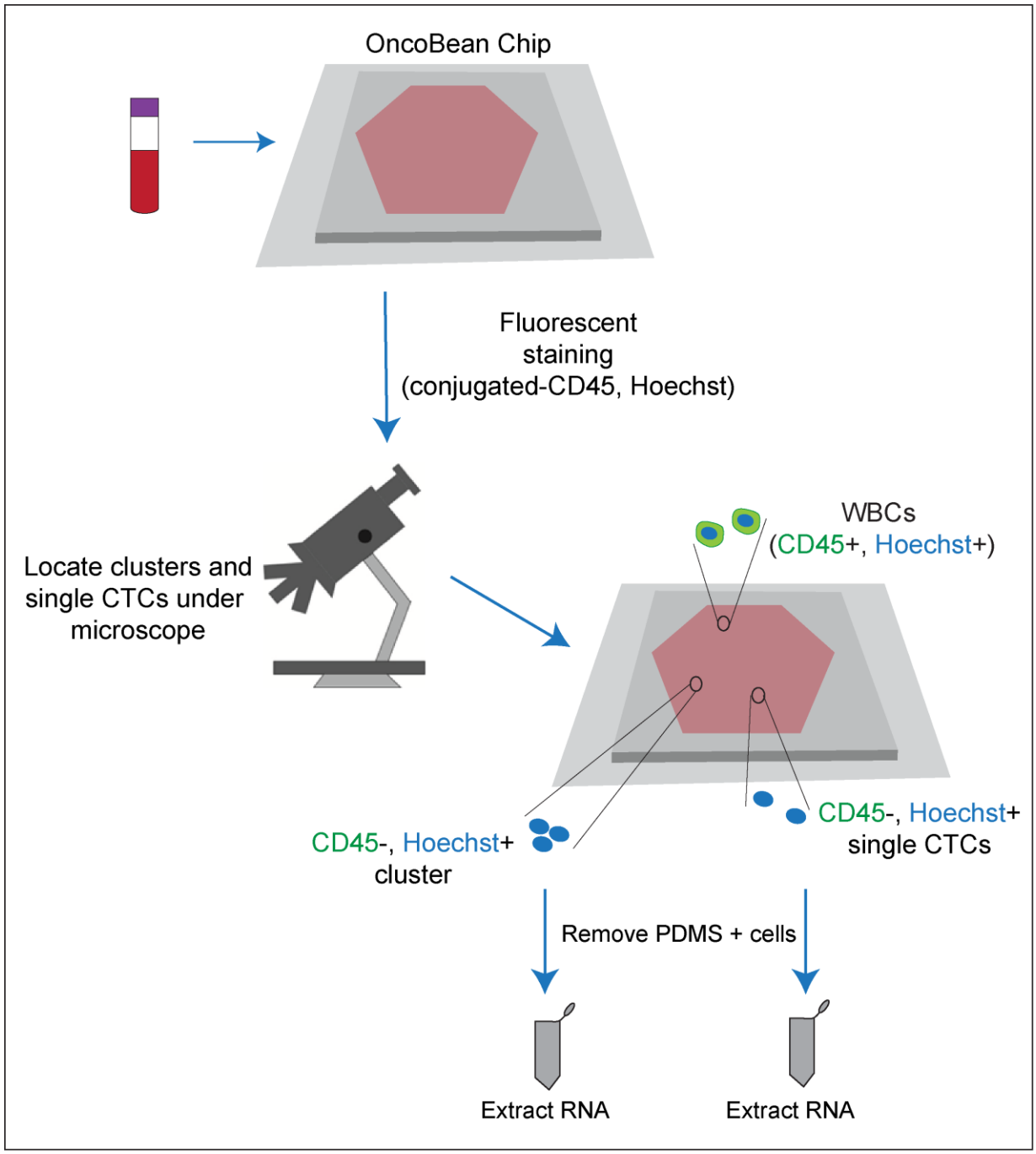

Figure 4.1 Schematic of CTC cluster and single CTC analysis
Pulmonary vein (PV) blood will be processed through the OncoBean Chip. After capture, cells will be stained with AF488 conjugated CD45 and Hoechst followed by microscopic imaging. CD45- clusters and single CTCs will be located on the device, and regions of interest will be removed by punching of PDMS (embedded with cells). This will be followed by RNA extraction using the RNeasy FFPE kit.

4.3.2. Blood sample processing

Previously described protocols for antibody immobilization were observed. Pulmonary vein blood was procured from patients undergoing tumor resection as described in Chapter 3. Procedures consequent to cell capture and PBS wash were modified as follows. After a brief PBS wash, anti-CD45 was applied and live cells were allowed to incubate at 4 °C overnight. Next day, devices were washed with PBS and secondary stain was applied if needed, followed by Hoechst nuclear stain. Devices were then fresh fixed with 4% para-formaldehyde before or during microscopic imaging, and RNA extracted if applicable, within 2 days (**Figure 4.1**).

4.3.3. Cell isolation and RNA extraction process

Devices freshly stained for CD45 were immediately imaged under a Nikon Ti Eclipse fluorescence microscope. Spatial locations of groups of 2 or more Hoechst positive cells, absent for CD45 staining, were identified. Single CTCs (absent for CD45) were also identified when feasible. As controls, a few white blood cells (WBCs) (positive for CD45) were also noted. These locations were carefully punched out from the glass slide, and immediately transferred to a microcentrifuge tube. Clusters from the same patient sample were pooled together to increase the feasibility of sufficient RNA procurement. The same was performed for single CTCs or WBCs. RNA was extracted using Qiagen's RNeasy FFPE kit following manufacturer's protocol for "microdissected FFPE tissue sections". Purified RNA was then stored at -80°C until use.

4.3.4. qRT-PCR

Total RNA extracted using the Qiagen kit will be used for cDNA synthesis, followed by preamplification for 96 genes, which will then be subjected to RT-qPCR using the Biomark HD

system (Fluidigm). The gene set **(Table 4.1)** will be comprised of genes implicated in CTC clusters and single CTC –related pathways [48, 49, 100, 101, 176].

Table 4.1 Gene set for analysis of CTC clusters and single CTCs

GAPDH	ACTB	EPCAM	VIMENTIN	ERBB2	CD24	CD44	CD44v6
CD133	ALDH1A1	ALDH1A3	CDH1	CDH2	TGFB1	BCL2	CTNNB1
KRT5	KRT7	KRT8	KRT14	EMP2	TP53	PTEN	RB1
MMP2	MMP9	TIMP1	TIMP2	PD-1	PDL-1	COL1A2	LGALS3BP
JUP	EVPL	NTRK2	MUC1	PSME3	XBP1	FOXC1	FOXC2
ELF3	CHP1	PKP2	CDH11	BCL-xL	XIAP	CASP3	UBB
SERPINB6	DSP	MLPH	TACSTD2	CTNND1	CTNNA1	NFKB1	AR
TMPRSS2	CXCL16	ETV1	ERG	KLK3	FOLH1	PTCH1	PTPRN2
IL6	IL8	MTOR	ALK	EGFR	BMi1	COL3A1	PIK3CA
CXCR1	CXCR4	ERCC1	KLF4	MAPK1	IGFBP5	ZEB1	ZEB2
MKI67	BAX	HOTAIR	KRAS	CCND1	SPARC	SNAI1	SNAI2
CD3D	CD11B	CD20	CD33	CD34	CD45	CD146	FGF18

4.4. Results

4.4.1. Capture of CTC clusters

Four patients formed the initial study cohort, who provided pulmonary vein blood that was split and processed on two devices under identical capture conditions. Post-processing of the cells was performed as described above. For the enumeration device, CTCs were assessed by positivity of CK7/8 and DAPI, and absence of CD45. One out of four patients had 6 CTC clusters detected on the device, consisting of 15 CTCs in clusters and 17 CTCs as single cells, and a total of 40 CTCs calculated to a volume of 3 ml. The three other patients had 4.6, 0 and 3.5 CTCs per 3 ml.

4.4.2. Quality control for RNA extraction (spike in experiments)

Due to concerns on RNA degradation caused by formalin fixing, quality control checks were performed for RNA extracted using the protocols described above. RNA quality was determined using the Agilent Bioanalyzer system (DNA sequencing core, University of Michigan). Different fixing durations and different conditions of samples (live or fixed) were tested using clusters generated from cell lines and captured on the device. Five conditions were tested – fixed 3 weeks, fixed 5 weeks, fixed 2 days, live cells captured on device, and direct spiking of live cells into the extraction buffer. Longer fixing times served to represent clinical samples that have been stored long term, while the minimum fixing time of 2 days was chosen to account for cell capture and staining durations. It was observed that RNA quality was poor for samples fixed more than 3 weeks (**Table 4.2**). Live cells represented the best RNA quality, closely followed by cells that had been fixed for 2 days.

Table 4.2 RNA Quality Control

Sample	Cells	Fixing duration	Number of PDMS regions extracted	RNA concentration	260/280	RNA Integrity Number (RIN)
1	H1650	Fixed 3 weeks	5	53 pg/ul	1.46	1
2	H1650	Fixed 5 weeks	5	74 pg/ul	1.26	1
3	MCF7	Fixed 2 days	2	23 ng/ul	1.74	5.6
4	MCF7	Live on device	2	37 ng/ul	1.82	6.5
5	MCF7	Live cells (direct extraction by spiking)	-	1371 pg/ul	1.42	7.2

4.4.3. RT-qPCR test for cell spike for RNA controls

Samples 2-5 shown in **Table 4.2** were subjected to RT-qPCR using Biomark HD. All samples except sample 2 showed good gene expression profiles as gauged by raw Ct values (**Figure 4.2**). The gene expression profile of sample 2 suggested RNA degradation, likely due to the high fixing duration.

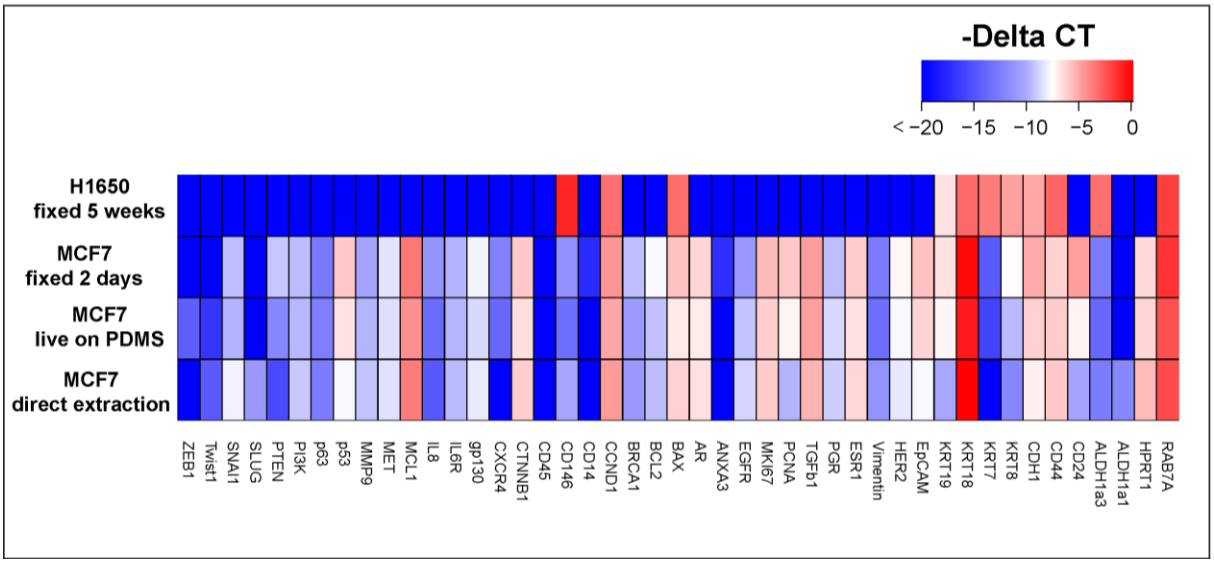

Figure 4.2 Heatmap showing expression profile of cell line spiked controls
Heatmap shows –Delta Ct profiles of selected genes after RNA extraction from cells captured on the OncoBean Chip to test quality of RNA after fixing.

4.4.4. Quality control for RNA extraction (patient samples)

After microscopic imaging of captured cells, putative CTCs and CTC clusters were isolated, and RNA was extracted from punched PDMS samples as described. Retrospective analysis revealed only one patient with positive CTC clusters, and the RNA of extracted clusters was determined to have a 260/280 ratio of 1.63, deeming it of sufficient quality for subsequent analysis (**Table 4.3**).

Table 4.3 Capture of CTC clusters and RNA extraction from patient samples

Sample	Number of PDMS regions extracted	RNA concentration	260/280	RNA Integrity Number (RIN)	Clusters
PV-31 “Clusters”	2	89 pg/ul	1.22	1.1	No
PV-32 “Clusters”	4	302 pg/ul	1.33	1.9	No
PV-32 “WBCs”	5	107 pg/ul	1.39	2.5	-
PV-33 “Clusters”	4	95 pg/ul	1.63	1.6	Yes
PV-33 “Single”	4	75 pg/ul	1.28	2.1	-

4.5. Conclusion

The analysis of CTC clusters and single CTCs individually was limited by lack of cell releasing capabilities on the OncoBean Chip. This was resolved by developing a method for removal of immobilized cells along with the embedding substrate (PDMS), followed by RNA extraction from fixed cells. Cells were captured on the microfluidic device and were identified using immunofluorescence staining for CD45 and Hoechst. Cells and cell clusters absent for CD45, and positive for the nuclear stain were located, and the PDMS regions were extracted. RNA was extracted using the Qiagen RNeasy FFPE kit, and fixing durations were optimized with cell line experiments for obtaining RNA of optimal quality. Patient samples were also processed for obtaining CTC clusters. The analysis of the gene expression profiles will potentially reveal the significance of cancer cell clusters in circulation.

Chapter 5

Application of high-throughput microfluidic device in the identification of CTCs in other cancers

5.1. Abstract

Circulating tumor cells (CTCs) have found widespread use in cancer research due to the relative ease of blood sampling, in contrast to standard tissue biopsies. They have been identified as prognostic indicators in breast, colon and prostate cancer. CTCs have also been proven useful monitoring aids to predict treatment efficacy or changing tumor burden. They have been studied in a variety of cancers such as breast, colon, prostate, lung, pancreatic, renal cancers, melanoma and various other malignancies. In this study, the aforementioned OncoBean Chip, a radial flow microfluidic device enabling high-throughput CTC capture by antibody-antigen interactions, was utilized for the identification and characterization of CTCs from melanoma (skin cancer) patients, wherein CTCs are presumably devoid of the commonly-used Epithelial Cell Adhesion Molecular (EpCAM) antigen. Melanoma CTCs from 11 patients were captured by the use of a cocktail of MCAM (CD146) and MCSP antibodies. A range of 1.2 to 10.5 CTCs per 3 ml were observed, with a mean count of 3.7 CTCs per 3 ml. The captured CTCs will be characterized by downstream analysis of RNA for frequently mutated genes in melanoma such as BRAF. The study demonstrates the versatility of the OncoBean Chip in being tailored for CTC capture in any type of cancer with known biomarkers.

5.2. Motivation

Melanoma is an aggressive cancer of the skin originating from melanocytes in the epidermal skin layer [186]. With a high incidence of mortality, melanoma metastasis is believed to be an early event and may be local or distant [186, 187]. With metastatic disease, the 5-year survival rate can be as low as 6% and poses limited treatment options [186]. The poor survival calls for detection of disease well in advance of clinically detectable metastasis [186]. Circulating tumor cells or CTCs act as couriers of metastasis and serve to offer prognostic and clinically useful information about tumors [4, 9]. Their presence in the blood provides a less-invasive blood-based biopsy of the tumor [8]. Indeed, melanoma was the first solid tumor with detectable CTCs, detected at the time by reverse-transcriptase polymerase chain reaction [19, 188].

There have been very few studies characterizing melanoma CTCs, also known as circulating melanoma cells (CMCs). Of these studies, a very small percentage has demonstrated CTC isolation with the use of microfluidics, a platform that enables an efficient and sensitive isolation strategy for rare cells like CTCs [15]. Luo et al. used the ^{HB}CTC-Chip for the capture of CTCs from melanoma mouse models and monitored CTC numbers through treatment with a BRAF inhibitor, and demonstrated CTC isolation in 41 patient samples [189]. Another study used an improved version of the nanovelcro chip for melanoma CTC capture against the CD146 antigen, followed by retrieval of single cells for genomic analysis [35]. The authors demonstrated a proof-of-concept study of two metastatic patients with a BRAF mutation that could also be detected in CTCs isolated from the patients [35]. Other studies utilizing approaches other than microfluidics include the CellSearch platform using melanoma specific markers [190], *in vivo*

CTC detection by photoacoustic flow cytometry [191], plating of cells on glass slide [192], immunomagnetic CTC sorting [193] and size-based filtration [63].

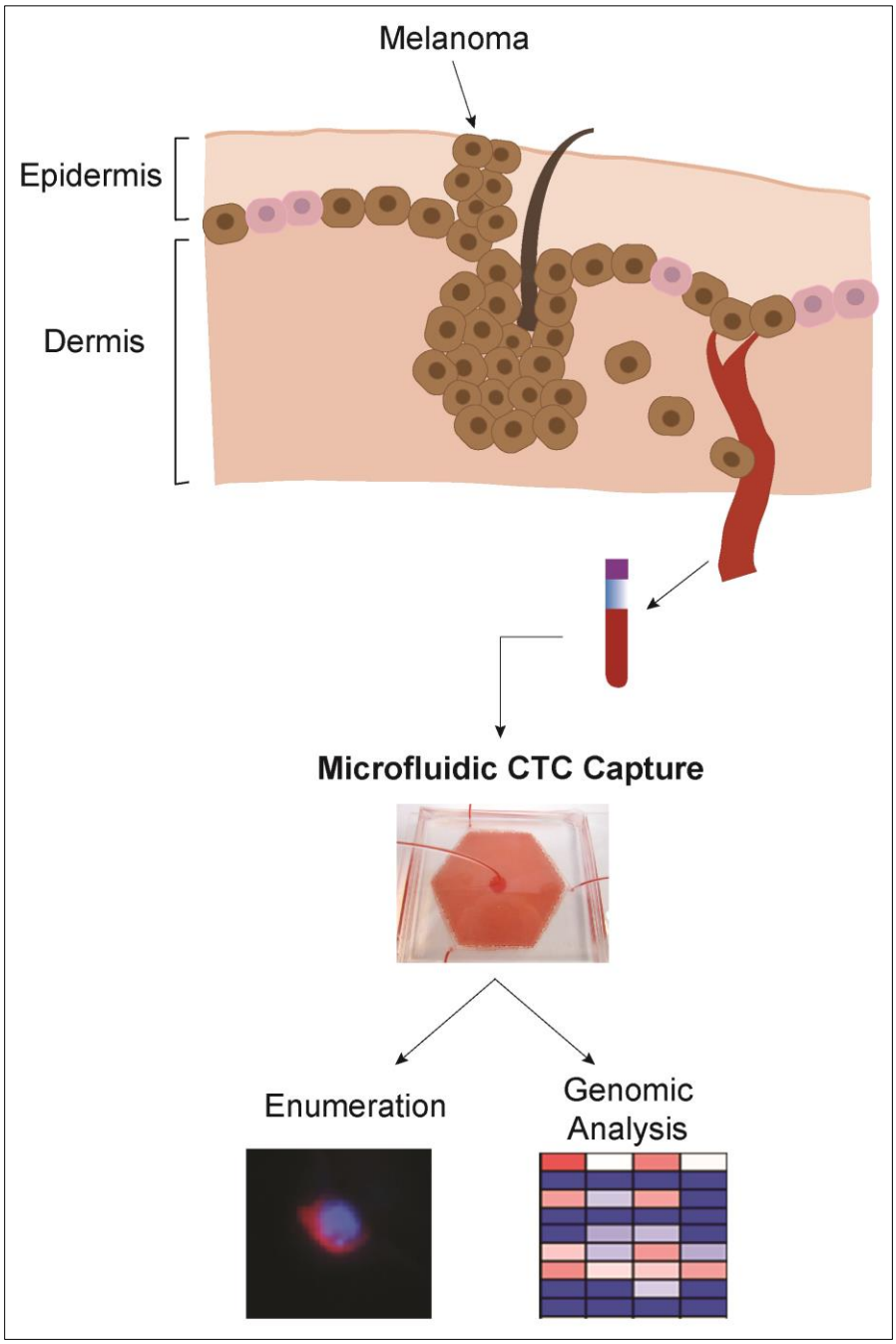

Figure 5.1 Schematic of melanoma CTC study
Melanoma originates in the epidermal skin layer, and disseminates into the lymphatic system and blood circulation to cause metastasis. Blood from melanoma patients is processed through the microfluidic OncoBean Chip, and CTCs are captured for enumerative and genomic analyses.

Melanoma CTCs cannot be isolated by Epithelial Cell Adhesion Molecule (EpCAM) -based strategies due to their lack of surface EpCAM expression [189]. Various other markers have been explored in melanoma, such as tyrosinase, S100, Melan-A/MART-1, MCSP and MCAM [194]. MCAM or melanoma cell adhesion molecule, also known as CD146, is implicated in melanoma metastasis and progression [195], and a few investigators have demonstrated its use in the immunomagnetic capture of melanoma CTCs [192, 196]. Melanoma-associated chondroitin sulphate proteoglycan (MCSP), also known as high molecular weight melanoma-associated antigen (HMW-MAA) is abundantly expressed in 80-85% of melanoma tumors [192, 195]. Melanoma antigen recognized by T cells-1 (MART-1) or Melan-A is a melanoma specific antigen that has been detected in late stage melanoma patients [195]. S100β is a routine marker for histological analysis of melanoma tumors [195]. In the proposed study (**Figure 5.1**), we have thus chosen to use a cocktail of MCAM and MCSP antibodies for circulating melanoma cell capture, followed by detection by the use of combined Melan-A and S100 antibodies. The use of antibody cocktails has shown effective capture of circulating tumor cells in a number of studies [31, 37].

5.3. Materials and Methods

5.3.1. Cell culture and labeling

Melanoma cell line SK-Mel-103 was grown in adherent cell culture flasks at 37 °C and 5% CO_2. DMEM media supplemented with 10% fetal bovine serum (FBS) and 1% antibiotic-antimycotic was renewed every 2-3 days. Cells were passaged with 0.05% Trypsin - 0.53mM EDTA. Cells at 70-80% confluence were split and labeled with fluorescent dye CellTracker Green (Life

Technologies) or CellMask Orange (Life Technologies). Labeled cells were spiked into blood at a concentration of 1000 cells/ml for cell capture experiments.

5.3.2. Strategy of melanoma CTC study

Patients were enrolled into the study with informed consent. Out of 11 patients, 1 had unknown clinical status. Of the 10 remaining patients, 7 were male and 3 were female. The median age of the 10 patients was 73.5 years. 4 patients had stage I disease, 4 patients had stage II disease and 2 patients had stage III disease. Whole blood drawn into EDTA tubes was processed through the OncoBean Chip coated with a combination of MCAM and MCSP, at a flow rate of 5 ml/hr. An average of 3.4 ml of blood was processed through the device.

5.3.3. Isolation and identification of melanoma CTCs

Previously described protocol for whole blood processing was followed [8, 50]. Briefly, a combination of 10ug/ml each of biotinylated MCAM (Miltenyi-Biotec) and biotinylated MCSP (RnD Systems) were immobilized on the OncoBean Chip. After a brief wash, devices were blocked with 3% bovine serum albumin (BSA). Whole blood was then processed at 5 ml/hr. This was followed by washing with phosphate buffer saline (PBS) and fixing the cells with 4% PFA for enumeration. On a parallel device where the same processing methods were observed, the washing step was followed by lysing of cells using the Arcturus PicoPure RNA extraction buffer.

Fixed cells were immunostained after permeabilizing with 0.2% Triton-X 100 and blocking with 3% bovine serum albumin + 2% normal goat serum. Primary antibodies used for immunostaining were Melan-A (RnD Systems), S100 (Life Technologies/ Thermo Fisher Scientific) (cocktail) and CD45 (Santa Cruz Biotechnology), which were visualized with secondary antibodies Alexa Fluor 546 and Alexa Fluor 488 respectively. DAPI was used to stain

the nuclei. Devices were automatically scanned under a fluorescence microscope (Nikon Ti Eclipse). A positive melanoma CTC was scored as Melan-A + S100 cocktail positive, CD45 negative and DAPI positive **(Figure 5.2A)**.

5.4. Results

5.4.1. Cell capture optimization

SK-Mel-103 cells were fluorescently labeled and spiked into blood. Cells captured on the device were fixed, permeabilized and stained for DAPI. After a quick microscope scan, number of captured cells were manually counted and compared with the original number of cells spiked. Cell line capture in blood at 5 ml/hr against MCAM and MCSP gave a mean capture efficiency of 73.6% (**Figure 5.2B**) from two experiments.

5.4.2. Melanoma CTC capture from patient specimens

Patient blood was processed on the OncoBean Chip at 5 ml/hr and cells were captured against MCAM and MCSP antibodies. CTC identification criteria included Melan-A+S100 positive, CD45 negative and DAPI positive. A total of 11 patients were included in the study. At least 1 CTC was detected in 11/11 (100%) patients (**Figure 5.2C**). A mean and median of 3.7 CTCs and 3.0 CTCs per 3 ml respectively, and a range of 1.2 to 10.5 CTCs per 3 ml were detected in all patients.

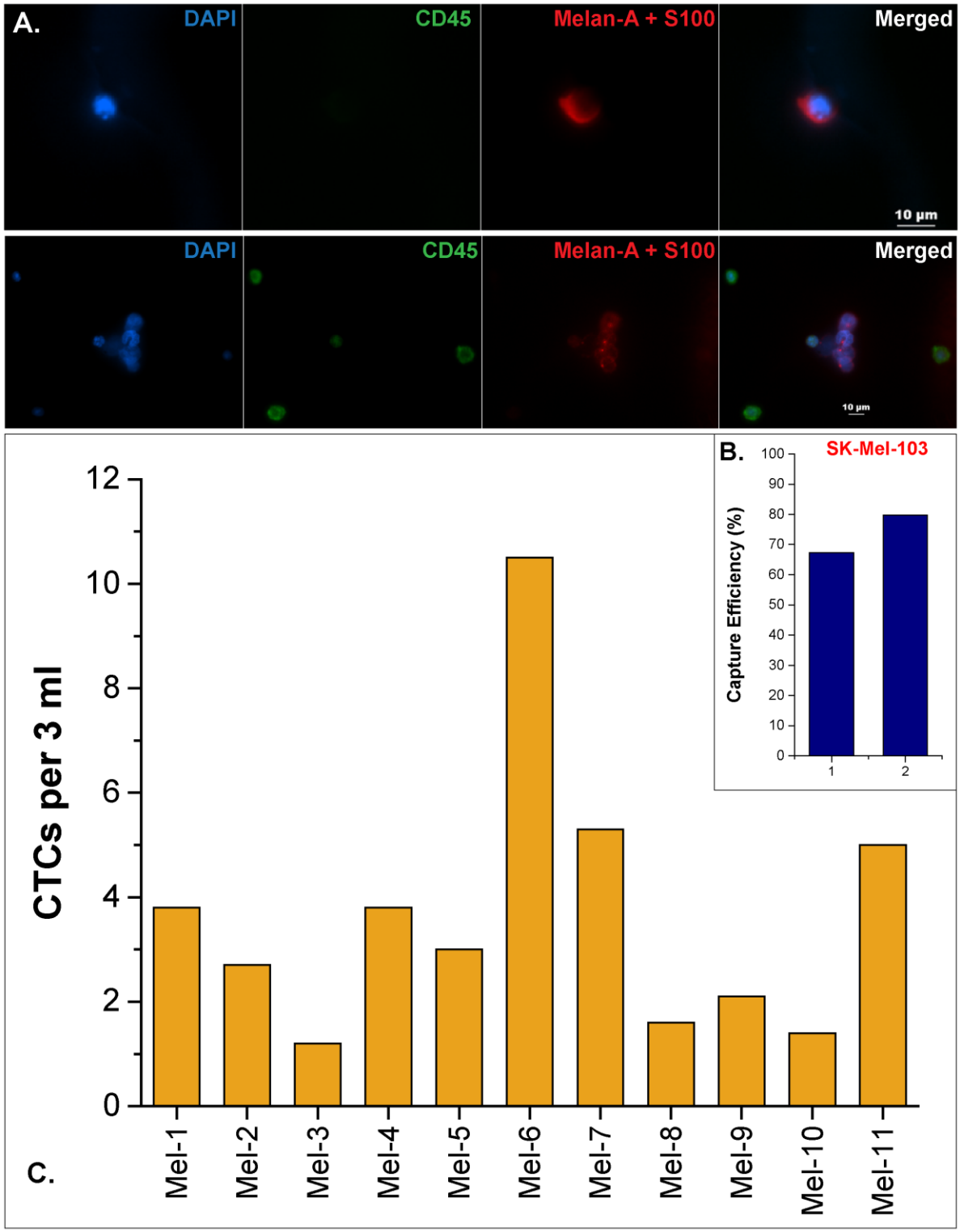

Figure 5.2 CTC capture and identification in melanoma
(A). Immunofluorescent staining showing a single CTC and a CTC cluster positive for Melan-A+S100 and DAPI; white blood cells are shown as CD45 positive (green), (B). Cell capture optimization of OncoBean Chip with SK-Mel-103 cells showing capture efficiency in blood from two experiments, (C). CTC enumeration from patient specimens ('Mel') and healthy controls ('H').

5.5. Future Work

5.5.1. CTC capture from healthy and metastatic patient specimens (ongoing)

The next goals for the melanoma CTC study include processing of blood samples from healthy volunteers and metastatic/late-stage melanoma patients in order to obtain quantitative estimates of the CTC burden for negative and positive controls respectively. Whole blood from five healthy donors and five advanced disease patients will be processed as above, at 5 ml/hr against MCAM and MCSP targets. The average CTCs per 3ml from healthy controls will be used as a threshold for positivity of patient specimens.

5.5.2. Genomic characterization of melanoma CTCs

Captured cells will be lysed using the PicoPure RNA extraction buffer. RNA from patient samples and healthy control samples will then be analyzed. As cell spike controls, melanoma cells SK-Mel-103 will be spiked into blood at concentrations of 10 and 50 cells per 3 ml of blood and captured on the device. RNA extracted from these controls will serve to obtain the limit of detection for the downstream genomic assays. The downstream analysis will include gene mutation profiling for mutations in BRAF, which is known in melanoma [35].

5.5.3. CTC isolation in head and neck cancers

The OncoBean Chip will also be applied in monitoring CTC burden in patients with cancers of the head and neck. Most head and neck cancers are epithelial, squamous cell cancers [197, 198]. They express markers similar to lung cancer, such as cytokeratins [199], EpCAM [200], EGFR [201] and CD133 [202], and a strategy similar to that of lung CTC isolation used in Chapter 3 will be employed.

Chapter 6

Conclusions

6.1. Summary of Research

6.1.1. High-throughput OncoBean Chip for CTC capture

A high-throughput microfluidic device, termed the OncoBean Chip was developed (Chapter 2) for immuno-affinity based CTC capture and analysis. The device was optimized for a capture efficiency of 80% at a throughput of 10 ml/hr with lung cancer cell line H1650. The OncoBean Chip also performed more efficiently at higher throughputs than the linear flow based CTC-chip [50]. The non-specific blood cell retention was also low at higher flow rates, which is favorable for downstream molecular analyses. Capture profiling studies suggested regions of differential capture that could depend on antigen expression levels. Comparing flow rates of 1 and 10 ml/hr for CTC capture from lung, breast and pancreatic patient samples, it was observed that the device was able to capture cells with similar efficiency at both the flow rates. The device was thus optimized for CTC capture from clinical specimens.

6.1.2. CTC capture and characterization in early lung cancer

Surgical resection of early stage lung cancer is considered curative [203], and assessing CTCs in early stages can shed light into the development of the disease. However, early stages are limited in CTC yields [148]. We analyzed CTCs from the pulmonary vein (tumor draining vein) as an

enriched source of CTCs, in comparison to peripheral blood (Chapter 3). Microfluidic CTC isolation on the OncoBean Chip from 36 patients from the pre-op peripheral (Pre-op Pe), intra-op peripheral (Intra-op Pe) and intra-op pulmonary veins (PV) showed a marked abundance of CTCs in the PV compared to the two Pe sources. CTC clusters also showed prevalence in the pulmonary vein. CTCs from the two sources (PV, Pe) were analyzed by RT-qPCR for gene expression of 96 target genes which revealed higher expression of epithelial-mesenchymal genes in the PV than Pe, and higher expression of immune-modulating genes in the Pe than PV. CTC clusters were absent for Ki67 expression in most cases, suggestive of their potential for dormancy and evading therapy [138]. Moreover, CTC clusters also demonstrated signatures of cell migration. 85% of patients who recurred in the long term were positive for CTC clusters as well. Taken together, the data suggests the malignant potential of CTC clusters in the pulmonary vein, which may be missed in peripheral blood in early stages of lung cancer.

6.1.3. Characterization of CTC clusters in early lung cancer

Probing further into circulating tumor cell clusters can provide understanding of tumor cell dissemination and metastasis. We thus proposed to capture CTC clusters from the pulmonary vein of early stage lung cancer patients (Chapter 4). Due to captured cells being adhered on to the microfluidic device, cells could not be segregated as single cells and collected in suspension. Hence, an alternate strategy following cell immunostaining was performed, consisting of physically removing portions of the PDMS device containing CTC clusters, and extracting RNA from fixed CTCs. Quality control with cell lines showed feasibility of the method, with sufficient quality obtained from cells fixed up to two days. The method will be adapted for analyzing gene expression profiles of CTC clusters obtained from patient specimens.

6.1.4. CTC capture from melanoma patients

Melanoma, or cancer of the skin, is an aggressive disease that quickly advances to metastatic disease [186]. CTCs can be useful to monitor this disease during progression or treatment [190]. We analyzed samples from 11 patients diagnosed with melanoma (Chapter 5). A cocktail of MCAM and MCSP (melanoma specific antibodies) were used for capture, followed by detection using a combination of Melan-A + S100, CD45 and DAPI. A range of 1.2 to 10.5 CTCs per 3 ml were detected in the patient specimens. The captured cells will be analyzed for melanoma specific gene mutations such as BRAF [35]. The study shows the adaptability of the OncoBean Chip to capture CTCs from various cancers, including those that do not express EpCAM, such as melanoma.

6.2. Limitations and Future Directions

6.2.1. CTC capture technology

The last two decades have witnessed remarkable advancements in technologies for CTC isolation, including the CTC-chip, ^{HB}CTC-chip, GEDI chip, HTMSU, Nano-Velcro CTC chip, graphene oxide (GO) chip, to name a few [8, 15, 26, 32-34]. The OncoBean Chip (Chapter 2) is an improvement over existing affinity-based microfluidic technologies with regards to throughput. A high-throughput capture approach was proposed with the help of fluid dynamic simulations and by imparting a different geometry, thus achieving capture of 80% even at 10 ml/hr. However, the device suffers from certain limitations, the primary of which is the inability to release the captured cells. While the captured cells are viable and downstream analyses are feasible, cells remain strongly bound to the device and are not removable by convenient methods. This limits the scope for any single cell analysis that could enable tumor heterogeneity

studies. The ability to release cells may also enable easier ex vivo expansion, and xenograft studies [55, 185]. Improvements to the OncoBean Chip are possible to enable this release functionality. For example, our group has recently demonstrated the incorporation of a thermal sensitive polymer along with graphene oxide, that can efficiently capture CTCs, and the captured cells can be released by lowering the temperature [185]. Efforts are currently underway in our lab to develop a similar device employing radial flow for higher throughputs.

Another limitation includes the use of EpCAM based capture methodology, which has raised concerns in recent years due to the ability to target only epithelial cell populations and missing EMT-undergoing or mesenchymal CTCs [140, 204]. Morrow et al. have shown tumorigenicity of mesenchymal CTCs [204], and the use of EpCAM alone may miss these aggressive CTCs. We countered this issue by the use of multiple antibodies such as the incorporation of anti-EGFR and anti-CD133 in addition to anti-EpCAM for the capture of lung CTCs (Chapter 3).

6.2.2. CTCs from different venous sources in early lung cancer

The analysis of circulating tumor cells in lung cancer has been studied by various research groups, and most studies have focused on their clinical utility as a monitoring tool for disease burden during treatment [205], the acquisition of treatment resistant mutations [9], or to detect gene rearrangements [206]. However, non-invasive CTC testing has the potential to have tremendous impact as an early detection tool as well [2]. We proposed to study the biology of CTCs in early stages of lung cancer, but were hindered by the low numbers of these cells in early disease. The unique position of the pulmonary vein within the lung, combined with surgical tumor resection procedures provided an opportunity to draw blood from this tumor-draining vein. Albeit the pulmonary vein gave a much larger yield of CTCs compared to the peripheral

vein, the biggest limitation of our study is that the procedure is still an invasive one, as it is not feasible to obtain pulmonary vein blood during routine clinic visits. Also, it remains to be seen in larger clinical cohorts whether the CTCs gathered from the pulmonary vein will give us clinically useful information. Another drawback of the study was the lower blood volumes obtained from the pulmonary vein due to technical difficulties associated with the draw. However, we were able to detect a large number of CTCs and CTC clusters even in 1 ml of blood, possibly due to the higher sensitivities attributed to microfluidic devices [2].

The gene expression data was limited by statistical significance due to the lower number of samples analyzed by RT-qPCR. While the investigation provided leads on potentially important genes and pathways, the data can be confirmed only by analyzing a larger sample set. Furthermore, a good future direction would involve selecting a subset of the analyzed genes and testing cultured CTCs by induction or knockdown of those genes. Additionally, the larger CTC numbers found in the pulmonary vein can be exploited for generation of tumors in mice or expansion, to study tumorigenicity profiles or for predicting drug treatment efficacy [44, 91, 94, 207].

6.2.3. CTC cluster analysis

CTC clusters have been explored in depth in breast cancer [48, 87] and pancreatic cancer [180] recently, and we predict similar or more extensive studies in lung and prostate cancers. After observing CTC clusters in the pulmonary vein in our early lung cancer study (Chapter 3), we designed a future study to compare these clusters to their single cell counterparts with respect to gene expression profiles. Due to difficulties with cell release, we adopted a brute force method wherein cells immobilized on PDMS were manually removed and RNA was extracted similar to

extraction from fixed tissue samples (Qiagen RNeasy FFPE kit). However the procedure is not optimal and RNA studies are most often performed using live cells. Furthermore, the physical removal of cells with PDMS may be inefficient and clusters may not be removed intact. It may also be detrimental to cell morphology. Contaminating white blood cells may still be present in the extracted RNA as it is difficult to target a specific amount of cells. In the future, we are aiming to develop a high-throughput device incorporating a temperature sensitive polymer that enables release of captured cells [185] in suspension, which can then be micromanipulated for separating single CTCs from CTC clusters [11, 48, 176].

Recently, novel technologies for the specialized isolation of CTC clusters from patient blood have been developed. The Cluster-Chip is a microfluidic platform that can isolate clusters of as small as two cells by a label free isolation [176]. The device was shown to isolate clusters from metastatic melanoma, breast and prostate cancers. Clusters were also released by a combination of reverse flow and cooling to 4 °C [176]. By incorporating such novel techniques, we can potentially conceive a microfluidic technology that integrates CTC cluster capture and single CTC capture within separate modules in the same device, from the same patient sample. Whole blood can first be processed through label free cluster isolation module, followed by capture of single CTCs from the remainder of the sample on the aforementioned thermal sensitive polymer coated immuno-affinity device. Following this, clusters and single CTCs can then be removed using respective mechanisms, thereby facilitating easier cell release, while also maintaining segregation of CTC clusters and single cells.

Another alternative to cell release includes the use of photocleavable cross linking agents. Linkers that can be cleaved by exposure of light have been reported, and biomolecules such as biotin can be tethered to the linker [208]. Applications with cell attachment and release were also

demonstrated [208], thereby providing a promising approach toward incorporation into CTC capture devices.

6.2.4. CTCs in melanoma

Melanoma CTC studies began more than two decades ago, where the presence of CTCs was identified using reverse-transciptase PCR [19]. Microfluidics for CTC analyses have improved since, yet there have been only a handful of studies on melanoma CTCs using microfluidic devices. Our studies show potential for adapting the OncoBean Chip to non-EpCAM based platforms, such as in melanoma. Melanoma CTCs were captured using a combination of MCAM and MCSP (Chapter 5). The major limitation of our study was the low number of cells detected. However, this was expected as the majority of patients were in early stages. Metastatic samples will be processed in order to compare CTC numbers in advanced stages. Another drawback was the large amount of contaminating cells captured on the device. The higher number of WBCs were likely captured due to MCAM (CD146), since CD146 is also expressed by endothelial cells [209]. The low purity of captured cells may cause background noise in downstream genetic analysis. However, this issue can be circumvented by the optimization of the previously proposed cell release and single cell picking protocols.

6.3. Conclusion

In conclusion, the radial flow OncoBean Chip offers a microfluidic technology to address the imminent need for developing biomarkers for early diagnosis of lung cancer. Future work will focus on developing the technology further to be able to manipulate cells at a single cell resolution, in order to elucidate mechanisms of tumor heterogeneity and metastasis.

Bibliography

1. Ashworth, T. R., *Aust Med J* **1869,** *14.3*, 146-149.
2. Haber, D. A.; Velculescu, V. E., *Cancer discovery* **2014,** *4* (6), 650-61. DOI 10.1158/2159-8290.CD-13-1014.
3. Miller, M. C.; Doyle, G. V.; Terstappen, L. W., *Journal of oncology* **2010,** *2010*, 617421. DOI 10.1155/2010/617421 [doi].
4. Cristofanilli, M.; Budd, G. T.; Ellis, M. J.; Stopeck, A.; Matera, J.; Miller, M. C.; Reuben, J. M.; Doyle, G. V.; Allard, W. J.; Terstappen, L. W.; Hayes, D. F., *N Engl J Med* **2004,** *351* (8), 781-91. DOI 10.1056/NEJMoa040766.
5. Fan, T.; Zhao, Q.; Chen, J. J.; Chen, W. T.; Pearl, M. L., *Gynecologic oncology* **2009,** *112* (1), 185-91. DOI 10.1016/j.ygyno.2008.09.021.
6. Hayes, D. F.; Cristofanilli, M.; Budd, G. T.; Ellis, M. J.; Stopeck, A.; Miller, M. C.; Matera, J.; Allard, W. J.; Doyle, G. V.; Terstappen, L. W., *Clinical cancer research : an official journal of the American Association for Cancer Research* **2006,** *12* (14 Pt 1), 4218-4224. DOI 12/14/4218 [pii].
7. Kurkuri, M. D.; Al-Ejeh, F.; Shi, J. Y.; Palms, D.; Prestidge, C.; Griesser, H. J.; Brown, M. P.; Thierry, B., *Journal of Materials Chemistry* **2011,** *21* (24), 8841. DOI 10.1039/c1jm10317b.
8. Nagrath, S.; Sequist, L. V.; Maheswaran, S.; Bell, D. W.; Irimia, D.; Ulkus, L.; Smith, M. R.; Kwak, E. L.; Digumarthy, S.; Muzikansky, A.; Ryan, P.; Balis, U. J.; Tompkins, R. G.; Haber, D. A.; Toner, M., *Nature* **2007,** *450* (7173), 1235-9. DOI 10.1038/nature06385.
9. Maheswaran, S.; Sequist, L. V.; Nagrath, S.; Ulkus, L.; Brannigan, B.; Collura, C. V.; Inserra, E.; Diederichs, S.; Iafrate, A. J.; Bell, D. W.; Digumarthy, S.; Muzikansky, A.; Irimia, D.; Settleman, J.; Tompkins, R. G.; Lynch, T. J.; Toner, M.; Haber, D. A., *N Engl J Med* **2008,** *359* (4), 366-77. DOI 10.1056/NEJMoa0800668.
10. Riethdorf, S.; Fritsche, H.; Muller, V.; Rau, T.; Schindlbeck, C.; Rack, B.; Janni, W.; Coith, C.; Beck, K.; Janicke, F.; Jackson, S.; Gornet, T.; Cristofanilli, M.; Pantel, K., *Clin Cancer Res* **2007,** *13* (3), 920-8. DOI 10.1158/1078-0432.CCR-06-1695.
11. Ozkumur, E.; Shah, A. M.; Ciciliano, J. C.; Emmink, B. L.; Miyamoto, D. T.; Brachtel, E.; Yu, M.; Chen, P. I.; Morgan, B.; Trautwein, J.; Kimura, A.; Sengupta, S.; Stott, S. L.; Karabacak, N. M.; Barber, T. A.; Walsh, J. R.; Smith, K.; Spuhler, P. S.; Sullivan, J. P.; Lee, R. J.; Ting, D. T.; Luo, X.; Shaw, A. T.; Bardia, A.; Sequist, L. V.; Louis, D. N.; Maheswaran, S.; Kapur, R.; Haber, D. A.; Toner, M., *Science translational medicine* **2013,** *5* (179), 179ra47. DOI 10.1126/scitranslmed.3005616.
12. Punnoose, E. A.; Atwal, S.; Liu, W.; Raja, R.; Fine, B. M.; Hughes, B. G.; Hicks, R. J.; Hampton, G. M.; Amler, L. C.; Pirzkall, A.; Lackner, M. R., *Clin Cancer Res* **2012,** *18* (8), 2391-401. DOI 10.1158/1078-0432.CCR-11-3148.
13. Rudin, C. M.; Hann, C. L.; Garon, E. B.; Ribeiro de Oliveira, M.; Bonomi, P. D.; Camidge, D. R.; Chu, Q.; Giaccone, G.; Khaira, D.; Ramalingam, S. S.; Ranson, M. R.; Dive, C.; McKeegan, E. M.; Chyla, B. J.; Dowell, B. L.; Chakravartty, A.; Nolan, C. E.; Rudersdorf, N.; Busman, T. A.; Mabry, M. H.; Krivoshik, A. P.; Humerickhouse, R. A.; Shapiro, G. I.; Gandhi, L., *Clin Cancer Res* **2012,** *18* (11), 3163-9. DOI 10.1158/1078-0432.CCR-11-3090.

14. Khoja, L.; Backen, A.; Sloane, R.; Menasce, L.; Ryder, D.; Krebs, M.; Board, R.; Clack, G.; Hughes, A.; Blackhall, F.; Valle, J. W.; Dive, C., *British journal of cancer* **2012,** *106* (3), 508-16. DOI 10.1038/bjc.2011.545.
15. Stott, S. L.; Hsu, C. H.; Tsukrov, D. I.; Yu, M.; Miyamoto, D. T.; Waltman, B. A.; Rothenberg, S. M.; Shah, A. M.; Smas, M. E.; Korir, G. K.; Floyd, F. P., Jr.; Gilman, A. J.; Lord, J. B.; Winokur, D.; Springer, S.; Irimia, D.; Nagrath, S.; Sequist, L. V.; Lee, R. J.; Isselbacher, K. J.; Maheswaran, S.; Haber, D. A.; Toner, M., *Proceedings of the National Academy of Sciences of the United States of America* **2010,** *107* (43), 18392-7. DOI 10.1073/pnas.1012539107.
16. Dong, Y.; Skelley, A. M.; Merdek, K. D.; Sprott, K. M.; Jiang, C.; Pierceall, W. E.; Lin, J.; Stocum, M.; Carney, W. P.; Smirnov, D. A., *The Journal of molecular diagnostics : JMD* **2013,** *15* (2), 149-57. DOI 10.1016/j.jmoldx.2012.09.004.
17. Yu, M.; Stott, S.; Toner, M.; Maheswaran, S.; Haber, D. A., *The Journal of cell biology* **2011,** *192* (3), 373-382. DOI 10.1083/jcb.201010021 [doi].
18. den Toonder, J., *Lab on a chip* **2011,** *11* (3), 375-7. DOI 10.1039/c0lc90100h.
19. Smith, B.; Selby, P.; Southgate, J.; Pittman, K.; Bradley, C.; Blair, G. E., *Lancet* **1991,** *338* (8777), 1227-9.
20. Murlidhar, V.; Rivera-Baez, L.; Nagrath, S., *Small* **2016**. DOI 10.1002/smll.201601394.
21. Bhagat, A. A.; Hou, H. W.; Li, L. D.; Lim, C. T.; Han, J., *Lab on a chip* **2011,** *11* (11), 1870-8. DOI 10.1039/c0lc00633e.
22. Sheng, W.; Chen, T.; Kamath, R.; Xiong, X.; Tan, W.; Fan, Z. H., *Analytical chemistry* **2012,** *84* (9), 4199-206. DOI 10.1021/ac3005633.
23. Dharmasiri, U.; Balamurugan, S.; Adams, A. A.; Okagbare, P. I.; Obubuafo, A.; Soper, S. A., *Electrophoresis* **2009,** *30* (18), 3289-300. DOI 10.1002/elps.200900141.
24. Nora Dickson, M.; Tsinberg, P.; Tang, Z.; Bischoff, F. Z.; Wilson, T.; Leonard, E. F., *Biomicrofluidics* **2011,** *5* (3), 34119-3411915. DOI 10.1063/1.3623748.
25. Liu, Z.; Zhang, W.; Huang, F.; Feng, H.; Shu, W.; Xu, X.; Chen, Y., *Biosensors & bioelectronics* **2013,** *47*, 113-9. DOI 10.1016/j.bios.2013.03.017.
26. Gleghorn, J. P.; Pratt, E. D.; Denning, D.; Liu, H.; Bander, N. H.; Tagawa, S. T.; Nanus, D. M.; Giannakakou, P. A.; Kirby, B. J., *Lab on a chip* **2010,** *10* (1), 27-9. DOI 10.1039/b917959c.
27. Paterlini-Brechot, P.; Benali, N. L., *Cancer letters* **2007,** *253* (2), 180-204. DOI 10.1016/j.canlet.2006.12.014.
28. Sun, Y. F.; Yang, X. R.; Zhou, J.; Qiu, S. J.; Fan, J.; Xu, Y., *Journal of cancer research and clinical oncology* **2011,** *137* (8), 1151-73. DOI 10.1007/s00432-011-0988-y.
29. Alix-Panabières, C.; Pantel, K., *Lab on a chip* **2014,** *14* (1), 57-62.
30. Mittal, S.; Wong, I. Y.; Deen, W. M.; Toner, M., *Biophysical journal* **2012,** *102* (4), 721-30. DOI 10.1016/j.bpj.2011.12.044.
31. Pecot, C. V.; Bischoff, F. Z.; Mayer, J. A.; Wong, K. L.; Pham, T.; Bottsford-Miller, J.; Stone, R. L.; Lin, Y. G.; Jaladurgam, P.; Roh, J. W.; Goodman, B. W.; Merritt, W. M.; Pircher, T. J.; Mikolajczyk, S. D.; Nick, A. M.; Celestino, J.; Eng, C.; Ellis, L. M.; Deavers, M. T.; Sood, A. K., *Cancer discovery* **2011,** *1* (7), 580-6. DOI 10.1158/2159-8290.CD-11-0215.
32. Adams, A. A.; Okagbare, P. I.; Feng, J.; Hupert, M. L.; Patterson, D.; Gottert, J.; McCarley, R. L.; Nikitopoulos, D.; Murphy, M. C.; Soper, S. A., *Journal of the American Chemical Society* **2008,** *130* (27), 8633-41. DOI 10.1021/ja8015022.
33. Yoon, H. J.; Kim, T. H.; Zhang, Z.; Azizi, E.; Pham, T. M.; Paoletti, C.; Lin, J.; Ramnath, N.; Wicha, M. S.; Hayes, D. F., *Nature nanotechnology* **2013,** *8* (10), 735-741.
34. Lu, Y. T.; Zhao, L.; Shen, Q.; Garcia, M. A.; Wu, D.; Hou, S.; Song, M.; Xu, X.; Ouyang, W. H.; Ouyang, W. W.; Lichterman, J.; Luo, Z.; Xuan, X.; Huang, J.; Chung, L. W.; Rettig, M.; Tseng, H. R.; Shao, C.; Posadas, E. M., *Methods* **2013,** *64* (2), 144-52. DOI 10.1016/j.ymeth.2013.06.019.

35. Hou, S.; Zhao, L.; Shen, Q.; Yu, J.; Ng, C.; Kong, X.; Wu, D.; Song, M.; Shi, X.; Xu, X.; OuYang, W. H.; He, R.; Zhao, X. Z.; Lee, T.; Brunicardi, F. C.; Garcia, M. A.; Ribas, A.; Lo, R. S.; Tseng, H. R., *Angewandte Chemie* **2013,** *52* (12), 3379-83. DOI 10.1002/anie.201208452.
36. Galletti, G.; Sung, M. S.; Vahdat, L. T.; Shah, M. A.; Santana, S. M.; Altavilla, G.; Kirby, B. J.; Giannakakou, P., *Lab on a chip* **2014,** *14* (1), 147-56. DOI 10.1039/c3lc51039e.
37. Yu, M.; Bardia, A.; Wittner, B. S.; Stott, S. L.; Smas, M. E.; Ting, D. T.; Isakoff, S. J.; Ciciliano, J. C.; Wells, M. N.; Shah, A. M.; Concannon, K. F.; Donaldson, M. C.; Sequist, L. V.; Brachtel, E.; Sgroi, D.; Baselga, J.; Ramaswamy, S.; Toner, M.; Haber, D. A.; Maheswaran, S., *Science* **2013,** *339* (6119), 580-4. DOI 10.1126/science.1228522.
38. Wong, L.; Bateman, W.; Morris, A.; Fraser, I., *British journal of surgery* **1995,** *82* (10), 1333-1337.
39. Hoshino, K.; Huang, Y. Y.; Lane, N.; Huebschman, M.; Uhr, J. W.; Frenkel, E. P.; Zhang, X., *Lab on a chip* **2011,** *11* (20), 3449-57. DOI 10.1039/c1lc20270g.
40. Casavant, B. P.; Mosher, R.; Warrick, J. W.; Maccoux, L. J.; Berry, S. M.; Becker, J. T.; Chen, V.; Lang, J. M.; McNeel, D. G.; Beebe, D. J., *Methods* **2013,** *64* (2), 137-43. DOI 10.1016/j.ymeth.2013.05.027.
41. Wu, Y.; Deighan, C. J.; Miller, B. L.; Balasubramanian, P.; Lustberg, M. B.; Zborowski, M.; Chalmers, J. J., *Methods* **2013,** *64* (2), 169-82. DOI 10.1016/j.ymeth.2013.09.006.
42. Saucedo-Zeni, N.; Mewes, S.; Niestroj, R.; Gasiorowski, L.; Murawa, D.; Nowaczyk, P.; Tomasi, T.; Weber, E.; Dworacki, G.; Morgenthaler, N. G.; Jansen, H.; Propping, C.; Sterzynska, K.; Dyszkiewicz, W.; Zabel, M.; Kiechle, M.; Reuning, U.; Schmitt, M.; Lucke, K., *International journal of oncology* **2012,** *41* (4), 1241-50. DOI 10.3892/ijo.2012.1557.
43. Alix-Panabieres, C.; Pantel, K., *Clinical chemistry* **2013,** *59* (1), 110-8. DOI 10.1373/clinchem.2012.194258.
44. Zhang, Z.; Shiratsuchi, H.; Lin, J.; Chen, G.; Reddy, R. M.; Azizi, E.; Fouladdel, S.; Chang, A. C.; Lin, L.; Jiang, H.; Waghray, M.; Luker, G.; Simeone, D. M.; Wicha, M. S.; Beer, D. G.; Ramnath, N.; Nagrath, S., *Oncotarget* **2014,** *5* (23), 12383-97. DOI 10.18632/oncotarget.2592.
45. Thege, F. I.; Lannin, T. B.; Saha, T. N.; Tsai, S.; Kochman, M. L.; Hollingsworth, M. A.; Rhim, A. D.; Kirby, B. J., *Lab on a chip* **2014,** *14* (10), 1775-84. DOI 10.1039/c4lc00041b.
46. Riethdorf, S.; Muller, V.; Zhang, L.; Rau, T.; Loibl, S.; Komor, M.; Roller, M.; Huober, J.; Fehm, T.; Schrader, I.; Hilfrich, J.; Holms, F.; Tesch, H.; Eidtmann, H.; Untch, M.; von Minckwitz, G.; Pantel, K., *Clin Cancer Res* **2010,** *16* (9), 2634-45. DOI 10.1158/1078-0432.CCR-09-2042.
47. Mohamadi, R. M.; Besant, J. D.; Mepham, A.; Green, B.; Mahmoudian, L.; Gibbs, T.; Ivanov, I.; Malvea, A.; Stojcic, J.; Allan, A. L.; Lowes, L. E.; Sargent, E. H.; Nam, R. K.; Kelley, S. O., *Angewandte Chemie* **2015,** *54* (1), 139-43. DOI 10.1002/anie.201409376.
48. Aceto, N.; Bardia, A.; Miyamoto, D. T.; Donaldson, M. C.; Wittner, B. S.; Spencer, J. A.; Yu, M.; Pely, A.; Engstrom, A.; Zhu, H.; Brannigan, B. W.; Kapur, R.; Stott, S. L.; Shioda, T.; Ramaswamy, S.; Ting, D. T.; Lin, C. P.; Toner, M.; Haber, D. A.; Maheswaran, S., *Cell* **2014,** *158* (5), 1110-22. DOI 10.1016/j.cell.2014.07.013.
49. Aceto, N.; Toner, M.; Maheswaran, S.; Haber, D. A., *Trends in Cancer* **2015,** *1* (1), 44-52. DOI 10.1016/j.trecan.2015.07.006.
50. Murlidhar, V.; Zeinali, M.; Grabauskiene, S.; Ghannad-Rezaie, M.; Wicha, M. S.; Simeone, D. M.; Ramnath, N.; Reddy, R. M.; Nagrath, S., *Small* **2014,** *10* (23), 4895-904. DOI 10.1002/smll.201400719.
51. Sethi, N.; Kang, Y., *Nature reviews. Cancer* **2011,** *11* (10), 735-48. DOI 10.1038/nrc3125.
52. Gay, L. J.; Felding-Habermann, B., *Nature reviews. Cancer* **2011,** *11* (2), 123-34. DOI 10.1038/nrc3004.
53. Labelle, M.; Begum, S.; Hynes, R. O., *Cancer cell* **2011,** *20* (5), 576-90. DOI 10.1016/j.ccr.2011.09.009.

54. Wicha, M. S.; Hayes, D. F., *Journal of clinical oncology : official journal of the American Society of Clinical Oncology* **2011,** *29* (12), 1508-11. DOI 10.1200/JCO.2010.34.0026.
55. Shah, A. M.; Yu, M.; Nakamura, Z.; Ciciliano, J.; Ulman, M.; Kotz, K.; Stott, S. L.; Maheswaran, S.; Haber, D. A.; Toner, M., *Analytical chemistry* **2012,** *84* (8), 3682-8. DOI 10.1021/ac300190j.
56. Gerges, N.; Rak, J.; Jabado, N., *British medical bulletin* **2010,** *94*, 49-64. DOI 10.1093/bmb/ldq011.
57. McKenzie, S.; Williams, L., *Clinical laboratory hematology*. Prentice Hall: **2014**.
58. Phillips, K. G.; Kolatkar, A.; Rees, K. J.; Rigg, R.; Marrinucci, D.; Luttgen, M.; Bethel, K.; Kuhn, P.; McCarty, O. J., *Frontiers in oncology* **2012,** *2*.
59. Jin, C.; McFaul, S. M.; Duffy, S. P.; Deng, X.; Tavassoli, P.; Black, P. C.; Ma, H., *Lab on a chip* **2014,** *14* (1), 32-44.
60. Cima, I.; Yee, C. W.; Iliescu, F. S.; Phyo, W. M.; Lim, K. H.; Iliescu, C.; Tan, M. H., *Biomicrofluidics* **2013,** *7* (1), 011810.
61. Vona, G.; Sabile, A.; Louha, M.; Sitruk, V.; Romana, S.; Schütze, K.; Capron, F.; Franco, D.; Pazzagli, M.; Vekemans, M., *The American journal of pathology* **2000,** *156* (1), 57-63.
62. Hou, J.-M.; Krebs, M.; Ward, T.; Sloane, R.; Priest, L.; Hughes, A.; Clack, G.; Ranson, M.; Blackhall, F.; Dive, C., *The American journal of pathology* **2011,** *178* (3), 989-996.
63. De Giorgi, V.; Pinzani, P.; Salvianti, F.; Panelos, J.; Paglierani, M.; Janowska, A.; Grazzini, M.; Wechsler, J.; Orlando, C.; Santucci, M., *Journal of Investigative Dermatology* **2010,** *130* (10), 2440-2447.
64. Desitter, I.; Guerrouahen, B. S.; Benali-Furet, N.; Wechsler, J.; Jaenne, P. A.; Kuang, Y.; Yanagita, M.; Wang, L.; Berkowitz, J. A.; Distel, R. J., *Anticancer research* **2011,** *31* (2), 427-441.
65. Zheng, S.; Lin, H.; Liu, J.-Q.; Balic, M.; Datar, R.; Cote, R. J.; Tai, Y.-C., *Journal of Chromatography A* **2007,** *1162* (2), 154-161.
66. Lin, H. K.; Zheng, S.; Williams, A. J.; Balic, M.; Groshen, S.; Scher, H. I.; Fleisher, M.; Stadler, W.; Datar, R. H.; Tai, Y. C.; Cote, R. J., *Clinical cancer research : an official journal of the American Association for Cancer Research* **2010,** *16* (20), 5011-5018. DOI 10.1158/1078-0432.CCR-10-1105 [doi].
67. Zheng, S.; Lin, H. K.; Lu, B.; Williams, A.; Datar, R.; Cote, R. J.; Tai, Y.-C., *Biomedical microdevices* **2011,** *13* (1), 203-213.
68. Hosokawa, M.; Hayata, T.; Fukuda, Y.; Arakaki, A.; Yoshino, T.; Tanaka, T.; Matsunaga, T., *Analytical chemistry* **2010,** *82* (15), 6629-6635.
69. Lim, L. S.; Hu, M.; Huang, M. C.; Cheong, W. C.; Gan, A. T. L.; Looi, X. L.; Leong, S. M.; Koay, E. S.-C.; Li, M.-H., *Lab on a chip* **2012,** *12* (21), 4388-4396.
70. Zhou, M.-D.; Hao, S.; Williams, A. J.; Harouaka, R. A.; Schrand, B.; Rawal, S.; Ao, Z.; Brennaman, R.; Gilboa, E.; Lu, B., *Scientific reports* **2014,** *4*.
71. Cima, I.; Wen Yee, C.; Iliescu, F. S.; Phyo, W. M.; Lim, K. H.; Iliescu, C.; Tan, M. H., *Biomicrofluidics* **2013,** *7* (1), 11810. DOI 10.1063/1.4780062.
72. Di Carlo, D.; Irimia, D.; Tompkins, R. G.; Toner, M., *Proceedings of the National Academy of Sciences of the United States of America* **2007,** *104* (48), 18892-7. DOI 10.1073/pnas.0704958104.
73. Russom, A.; Gupta, A. K.; Nagrath, S.; Di Carlo, D.; Edd, J. F.; Toner, M., *New J Phys* **2009,** *11* (7), 75025. DOI 10.1088/1367-2630/11/7/075025.
74. Davis, J. A.; Inglis, D. W.; Morton, K. J.; Lawrence, D. A.; Huang, L. R.; Chou, S. Y.; Sturm, J. C.; Austin, R. H., *Proceedings of the National Academy of Sciences of the United States of America* **2006,** *103* (40), 14779-84. DOI 10.1073/pnas.0605967103.
75. Lee, A.; Park, J.; Lim, M.; Sunkara, V.; Kim, S. Y.; Kim, G. H.; Kim, M. H.; Cho, Y. K., *Analytical chemistry* **2014,** *86* (22), 11349-56. DOI 10.1021/ac5035049.
76. Hou, H. W.; Warkiani, M. E.; Khoo, B. L.; Li, Z. R.; Soo, R. A.; Tan, D. S.; Lim, W. T.; Han, J.; Bhagat, A. A.; Lim, C. T., *Sci Rep* **2013,** *3*, 1259. DOI 10.1038/srep01259.

77. Sollier, E.; Go, D. E.; Che, J.; Gossett, D. R.; O'Byrne, S.; Weaver, W. M.; Kummer, N.; Rettig, M.; Goldman, J.; Nickols, N.; McCloskey, S.; Kulkarni, R. P.; Di Carlo, D., *Lab on a chip* **2014,** *14* (1), 63-77. DOI 10.1039/c3lc50689d.
78. Hyun, K. A.; Kwon, K.; Han, H.; Kim, S. I.; Jung, H. I., *Biosensors & bioelectronics* **2013,** *40* (1), 206-12. DOI 10.1016/j.bios.2012.07.021.
79. Warkiani, M. E.; Guan, G.; Luan, K. B.; Lee, W. C.; Bhagat, A. A.; Chaudhuri, P. K.; Tan, D. S.; Lim, W. T.; Lee, S. C.; Chen, P. C.; Lim, C. T.; Han, J., *Lab on a chip* **2014,** *14* (1), 128-37. DOI 10.1039/c3lc50617g.
80. Warkiani, M. E.; Khoo, B. L.; Tan, D. S.; Bhagat, A. A.; Lim, W. T.; Yap, Y. S.; Lee, S. C.; Soo, R. A.; Han, J.; Lim, C. T., *Analyst* **2014,** *139* (13), 3245-55. DOI 10.1039/c4an00355a.
81. Becker, F. F.; Wang, X. B.; Huang, Y.; Pethig, R.; Vykoukal, J.; Gascoyne, P. R., *Proceedings of the National Academy of Sciences of the United States of America* **1995,** *92* (3), 860-4.
82. Jin, C.; McFaul, S. M.; Duffy, S. P.; Deng, X.; Tavassoli, P.; Black, P. C.; Ma, H., *Lab on a chip* **2014,** *14* (1), 32-44. DOI 10.1039/c3lc50625h.
83. Shim, S.; Stemke-Hale, K.; Tsimberidou, A. M.; Noshari, J.; Anderson, T. E.; Gascoyne, P. R., *Biomicrofluidics* **2013,** *7* (1), 11807. DOI 10.1063/1.4774304.
84. Warkiani, M. E.; Khoo, B. L.; Tan, D. S.-W.; Bhagat, A. A. S.; Lim, W.-T.; Yap, Y. S.; Lee, S. C.; Soo, R. A.; Han, J.; Lim, C. T., *Analyst* **2014,** *139* (13), 3245-3255.
85. Warkiani, M. E.; Guan, G.; Luan, K. B.; Lee, W. C.; Bhagat, A. A. S.; Chaudhuri, P. K.; Tan, D. S.-W.; Lim, W. T.; Lee, S. C.; Chen, P. C. Y., *Lab on a chip* **2014,** *14* (1), 128-137.
86. Sollier, E.; Go, D. E.; Che, J.; Gossett, D. R.; O'Byrne, S.; Weaver, W. M.; Kummer, N.; Rettig, M.; Goldman, J.; Nickols, N., *Lab on a chip* **2014,** *14* (1), 63-77.
87. Cheung, K. J.; Padmanaban, V.; Silvestri, V.; Schipper, K.; Cohen, J. D.; Fairchild, A. N.; Gorin, M. A.; Verdone, J. E.; Pienta, K. J.; Bader, J. S.; Ewald, A. J., *Proceedings of the National Academy of Sciences of the United States of America* **2016,** *113* (7), E854-63. DOI 10.1073/pnas.1508541113.
88. Marrinucci, D.; Bethel, K.; Lazar, D.; Fisher, J.; Huynh, E.; Clark, P.; Bruce, R.; Nieva, J.; Kuhn, P., *Journal of oncology* **2010,** *2010*.
89. Gossett, D. R.; Weaver, W. M.; Mach, A. J.; Hur, S. C.; Tse, H. T.; Lee, W.; Amini, H.; Di Carlo, D., *Analytical and bioanalytical chemistry* **2010,** *397* (8), 3249-67. DOI 10.1007/s00216-010-3721-9.
90. Yu, Z. T.; Aw Yong, K. M.; Fu, J., *Small* **2014,** *10* (9), 1687-703. DOI 10.1002/smll.201302907.
91. Hodgkinson, C. L.; Morrow, C. J.; Li, Y.; Metcalf, R. L.; Rothwell, D. G.; Trapani, F.; Polanski, R.; Burt, D. J.; Simpson, K. L.; Morris, K.; Pepper, S. D.; Nonaka, D.; Greystoke, A.; Kelly, P.; Bola, B.; Krebs, M. G.; Antonello, J.; Ayub, M.; Faulkner, S.; Priest, L.; Carter, L.; Tate, C.; Miller, C. J.; Blackhall, F.; Brady, G.; Dive, C., *Nature medicine* **2014,** *20* (8), 897-903. DOI 10.1038/nm.3600.
92. Yu, M.; Bardia, A.; Aceto, N.; Bersani, F.; Madden, M. W.; Donaldson, M. C.; Desai, R.; Zhu, H.; Comaills, V.; Zheng, Z.; Wittner, B. S.; Stojanov, P.; Brachtel, E.; Sgroi, D.; Kapur, R.; Shioda, T.; Ting, D. T.; Ramaswamy, S.; Getz, G.; Iafrate, A. J.; Benes, C.; Toner, M.; Maheswaran, S.; Haber, D. A., *Science* **2014,** *345* (6193), 216-20. DOI 10.1126/science.1253533.
93. Cayrefourcq, L.; Mazard, T.; Joosse, S.; Solassol, J.; Ramos, J.; Assenat, E.; Schumacher, U.; Costes, V.; Maudelonde, T.; Pantel, K., *Cancer research* **2015**, canres. 2613.2014.
94. Morrow, C. J.; Trapani, F.; Metcalf, R. L.; Bertolini, G.; Hodgkinson, C. L.; Khandelwal, G.; Kelly, P.; Galvin, M.; Carter, L.; Simpson, K. L.; Williamson, S.; Wirth, C.; Simms, N.; Frankliln, L.; Frese, K.; Rothwell, D. G.; Nonaka, D.; Miller, C. J.; Brady, G.; Blackhall, F. H.; Dive, C., *Annals of oncology : official journal of the European Society for Medical Oncology / ESMO* **2016**. DOI 10.1093/annonc/mdw122.
95. Cayrefourcq, L.; Mazard, T.; Joosse, S.; Solassol, J.; Ramos, J.; Assenat, E.; Schumacher, U.; Costes, V.; Maudelonde, T.; Pantel, K.; Alix-Panabieres, C., *Cancer Res* **2015,** *75* (5), 892-901. DOI 10.1158/0008-5472.CAN-14-2613.
96. Alix-Panabières, C.; Pantel, K., *Nature Reviews Cancer* **2014,** *14* (9), 623-631.

97. Joosse, S. A.; Gorges, T. M.; Pantel, K., *EMBO molecular medicine* **2015,** *7* (1), 1-11.
98. de Bono, J. S.; Scher, H. I.; Montgomery, R. B.; Parker, C.; Miller, M. C.; Tissing, H.; Doyle, G. V.; Terstappen, L. W.; Pienta, K. J.; Raghavan, D., *Clin Cancer Res* **2008,** *14* (19), 6302-9. DOI 10.1158/1078-0432.CCR-08-0872.
99. Smirnov, D. A.; Zweitzig, D. R.; Foulk, B. W.; Miller, M. C.; Doyle, G. V.; Pienta, K. J.; Meropol, N. J.; Weiner, L. M.; Cohen, S. J.; Moreno, J. G.; Connelly, M. C.; Terstappen, L. W.; O'Hara, S. M., *Cancer Res* **2005,** *65* (12), 4993-7. DOI 10.1158/0008-5472.CAN-04-4330.
100. Ting, D. T.; Wittner, B. S.; Ligorio, M.; Vincent Jordan, N.; Shah, A. M.; Miyamoto, D. T.; Aceto, N.; Bersani, F.; Brannigan, B. W.; Xega, K.; Ciciliano, J. C.; Zhu, H.; MacKenzie, O. C.; Trautwein, J.; Arora, K. S.; Shahid, M.; Ellis, H. L.; Qu, N.; Bardeesy, N.; Rivera, M. N.; Deshpande, V.; Ferrone, C. R.; Kapur, R.; Ramaswamy, S.; Shioda, T.; Toner, M.; Maheswaran, S.; Haber, D. A., *Cell reports* **2014,** *8* (6), 1905-18. DOI 10.1016/j.celrep.2014.08.029.
101. Yu, M.; Ting, D. T.; Stott, S. L.; Wittner, B. S.; Ozsolak, F.; Paul, S.; Ciciliano, J. C.; Smas, M. E.; Winokur, D.; Gilman, A. J.; Ulman, M. J.; Xega, K.; Contino, G.; Alagesan, B.; Brannigan, B. W.; Milos, P. M.; Ryan, D. P.; Sequist, L. V.; Bardeesy, N.; Ramaswamy, S.; Toner, M.; Maheswaran, S.; Haber, D. A., *Nature* **2012,** *487* (7408), 510-3. DOI 10.1038/nature11217.
102. Leversha, M. A.; Han, J.; Asgari, Z.; Danila, D. C.; Lin, O.; Gonzalez-Espinoza, R.; Anand, A.; Lilja, H.; Heller, G.; Fleisher, M.; Scher, H. I., *Clin Cancer Res* **2009,** *15* (6), 2091-7. DOI 10.1158/1078-0432.CCR-08-2036.
103. Attard, G.; Swennenhuis, J. F.; Olmos, D.; Reid, A. H.; Vickers, E.; A'Hern, R.; Levink, R.; Coumans, F.; Moreira, J.; Riisnaes, R.; Oommen, N. B.; Hawche, G.; Jameson, C.; Thompson, E.; Sipkema, R.; Carden, C. P.; Parker, C.; Dearnaley, D.; Kaye, S. B.; Cooper, C. S.; Molina, A.; Cox, M. E.; Terstappen, L. W.; de Bono, J. S., *Cancer Res* **2009,** *69* (7), 2912-8. DOI 10.1158/0008-5472.CAN-08-3667.
104. Chimonidou, M.; Strati, A.; Malamos, N.; Georgoulias, V.; Lianidou, E. S., *Clinical chemistry* **2013,** *59* (1), 270-9. DOI 10.1373/clinchem.2012.191551.
105. Chimonidou, M.; Kallergi, G.; Georgoulias, V.; Welch, D. R.; Lianidou, E. S., *Molecular cancer research : MCR* **2013,** *11* (10), 1248-57. DOI 10.1158/1541-7786.MCR-13-0096.
106. Malara, N.; Coluccio, M. L.; Limongi, T.; Asande, M.; Trunzo, V.; Cojoc, G.; Raso, C.; Candeloro, P.; Perozziello, G.; Raimondo, R.; De Vitis, S.; Roveda, L.; Renne, M.; Prati, U.; Mollace, V.; Di Fabrizio, E., *Small* **2014,** *10* (21), 4324-31. DOI 10.1002/smll.201400498.
107. Zhou, J.; Ellis, A. V.; Voelcker, N. H., *Electrophoresis* **2010,** *31* (1), 2-16. DOI 10.1002/elps.200900475.
108. McDonald, J. C.; Duffy, D. C.; Anderson, J. R.; Chiu, D. T.; Wu, H.; Schueller, O. J.; Whitesides, G. M., *Electrophoresis* **2000,** *21* (1), 27-40. DOI 10.1002/(SICI)1522-2683(20000101)21:1<27::AID-ELPS27>3.0.CO;2-C.
109. McDonald, J. C.; Whitesides, G. M., *Accounts of chemical research* **2002,** *35* (7), 491-9.
110. Becker, H.; Locascio, L. E., *Talanta* **2002,** *56* (2), 267-87.
111. Shaw, J. M.; Gelorme, J. D.; LaBianca, N. C.; Conley, W. E.; Holmes, S. J., *IBM Journal of Research and Development* **1997,** *41* (1.2), 81-94.
112. Murthy, S. K.; Sin, A.; Tompkins, R. G.; Toner, M., *Langmuir : the ACS journal of surfaces and colloids* **2004,** *20* (26), 11649-55. DOI 10.1021/la048047b.
113. Sequist, L. V.; Nagrath, S.; Toner, M.; Haber, D. A.; Lynch, T. J., *Journal of thoracic oncology : official publication of the International Association for the Study of Lung Cancer* **2009,** *4* (3), 281-3. DOI 10.1097/JTO.0b013e3181989565.
114. Karabacak, N. M.; Spuhler, P. S.; Fachin, F.; Lim, E. J.; Pai, V.; Ozkumur, E.; Martel, J. M.; Kojic, N.; Smith, K.; Chen, P. I.; Yang, J.; Hwang, H.; Morgan, B.; Trautwein, J.; Barber, T. A.; Stott, S. L.; Maheswaran, S.; Kapur, R.; Haber, D. A.; Toner, M., *Nature protocols* **2014,** *9* (3), 694-710. DOI 10.1038/nprot.2014.044.

115. Mittal, S.; Wong, I. Y.; Yanik, A. A.; Deen, W. M.; Toner, M., *Small* **2013,** *9* (24), 4207-14. DOI 10.1002/smll.201300977.
116. Powell, A. A.; Talasaz, A. H.; Zhang, H.; Coram, M. A.; Reddy, A.; Deng, G.; Telli, M. L.; Advani, R. H.; Carlson, R. W.; Mollick, J. A.; Sheth, S.; Kurian, A. W.; Ford, J. M.; Stockdale, F. E.; Quake, S. R.; Pease, R. F.; Mindrinos, M. N.; Bhanot, G.; Dairkee, S. H.; Davis, R. W.; Jeffrey, S. S., *PloS one* **2012,** *7* (5), e33788. DOI 10.1371/journal.pone.0033788.
117. Zheng, X.; Cheung, L. S.; Schroeder, J. A.; Jiang, L.; Zohar, Y., *Lab on a chip* **2011,** *11* (19), 3269-76. DOI 10.1039/c1lc20331b.
118. Zhang, H.; Williams, P. S.; Zborowski, M.; Chalmers, J. J., *Biotechnol Bioeng* **2006,** *95* (5), 812-29. DOI 10.1002/bit.21024.
119. Jemal, A.; Siegel, R.; Xu, J.; Ward, E., *CA: a cancer journal for clinicians* **2010,** *60* (5), 277-300. DOI 10.3322/caac.20073.
120. Murlidhar, V.; Ramnath, N.; Nagrath, S.; Reddy, R. M., *Cancers (Basel)* **2016,** *8* (7). DOI 10.3390/cancers8070061.
121. **2015**.
122. National Lung Screening Trial Research, T.; Aberle, D. R.; Adams, A. M.; Berg, C. D.; Black, W. C.; Clapp, J. D.; Fagerstrom, R. M.; Gareen, I. F.; Gatsonis, C.; Marcus, P. M.; Sicks, J. D., *N Engl J Med* **2011,** *365* (5), 395-409. DOI 10.1056/NEJMoa1102873.
123. Albert, J. M., *AJR. American journal of roentgenology* **2013,** *201* (1), W81-7. DOI 10.2214/AJR.12.9226.
124. Lokhandwala, T.; Dann, R.; Johnson, M.; D'Souza, A., *International Journal of Radiation Oncology• Biology• Physics* **2014,** *90* (5), S9-S10.
125. Husemann, Y.; Geigl, J. B.; Schubert, F.; Musiani, P.; Meyer, M.; Burghart, E.; Forni, G.; Eils, R.; Fehm, T.; Riethmuller, G.; Klein, C. A., *Cancer cell* **2008,** *13* (1), 58-68. DOI 10.1016/j.ccr.2007.12.003.
126. Izbicki, J. R.; Passlick, B.; Hosch, S. B.; Kubuschock, B.; Schneider, C.; Busch, C.; Knoefel, W. T.; Thetter, O.; Pantel, K., *The Journal of thoracic and cardiovascular surgery* **1996,** *112* (3), 623-30. DOI 10.1016/S0022-5223(96)70044-2.
127. Maruyama, R.; Sugio, K.; Mitsudomi, T.; Saitoh, G.; Ishida, T.; Sugimachi, K., *The Journal of thoracic and cardiovascular surgery* **1997,** *114* (4), 535-43. DOI 10.1016/S0022-5223(97)70041-2.
128. Wong, S. Y.; Hynes, R. O., *Cell cycle* **2006,** *5* (8), 812-7.
129. Nakagawa, T.; Martinez, S. R.; Goto, Y.; Koyanagi, K.; Kitago, M.; Shingai, T.; Elashoff, D. A.; Ye, X.; Singer, F. R.; Giuliano, A. E.; Hoon, D. S., *Clin Cancer Res* **2007,** *13* (14), 4105-10. DOI 10.1158/1078-0432.CCR-07-0419.
130. Krishnamurthy, S.; Cristofanilli, M.; Singh, B.; Reuben, J.; Gao, H.; Cohen, E. N.; Andreopoulou, E.; Hall, C. S.; Lodhi, A.; Jackson, S.; Lucci, A., *Cancer* **2010,** *116* (14), 3330-7. DOI 10.1002/cncr.25145.
131. Ilie, M.; Hofman, V.; Long-Mira, E.; Selva, E.; Vignaud, J. M.; Padovani, B.; Mouroux, J.; Marquette, C. H.; Hofman, P., *PloS one* **2014,** *9* (10), e111597. DOI 10.1371/journal.pone.0111597.
132. Chen, H. Y.; Yu, S. L.; Chen, C. H.; Chang, G. C.; Chen, C. Y.; Yuan, A.; Cheng, C. L.; Wang, C. H.; Terng, H. J.; Kao, S. F.; Chan, W. K.; Li, H. N.; Liu, C. C.; Singh, S.; Chen, W. J.; Chen, J. J.; Yang, P. C., *N Engl J Med* **2007,** *356* (1), 11-20. DOI 10.1056/NEJMoa060096.
133. Flehinger, B. J.; Kimmel, M.; Melamed, M. R., *Chest* **1992,** *101* (4), 1013-8.
134. Martin, K. J.; Fournier, M. V.; Reddy, G. P.; Pardee, A. B., *Cancer Res* **2010,** *70* (13), 5203-6. DOI 10.1158/0008-5472.CAN-10-0987.
135. Wendel, M.; Bazhenova, L.; Boshuizen, R.; Kolatkar, A.; Honnatti, M.; Cho, E. H.; Marrinucci, D.; Sandhu, A.; Perricone, A.; Thistlethwaite, P.; Bethel, K.; Nieva, J.; Heuvel, M.; Kuhn, P., *Physical biology* **2012,** *9* (1), 016005. DOI 10.1088/1478-3967/9/1/016005.
136. Pantel, K.; Alix-Panabieres, C., *Clinical chemistry* **2016,** *62* (2), 328-34. DOI 10.1373/clinchem.2015.242537.

137. Bockhorn, M.; Jain, R. K.; Munn, L. L., *The Lancet Oncology* **2007,** *8* (5), 444-448. DOI 10.1016/s1470-2045(07)70140-7.
138. Pantel, K.; Speicher, M. R., *Oncogene* **2015**. DOI 10.1038/onc.2015.192.
139. Kallergi, G.; Konstantinidis, G.; Markomanolaki, H.; Papadaki, M. A.; Mavroudis, D.; Stournaras, C.; Georgoulias, V.; Agelaki, S., *Molecular cancer therapeutics* **2013,** *12* (9), 1886-95. DOI 10.1158/1535-7163.MCT-12-1167.
140. Lecharpentier, A.; Vielh, P.; Perez-Moreno, P.; Planchard, D.; Soria, J. C.; Farace, F., *British journal of cancer* **2011,** *105* (9), 1338-41. DOI 10.1038/bjc.2011.405.
141. Hirsch, F. R.; Franklin, W. A.; Gazdar, A. F.; Bunn, P. A., Jr., *Clin Cancer Res* **2001,** *7* (1), 5-22.
142. Reddy, R. M.; Murlidhar, V.; Zhao, L.; Grabauskiene, S.; Zhang, Z.; Ramnath, N.; Lin, J.; Chang, A. C.; Carrott, P.; Lynch, W.; Orringer, M. B.; Beer, D. G.; Nagrath, S., *The Journal of thoracic and cardiovascular surgery* **2015**. DOI 10.1016/j.jtcvs.2015.09.126.
143. Wu, C.; Hao, H.; Li, L.; Zhou, X.; Guo, Z.; Zhang, L.; Zhang, X.; Zhong, W.; Guo, H.; Bremner, R. M.; Lin, P., *Journal of thoracic oncology : official publication of the International Association for the Study of Lung Cancer* **2009,** *4* (1), 30-6. DOI 10.1097/JTO.0b013e3181914125.
144. Krebs, M. G.; Hou, J. M.; Sloane, R.; Lancashire, L.; Priest, L.; Nonaka, D.; Ward, T. H.; Backen, A.; Clack, G.; Hughes, A.; Ranson, M.; Blackhall, F. H.; Dive, C., *Journal of thoracic oncology : official publication of the International Association for the Study of Lung Cancer* **2012,** *7* (2), 306-15. DOI 10.1097/JTO.0b013e31823c5c16.
145. Aguirre-Ghiso, J. A.; Bragado, P.; Sosa, M. S., *Nature medicine* **2013,** *19* (3), 276-7. DOI 10.1038/nm.3120.
146. Poveda, A.; Kaye, S. B.; McCormack, R.; Wang, S.; Parekh, T.; Ricci, D.; Lebedinsky, C. A.; Tercero, J. C.; Zintl, P.; Monk, B. J., *Gynecologic oncology* **2011,** *122* (3), 567-72. DOI 10.1016/j.ygyno.2011.05.028.
147. Pantel, K.; Alix-Panabieres, C., *Clinical chemistry* **2015**. DOI 10.1373/clinchem.2015.242537.
148. Alix-Panabieres, C.; Pantel, K., *Nature reviews. Cancer* **2014,** *14* (9), 623-31. DOI 10.1038/nrc3820.
149. Nanguzgambo, A. B.; Razack, R.; Louw, M.; Bolliger, C. T., *Oncology* **2011,** *80* (3-4), 247-56. DOI 10.1159/000329064.
150. Stott, S. L.; Lee, R. J.; Nagrath, S.; Yu, M.; Miyamoto, D. T.; Ulkus, L.; Inserra, E. J.; Ulman, M.; Springer, S.; Nakamura, Z.; Moore, A. L.; Tsukrov, D. I.; Kempner, M. E.; Dahl, D. M.; Wu, C. L.; Iafrate, A. J.; Smith, M. R.; Tompkins, R. G.; Sequist, L. V.; Toner, M.; Haber, D. A.; Maheswaran, S., *Science translational medicine* **2010,** *2* (25), 25ra23. DOI 10.1126/scitranslmed.3000403.
151. Marrinucci, D.; Bethel, K.; Bruce, R. H.; Curry, D. N.; Hsieh, B.; Humphrey, M.; Krivacic, R. T.; Kroener, J.; Kroener, L.; Ladanyi, A.; Lazarus, N. H.; Nieva, J.; Kuhn, P., *Human pathology* **2007,** *38* (3), 514-9. DOI 10.1016/j.humpath.2006.08.027.
152. Okumura, Y.; Tanaka, F.; Yoneda, K.; Hashimoto, M.; Takuwa, T.; Kondo, N.; Hasegawa, S., *The Annals of thoracic surgery* **2009,** *87* (6), 1669-75. DOI 10.1016/j.athoracsur.2009.03.073.
153. Sienel, W.; Seen-Hibler, R.; Mutschler, W.; Pantel, K.; Passlick, B., *European journal of cardio-thoracic surgery : official journal of the European Association for Cardio-thoracic Surgery* **2003,** *23* (4), 451-6.
154. Hashimoto, M.; Tanaka, F.; Yoneda, K.; Takuwa, T.; Matsumoto, S.; Okumura, Y.; Kondo, N.; Tsubota, N.; Tsujimura, T.; Tabata, C.; Nakano, T.; Hasegawa, S., *Interactive cardiovascular and thoracic surgery* **2014,** *18* (6), 775-83. DOI 10.1093/icvts/ivu048.
155. Funaki, S.; Sawabata, N.; Abulaiti, A.; Nakagiri, T.; Shintani, Y.; Inoue, M.; Minami, M.; Okumura, M., *European journal of cardio-thoracic surgery : official journal of the European Association for Cardio-thoracic Surgery* **2013,** *43* (6), 1126-30. DOI 10.1093/ejcts/ezs553.

156. Pirozzi, G.; Tirino, V.; Camerlingo, R.; La Rocca, A.; Martucci, N.; Scognamiglio, G.; Franco, R.; Cantile, M.; Normanno, N.; Rocco, G., *Oncology reports* **2013,** *29* (5), 1763-8. DOI 10.3892/or.2013.2294.
157. Funaki, S.; Sawabata, N.; Nakagiri, T.; Shintani, Y.; Inoue, M.; Kadota, Y.; Minami, M.; Okumura, M., *European journal of cardio-thoracic surgery : official journal of the European Association for Cardio-thoracic Surgery* **2011,** *40* (2), 322-7. DOI 10.1016/j.ejcts.2010.11.029.
158. Schmittgen, T. D.; Livak, K. J., *Nature protocols* **2008,** *3* (6), 1101-8.
159. Livak, K. J.; Schmittgen, T. D., *Methods* **2001,** *25* (4), 402-8. DOI 10.1006/meth.2001.1262.
160. Luo, M.; Brooks, M.; Wicha, M. S., *Current pharmaceutical design* **2015,** *21* (10), 1301-10.
161. Yip, K. W.; Reed, J. C., *Oncogene* **2008,** *27* (50), 6398-406. DOI 10.1038/onc.2008.307.
162. Kasimir-Bauer, S.; Bittner, A. K.; Konig, L.; Reiter, K.; Keller, T.; Kimmig, R.; Hoffmann, O., *Breast cancer research : BCR* **2016,** *18* (1), 20. DOI 10.1186/s13058-016-0679-3.
163. Carlsson, A.; Nair, V. S.; Luttgen, M. S.; Keu, K. V.; Horng, G.; Vasanawala, M.; Kolatkar, A.; Jamali, M.; Iagaru, A. H.; Kuschner, W.; Loo, B. W., Jr.; Shrager, J. B.; Bethel, K.; Hoh, C. K.; Bazhenova, L.; Nieva, J.; Kuhn, P.; Gambhir, S. S., *Journal of thoracic oncology : official publication of the International Association for the Study of Lung Cancer* **2014,** *9* (8), 1111-9. DOI 10.1097/JTO.0000000000000235.
164. Baccelli, I.; Schneeweiss, A.; Riethdorf, S.; Stenzinger, A.; Schillert, A.; Vogel, V.; Klein, C.; Saini, M.; Bauerle, T.; Wallwiener, M.; Holland-Letz, T.; Hofner, T.; Sprick, M.; Scharpff, M.; Marme, F.; Sinn, H. P.; Pantel, K.; Weichert, W.; Trumpp, A., *Nature biotechnology* **2013,** *31* (6), 539-44. DOI 10.1038/nbt.2576.
165. Peeters, D. J.; Brouwer, A.; Van den Eynden, G. G.; Rutten, A.; Onstenk, W.; Sieuwerts, A. M.; Van Laere, S. J.; Huget, P.; Pauwels, P.; Peeters, M.; Vermeulen, P. B.; Dirix, L. Y., *Cancer letters* **2015,** *356* (2 Pt B), 872-9. DOI 10.1016/j.canlet.2014.10.039.
166. Bissolati, M.; Sandri, M. T.; Burtulo, G.; Zorzino, L.; Balzano, G.; Braga, M., *Tumour biology : the journal of the International Society for Oncodevelopmental Biology and Medicine* **2014**. DOI 10.1007/s13277-014-2716-0.
167. Rahbari, N. N.; Bork, U.; Kircher, A.; Nimitz, T.; Scholch, S.; Kahlert, C.; Schmidt, T.; Steinert, G.; Ulrich, A. B.; Reissfelder, C.; Buchler, M. W.; Koch, M.; Weitz, J., *Annals of surgical oncology* **2012,** *19* (7), 2195-202. DOI 10.1245/s10434-011-2178-1.
168. Liotta, L. A.; Saidel, M. G.; Kleinerman, J., *Cancer Res* **1976,** *36* (3), 889-94.
169. Guo, Y.; Xu, F.; Lu, T.; Duan, Z.; Zhang, Z., *Cancer treatment reviews* **2012,** *38* (7), 904-10. DOI 10.1016/j.ctrv.2012.04.007.
170. Laubli, H.; Alisson-Silva, F.; Stanczak, M. A.; Siddiqui, S. S.; Deng, L.; Verhagen, A.; Varki, N.; Varki, A., *The Journal of biological chemistry* **2014,** *289* (48), 33481-91. DOI 10.1074/jbc.M114.593129.
171. Noh, K. H.; Kim, B. W.; Song, K. H.; Cho, H.; Lee, Y. H.; Kim, J. H.; Chung, J. Y.; Kim, J. H.; Hewitt, S. M.; Seong, S. Y.; Mao, C. P.; Wu, T. C.; Kim, T. W., *The Journal of clinical investigation* **2012,** *122* (11), 4077-93. DOI 10.1172/JCI64057.
172. Cheung, K. J.; Padmanaban, V.; Silvestri, V.; Schipper, K.; Cohen, J. D.; Fairchild, A. N.; Gorin, M. A.; Verdone, J. E.; Pienta, K. J.; Bader, J. S.; Ewald, A. J., *Proceedings of the National Academy of Sciences of the United States of America* **2016**. DOI 10.1073/pnas.1508541113.
173. Cheung, K. J.; Ewald, A. J., *Science* **2016,** *352* (6282), 167-9. DOI 10.1126/science.aaf6546.
174. Hou, J. M.; Krebs, M. G.; Lancashire, L.; Sloane, R.; Backen, A.; Swain, R. K.; Priest, L. J.; Greystoke, A.; Zhou, C.; Morris, K.; Ward, T.; Blackhall, F. H.; Dive, C., *Journal of clinical oncology : official journal of the American Society of Clinical Oncology* **2012,** *30* (5), 525-32. DOI 10.1200/JCO.2010.33.3716.
175. Das, M.; Riess, J. W.; Frankel, P.; Schwartz, E.; Bennis, R.; Hsieh, H. B.; Liu, X.; Ly, J. C.; Zhou, L.; Nieva, J. J.; Wakelee, H. A.; Bruce, R. H., *Lung cancer* **2012,** *77* (2), 421-6. DOI 10.1016/j.lungcan.2012.04.005.

176. Sarioglu, A. F.; Aceto, N.; Kojic, N.; Donaldson, M. C.; Zeinali, M.; Hamza, B.; Engstrom, A.; Zhu, H.; Sundaresan, T. K.; Miyamoto, D. T.; Luo, X.; Bardia, A.; Wittner, B. S.; Ramaswamy, S.; Shioda, T.; Ting, D. T.; Stott, S. L.; Kapur, R.; Maheswaran, S.; Haber, D. A.; Toner, M., *Nat Methods* **2015,** *12* (7), 685-91. DOI 10.1038/nmeth.3404.
177. Offner, S.; Schmaus, W.; Witter, K.; Baretton, G. B.; Schlimok, G.; Passlick, B.; Riethmuller, G.; Pantel, K., *Proceedings of the National Academy of Sciences of the United States of America* **1999,** *96* (12), 6942-6.
178. Serrano, M. J.; Sanchez-Rovira, P.; Delgado-Rodriguez, M.; Juan Gaforio, J., *Cancer Biology & Therapy* **2014,** *8* (8), 671-675. DOI 10.4161/cbt.8.8.7834.
179. Levine, A. J., *Cell* **1997,** *88* (3), 323-31.
180. Maddipati, R.; Stanger, B. Z., *Cancer discovery* **2015,** *5* (10), 1086-97. DOI 10.1158/2159-8290.CD-15-0120.
181. Long, E.; Ilie, M.; Bence, C.; Butori, C.; Selva, E.; Lalvee, S.; Bonnetaud, C.; Poissonnet, G.; Lacour, J. P.; Bahadoran, P.; Brest, P.; Gilson, E.; Ballotti, R.; Hofman, V.; Hofman, P., *Cancer Med* **2016,** *5* (6), 1022-30. DOI 10.1002/cam4.661.
182. Fidler, I. J., *Eur J Cancer* **1973,** *9* (3), 223-7.
183. Au, S. H.; Storey, B. D.; Moore, J. C.; Tang, Q.; Chen, Y. L.; Javaid, S.; Sarioglu, A. F.; Sullivan, R.; Madden, M. W.; O'Keefe, R.; Haber, D. A.; Maheswaran, S.; Langenau, D. M.; Stott, S. L.; Toner, M., *Proceedings of the National Academy of Sciences of the United States of America* **2016,** *113* (18), 4947-52. DOI 10.1073/pnas.1524448113.
184. Reategui, E.; Aceto, N.; Lim, E. J.; Sullivan, J. P.; Jensen, A. E.; Zeinali, M.; Martel, J. M.; Aranyosi, A. J.; Li, W.; Castleberry, S.; Bardia, A.; Sequist, L. V.; Haber, D. A.; Maheswaran, S.; Hammond, P. T.; Toner, M.; Stott, S. L., *Adv Mater* **2015,** *27* (9), 1593-9. DOI 10.1002/adma.201404677.
185. Yoon, H. J.; Shanker, A.; Wang, Y.; Kozminsky, M.; Jin, Q.; Palanisamy, N.; Burness, M. L.; Azizi, E.; Simeone, D. M.; Wicha, M. S.; Kim, J.; Nagrath, S., *Adv Mater* **2016,** *28* (24), 4891-7. DOI 10.1002/adma.201600658.
186. Chudnovsky, Y.; Khavari, P. A.; Adams, A. E., *The Journal of clinical investigation* **2005,** *115* (4), 813-24. DOI 10.1172/JCI24808.
187. Meier, F.; Will, S.; Ellwanger, U.; Schlagenhauff, B.; Schittek, B.; Rassner, G.; Garbe, C., *Br J Dermatol* **2002,** *147* (1), 62-70.
188. Mocellin, S.; Hoon, D.; Ambrosi, A.; Nitti, D.; Rossi, C. R., *Clin Cancer Res* **2006,** *12* (15), 4605-13. DOI 10.1158/1078-0432.CCR-06-0823.
189. Luo, X.; Mitra, D.; Sullivan, R. J.; Wittner, B. S.; Kimura, A. M.; Pan, S.; Hoang, M. P.; Brannigan, B. W.; Lawrence, D. P.; Flaherty, K. T.; Sequist, L. V.; McMahon, M.; Bosenberg, M. W.; Stott, S. L.; Ting, D. T.; Ramaswamy, S.; Toner, M.; Fisher, D. E.; Maheswaran, S.; Haber, D. A., *Cell reports* **2014,** *7* (3), 645-53. DOI 10.1016/j.celrep.2014.03.039.
190. Khoja, L.; Lorigan, P.; Zhou, C.; Lancashire, M.; Booth, J.; Cummings, J.; Califano, R.; Clack, G.; Hughes, A.; Dive, C., *J Invest Dermatol* **2013,** *133* (6), 1582-90. DOI 10.1038/jid.2012.468.
191. Nedosekin, D. A.; Sarimollaoglu, M.; Ye, J. H.; Galanzha, E. I.; Zharov, V. P., *Cytometry A* **2011,** *79* (10), 825-33. DOI 10.1002/cyto.a.21102.
192. Ruiz, C.; Li, J.; Luttgen, M. S.; Kolatkar, A.; Kendall, J. T.; Flores, E.; Topp, Z.; Samlowski, W. E.; McClay, E.; Bethel, K.; Ferrone, S.; Hicks, J.; Kuhn, P., *Physical biology* **2015,** *12* (1), 016008. DOI 10.1088/1478-3975/12/1/016008.
193. Benez, A.; Geiselhart, A.; Handgretinger, R.; Schiebel, U.; Fierlbeck, G., *J Clin Lab Anal* **1999,** *13* (5), 229-33.
194. Khoja, L.; Lorigan, P.; Dive, C.; Keilholz, U.; Fusi, A., *Annals of oncology : official journal of the European Society for Medical Oncology / ESMO* **2015,** *26* (1), 33-9. DOI 10.1093/annonc/mdu207.

195. Medic, S.; Pearce, R. L.; Heenan, P. J.; Ziman, M., *Pigment Cell Res* **2007,** *20* (2), 80-91. DOI 10.1111/j.1600-0749.2006.00356.x.
196. Rao, C.; Bui, T.; Connelly, M.; Doyle, G.; Karydis, I.; Middleton, M. R.; Clack, G.; Malone, M.; Coumans, F. A.; Terstappen, L. W., *International journal of oncology* **2011,** *38* (3), 755-60. DOI 10.3892/ijo.2011.896.
197. Tong, X.; Yang, L.; Lang, J. C.; Zborowski, M.; Chalmers, J. J., *Cytometry B Clin Cytom* **2007,** *72* (5), 310-23. DOI 10.1002/cyto.b.20177.
198. Prince, M. E.; Sivanandan, R.; Kaczorowski, A.; Wolf, G. T.; Kaplan, M. J.; Dalerba, P.; Weissman, I. L.; Clarke, M. F.; Ailles, L. E., *Proceedings of the National Academy of Sciences of the United States of America* **2007,** *104* (3), 973-8. DOI 10.1073/pnas.0610117104.
199. Patel, V.; Hood, B. L.; Molinolo, A. A.; Lee, N. H.; Conrads, T. P.; Braisted, J. C.; Krizman, D. B.; Veenstra, T. D.; Gutkind, J. S., *Clin Cancer Res* **2008,** *14* (4), 1002-14. DOI 10.1158/1078-0432.CCR-07-1497.
200. Nichols, A. C.; Lowes, L. E.; Szeto, C. C.; Basmaji, J.; Dhaliwal, S.; Chapeskie, C.; Todorovic, B.; Read, N.; Venkatesan, V.; Hammond, A.; Palma, D. A.; Winquist, E.; Ernst, S.; Fung, K.; Franklin, J. H.; Yoo, J.; Koropatnick, J.; Mymryk, J. S.; Barrett, J. W.; Allan, A. L., *Head Neck* **2012,** *34* (10), 1440-4. DOI 10.1002/hed.21941.
201. Leemans, C. R.; Braakhuis, B. J.; Brakenhoff, R. H., *Nature reviews. Cancer* **2011,** *11* (1), 9-22. DOI 10.1038/nrc2982.
202. Chen, Y. S.; Wu, M. J.; Huang, C. Y.; Lin, S. C.; Chuang, T. H.; Yu, C. C.; Lo, J. F., *PloS one* **2011,** *6* (11), e28053. DOI 10.1371/journal.pone.0028053.
203. Bayarri-Lara, C.; Ortega, F. G.; Cueto Ladron de Guevara, A.; Puche, J. L.; Ruiz Zafra, J.; de Miguel-Perez, D.; Ramos, A. S.; Giraldo-Ospina, C. F.; Navajas Gomez, J. A.; Delgado-Rodriguez, M.; Lorente, J. A.; Serrano, M. J., *PloS one* **2016,** *11* (2), e0148659. DOI 10.1371/journal.pone.0148659.
204. Morrow, C. J.; Trapani, F.; Metcalf, R. L.; Bertolini, G.; Hodgkinson, C. L.; Khandelwal, G.; Kelly, P.; Galvin, M.; Carter, L.; Simpson, K. L.; Williamson, S.; Wirth, C.; Simms, N.; Frankliln, L.; Frese, K. K.; Rothwell, D. G.; Nonaka, D.; Miller, C. J.; Brady, G.; Blackhall, F. H.; Dive, C., *Annals of oncology : official journal of the European Society for Medical Oncology / ESMO* **2016,** *27* (6), 1155-60. DOI 10.1093/annonc/mdw122.
205. Hou, J. M.; Greystoke, A.; Lancashire, L.; Cummings, J.; Ward, T.; Board, R.; Amir, E.; Hughes, S.; Krebs, M.; Hughes, A.; Ranson, M.; Lorigan, P.; Dive, C.; Blackhall, F. H., *Am J Pathol* **2009,** *175* (2), 808-16. DOI 10.2353/ajpath.2009.090078.
206. Pailler, E.; Adam, J.; Barthelemy, A.; Oulhen, M.; Auger, N.; Valent, A.; Borget, I.; Planchard, D.; Taylor, M.; Andre, F.; Soria, J. C.; Vielh, P.; Besse, B.; Farace, F., *Journal of clinical oncology : official journal of the American Society of Clinical Oncology* **2013,** *31* (18), 2273-81. DOI 10.1200/JCO.2012.44.5932.
207. Zhang, Z.; Shiratsuchi, H.; Palanisamy, N.; Nagrath, S.; Ramnath, N., *Journal of thoracic oncology : official publication of the International Association for the Study of Lung Cancer* **2016**. DOI 10.1016/j.jtho.2016.07.027.
208. Wirkner, M.; Alonso, J. M.; Maus, V.; Salierno, M.; Lee, T. T.; Garcia, A. J.; del Campo, A., *Adv Mater* **2011,** *23* (34), 3907-10. DOI 10.1002/adma.201100925.
209. Elshal, M. F.; Khan, S. S.; Takahashi, Y.; Solomon, M. A.; McCoy, J. P., Jr., *Blood* **2005,** *106* (8), 2923-4. DOI 10.1182/blood-2005-06-2307.